Performance Monitoring and Diagnosis of a Binary Distillation Column

S.J. Burger 1367110

Master of Science Thesis

TU Delft Delft University of Technology

Delft Center for Systems and Control

Performance Monitoring and Diagnosis of a Binary Distillation Column

Master of Science Thesis

For the degree of Master of Science in Mechanical Engineering at Delft University of Technology

S.J. Burger 1367110

April 16, 2014

Faculty of Mechanical, Maritime and Materials Engineering (3mE) · Delft University of Technology

Abstract

The life-time performance of chemical processes is limited due to changes in the plant dynamics and disturbance characteristics over time. Such systems often make use of model-based controllers. When a dynamic change arises over time, a difference occurs between the dynamic models contained in the controller and the true system dynamics. The difference in dynamics could deteriorate the performance of a model-based control system. Monitoring the performance on-line is therefore of importance. Detection of a dynamic plant or disturbance change occurs by a classical performance monitoring method, which estimates the variance of the controlled outputs. A change is detected at the moment that a maximum performance bound is violated.

An important step is to distinguish between control-relevant plant changes and variations in disturbance characteristics due to different solutions strategies. With an existing performance diagnosis method which makes use of closed-loop prediction error identification the true plant dynamics are identified. Then it is verified whether a performance drop is caused by a change in control-relevant plant dynamics by making use of hypothesis testing. A set is considered that contains all plant dynamics which achieve a satisfactory performance and it is verified whether the identified model is located in or outside the set to make a decision. With an alternative second decision rule, a heuristic method is used where models are constructed around the estimated model by making use of a normal distribution. It is verified which percentage of these models are located outside the set to make a decision. A third decision rule is used which is a combination of the first and second decision rules and the confidence is compared between all considered decision rules.

In a simulation case study of a binary distillation column, the performance monitoring method detects a performance drop satisfactory without creating many false alarms. Furthermore, it is shown that with the heuristic method a significant increase in confidence is achieved compared to the first decision rule and only a minor difference with respect to the third decision rule.

Preface

This thesis is a part of my Master of Science graduation degree. By having a discussion with my supervisor, the idea of doing my thesis about identification and control of a binary distillation column arose. During the project multiple ideas have been discussed. Finally, we came up to investigate a classical performance monitoring and a novel diagnosis method and tested whether these methods are working properly on multiple-input multiple-output systems. In a simulation case study simulations are performed by making use of a model of a MIMO binary distillation column.

For people who are interested in how a performance monitoring and diagnosis method work, Chapter 2 is recommended. Chapter 3 discusses what a binary distillation column is, what it does and how to model such a system with a very simplified model. Finally, in Chapter 4 results are discussed with regard to the application of a performance monitoring and diagnosis method to a MIMO system.

I am very pleased with the results and I have learnt a lot with regard to doing research, scientific writing and public speaking. I want to thank my supervisors Dr. Ir. Xavier Bombois and Max Potters (MSc) for their help and advice.

Stefan Burger

Table of Contents

Chapter 1

Introduction

1-1 Problem Statement

Companies try to keep their costs as low as possible in order to be competitive. In particular, the operational costs from industrial processes are relatively high and need to be maintained or possibly lowered in order to remain acceptable. The costs can be indirectly maintained by monitoring the performance of a system. A performance monitoring method consist of a cost function which for example makes use of measurements of the controlled outputs from the past. The data can be used to estimate the variance of the outputs [1]. By applying a maximum bound on the performance a distinction can be made between satisfactory and degraded performance levels.

In industry models-based controllers are often used to achieve a desirable performance. These kind of controllers rely on the accuracy of the constructed models, where accuracy can be defined in terms of the modelling error. At the commissioning stage of a process, the controller is tuned so that the best possible performance is reached, i.e., nominal performance. Theoretically, the system will operate at nominal performance without developing problems. In reality it is possible that the performance of model-based control systems will deteriorate over time. Two causes are considered which could deteriorate the performance of a system [2]. The first cause is a change in control-relevant plant dynamics. This implies that we only consider plant changes that deteriorate the performance of our system (e.g. failures of sensors or actuators are not considered because we assume that these failures can be detected with existing methods). A control-relevant plant change increases the mismatch between the plant model contained in the controller and the actual system, such that nominal performance can not be reached any more. In this case the only solution is to perform a re-identification experiment to restore the performance of the system. Keep in mind that re-identification of the plant dynamics is highly expensive and should only be performed when necessary. This is of importance because the second cause, which are (temporary) variations in disturbance characteristics, occurs much more often. A full re-identification experiment is a waste of resources when a change in disturbance characteristics occurs, because it is unlikely to restore the systems performance. Instead, one should opt for tuning the controller to reject the

disturbances. To be able to perform the correct action after a performance deterioration is detected, the causes need to be distinguished by making use of a performance diagnosis.

Note that a change in dynamics can deteriorate the performance. For that reason the performance needs to be monitored on-line. Furthermore, the performance measure should not be too sensitive, which is the case when using a small amount of measured data. It could cause the performance monitoring method to detect many false alarms [3]. After an alarm of a possibly degraded performance is given, a performance diagnosis will be started which creates undesirable and unnecessary costs in the situation of a false alarm. Also, it is of importance that a change in plant dynamics or disturbance characteristics is detected as fast as possible to keep economical costs low. Therefore, the used performance monitoring method should be thoroughly investigated, such that it is able to meet certain expectations.

1-2 Literature Methodologies

A performance monitoring method is needed to measure the real-time performance of a system and a performance diagnosis method needs to be used to distinguish between a change in control-relevant plant dynamics and variations in disturbance characteristics. In literature, methodologies are found which are able to measure the performance on-line. In e.g. the survey paper of Isermann [4] a performance monitoring method is shortly explained. This method is based on obtaining information of the controlled outputs which are checked with regard to certain tolerances. If the tolerances are violated alarms are generated. Furthermore, in research of Potters et. al. [5] a performance monitoring method is discussed and applied to two different processes. They use a performance measure, i.e., a function which considers multiple issues. These issues are related to operational costs and acceptable product quality. Here, a trade-of was made between the production costs and so-called constraint violation costs. In Tyler and Morari [1] and in Basseville and Benveniste [3], detection of output changes are investigated. An often used classical performance monitoring method is considered to detect changes in signals/systems by making use of a squared distance measurement between outputs and set-points within a chosen time window, i.e., it is an estimation of the power of the measured outputs. Also, in Schäfer and Cinar [6] a same kind of performance measurement was considered. However, due to a model predictive controller which was used the performance measure included the computed future control actions and future outputs. In a simulation case study, the performance which was measured on-line was compared to the performance of the simulation model by making use of a ratio. It was found that the performance monitoring method worked well on model-based control systems.

After a detection of a performance deterioration, a performance diagnosis needs to be performed to be able to distinguish between various causes. In literature a distinction is made between multiple causes by making use of hypothesis testing as explained in Mesbah et. al. [2], Schäfer and Cinar [6], Gustafsson and Graebe [7] and Frank [8]. To find the cause which deteriorated the performance, a distinction is made between a change in disturbance characteristics which can seen as hypothesis $\mathcal{H}_0$ and a change in control-relevant plant dynamics which is seen as hypothesis $\mathcal{H}_1$. It can be noticed that the true plant dynamics are unknown. Therefore, in Mesbah et. al. [2] and Frank [8] the decision is based on an estimate of the true plant dynamics which is obtained via a short closed-loop re-identification experiment.

This thesis will make use of the diagnosis method of Mesbah et. al. [2], because it only considers changes in control-relevant plant dynamics and variations in disturbance character-

istics. Whereas, in, e.g., Basseville and Benveniste [3] or Huang and Tamayo [9] any plant change that deteriorates the performance is considered. Furthermore, in Ref. [2] a region is constructed, which contains all plant dynamics which do not deteriorate the closed-loop performance. The region is called $\mathcal{D}_{adm}$ and is defined by the set of all plant dynamics that achieve a satisfactory performance with the existing controller and under the original disturbance characteristics (at commissioning). Hypothesis $\mathcal{H}_1$ is only true if the true plant dynamics are located outside the region $\mathcal{D}_{adm}$. As mentioned, the true system is unknown and therefore the decision is based on the closed-loop performance which includes the identified model of the true dynamics. If the estimated model is found to be outside the region $\mathcal{D}_{adm}$, it is also considered that the true system is outside the region. Note that a wrong decision can be made and that therefore the confidence of making a wrong and correct decision needs to be assessed.

1-3 Objective

In this thesis an existing performance monitoring method and performance diagnosis are tested in a simulation case study, where we make use of a model of a multiple-input multiple-output (MIMO) binary distillation column. First the performance monitoring method of Ref. [1] is applied to our simulation model because it makes use of a classical performance measure which makes use of data of the measured outputs. It is investigated whether the performance can be measured satisfactory. Then a threshold value is applied to create a bound on the maximum performance and it was investigated whether a control-relevant plant change and a change in disturbance variations could be detected sufficiently. Also, a trade-off is made between the sensitivity and the accuracy of the performance measure. A question of interest is:

To what extent is it possible to detect the considered causes by making use of the performance monitoring method of Ref. [1] and what issues are of importance to tune variables within the performance monitoring method?

Secondly, it is considered that a performance deterioration is detected and it is investigated whether the performance diagnosis of Mesbah et. al. [2] could distinguish between the considered causes. Also, it is analysed how confident the decision will be. This is investigated by making use of Monte Carlo simulations to obtain a set of data which represents a distribution of many scenarios which can occur. With this second objective a second question of interest is:

How reliable will the made decision be, of opting for the correct cause, when applying the performance diagnosis methodology of Ref. [2] to a MIMO system?

This chapter introduced the main problems concerning model-based control systems/industrial processes and states its objectives. The thesis overview is structured as follows. In section 2-2 the principles of how a performance monitoring method of Ref. [1] can be used is discussed. A distinction is made between the performance measure used in the performance monitoring method and in the performance diagnosis. After explanation of the performance measure the performance diagnosis method is elaborated which distinguishes between a plant and a disturbance change as discussed in section 2-3. In section 3 a detailed description of the binary distillation column is given in terms of all the flows and parts in the column and how

certain flows affect other system properties when adjusting these flows. Furthermore, in section 3-2-2 the system variables are discussed in terms of control and simplifications are made by considering certain interactions in the system. In section 3-3 a case study is explained which makes use of a simulation model of a binary distillation column. Also, in section 3-3-3 it is explained how we model a plant change and a disturbance change. Finally, in section 4-2 results of the application of the performance measure and diagnosis method to the simulator are presented and explained. A final conclusion and future work is given in section 5.

Chapter 2

Closed-Loop Performance Monitoring and Diagnosis

2-1 Introduction

As mentioned in the introductory chapter a problem of model-based control systems is that the performance can deteriorate over time. A performance degradation occurs due to wear, dirt or any other reason which could affect the process dynamics. Therefore, on a system in operation the performance needs to be monitored continuously to be able to detect a performance deterioration. The performance can be monitored by making use of a performance measure, which can be expressed in many different ways. We will express the performance in terms of the power of the error between the outputs and the set-points as discussed in Ref. [1]. If a performance deterioration is measured it needs to be investigated what the cause could be. It is of importance to know the root cause of a performance deterioration, because each cause requires a different solution strategy. When a wrong strategy is performed, an undesired increase of economic costs will arise.

A diagnosis will be performed to investigate what the cause of a performance deterioration could be. In Mesbah et. al. [2] a distinction is made between two control relevant changes (process dynamics and disturbance characteristics) by making use of hypothesis testing and closed-loop performance analysis. In Ref. [2] the performance of a closed-loop stable linear time-invariant single-input single-output (SISO) system was analysed.

This thesis makes use of the performance diagnosis methodology of Mesbah to be able to find the correct cause which deteriorated the performance of the system. We will analyse the closed-loop performance of a stable linear time-invariant multiple-input multiple-output (MIMO) system and investigate whether it is possible, by making use of the diagnosis methodology of Ref. [2], to detect the correct cause which induces a performance deterioration.

Both the performance monitoring method as well as the performance diagnosis methodology used in this thesis are applicable to systems which operate in closed-loop and are controlled by linear PI or PID controllers. We solely focus on its application to linear PI controllers.

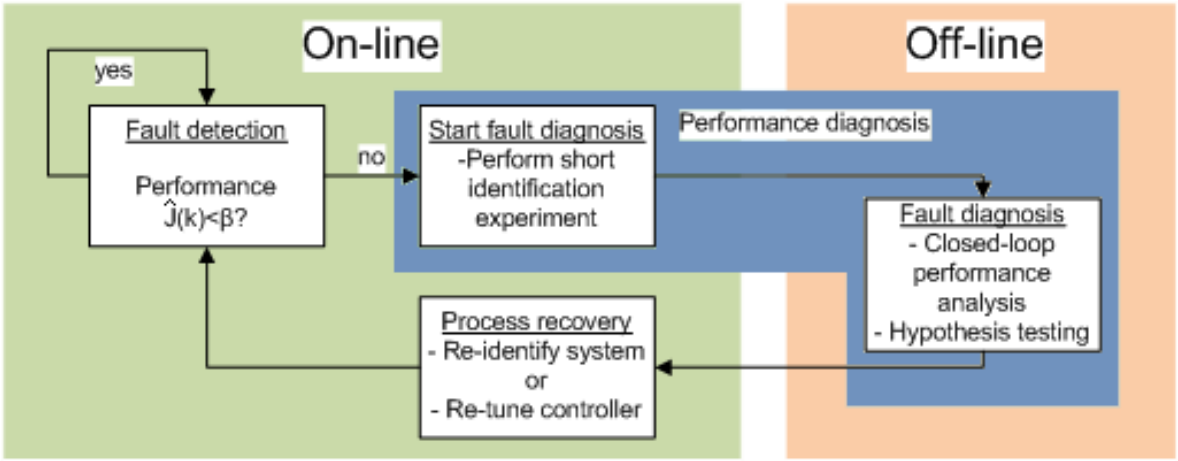

Figure 2-1: Loop of the performance monitor, diagnosis method and recovery of the system performance.

A global overview of the loop which is used to monitor the performance detect a performance drop and recover the performance of a system is shown in Fig. 2-1. Here it is shown whether an action is performed on-line (directly on the true system) or off-line (closed-loop performance analysis). First, the closed-loop system which will be used throughout this chapter is shortly discussed in section 2-2 and then a general description is given of the performance measure, i.e., fault detection. Here, we will distinguish between the performance measure used in the performance diagnosis and a performance measure for on-line performance monitoring. Secondly, the performance diagnosis method is explained in section 2-3, i.e., (start) fault diagnosis. Here, the issues about the control-relevant changes, hypothesis testing/decision rule, closed-loop performance analysis and the way to recover nominal performance are explained to be able to find the correct cause of a performance deterioration.

2-2 Performance Measure

An open-loop system is considered where the outputs are given by

$$\underline{y}(t) = G(z,\theta_0)\underline{u}(t) + H(z,\theta_0)\underline{e}(t) \tag{2-1}$$

Here, the inputs are given by $\underline{u}(t)$, zero-mean white noise signals are given by $\underline{e}(t)$ with corresponding variance matrix $\Sigma_e = \text{diag}(\left[\sigma^2_{e,1}...\sigma^2_{e,n}\right])$ and on the off-diagonal entries the matrix is zero. The vectors $\underline{y}(t)$ and $\underline{e}(t)$ are of size n. The input vector $\underline{u}(t)$ is of size m. Furthermore, the true system dynamics have been parametrized and $G_0(z) = G(z,\theta_0)$ represents a linear dynamic model of the true plant dynamics and is given by a discrete-time transfer matrix of size $m \times n$. Furthermore, $H_0(z) = H(z,\theta_0)$ represents a dynamic filter which is a diagonal discrete-time transfer matrix of size $n \times n$, is zero on the off-diagonal entries and is assumed to be monic and minimum-phase. It is assumed that the true process dynamics can be described by a linearised parametrization denoted by $\mathcal{M} = \{G(z,\theta), H(z,\theta)\}$. The linear dynamic model contains a parameter vector $\theta = \theta_0 \in \mathbb{R}^k$ which is the only parameter vector

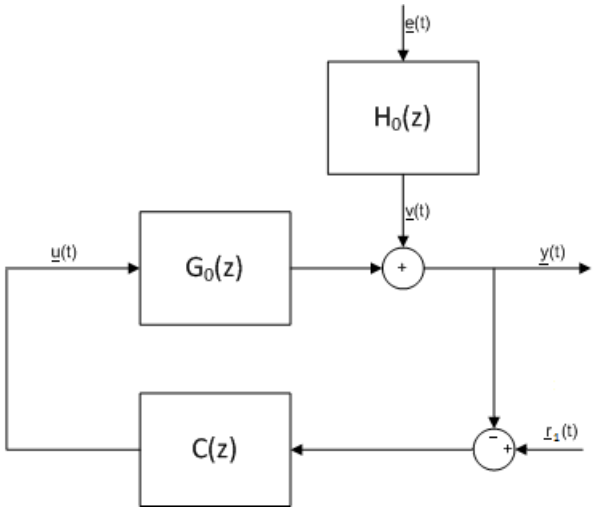

Figure 2-2: The closed-loop data generating system is shown with true process dynamics $G_0(z)$, dynamic filter $H_0(z)$ and controller $C(z)$. The outputs are given by $\underline{y}(t)$, the inputs by $\underline{u}(y)$, white-noise signals by $\underline{e}(t)$ and the set-points by $\underline{r}_1(t)$.

with which the true dynamics can be described.
As mentioned, the performance of stable closed-loop MIMO systems will be analysed. Therefore, we will consider a closed-loop system as depicted in Fig. 2-2. The outputs and the inputs of the true closed-loop system are given by

$$\begin{aligned}
\underline{y}(t) = \quad & (I + G(z,\theta_0)C(z))^{-1}(G(z,\theta_0)C(z)\underline{r}_1(t) + \underline{v}(t)) \\
= \quad & \underbrace{(I + G(z,\theta_0)C(z))^{-1}}_{T_0(z)}(\underbrace{G(z,\theta_0)}_{G_0(z)}C(z)\underline{r}_1(t) + \underbrace{H(z,\theta_0)}_{H_0(z)}\underline{e}(t)) \qquad (2\text{-}2) \\
\underline{u}(t) = \quad & \underbrace{(I + C(z)G(z,\theta_0))^{-1}}_{S_0(z)}(C(z)\underline{r}_1(t) - C(z)H(z,\theta_0)\underline{e}(t)) \qquad (2\text{-}3)
\end{aligned}$$

Derivation of Eqs. (2-2) and (2-3) is given in appendix A-1. $(.)^{-1}$ represents the inverse of a matrix, $C(z)$ represents the controller which is a discrete-time transfer matrix and closes the loop as shown in Fig. 2-2. The transfer matrices $T_0(z)$ and $S_0(z)$ represent the output and input sensitivity respectively. The set-points are indicated by $\underline{r}_1(t)$ and is of size n.

At commissioning, models of the process and noise dynamics, $G(z,\theta_{com})$ and $H(z,\theta_{com})$ respectively, are constructed to design the controller $C(z)$. The controller closes the loop of the true system as shown in Fig. 2-2 and is able to stabilize the true system $G_0(z)$. At commissioning it is known that nominal and good performance is reached for the constructed discrete closed-loop system $\{C(z), G(z,\theta_{com}), H(z,\theta_{com})\}$ and it is assumed that this also holds for the true discrete closed-loop system $\{C(z), G_0(z), H_0(z)\}$.

2-2-1 Performance Analysis of a Closed-Loop System

For a closed-loop system as given by Eq. (2-2) the performance can be formulated in more than one way. To express the performance of the closed-loop system we will consider

Ref. [1]. The difference in power between the measured outputs $\underline{y}(t)$ and the set-points $\underline{r}_1(t)$ is considered, where $\underline{r}_1(t)$ is considered to be a constant. Before a formulation can be given which can be used as a performance measure, Eq. (2-2) needs to be rewritten to show what power contributions are of importance. Subtract $\underline{r}_1(t)$ from Eq. (2-2) to define the error signal, which gives

$$\underline{y}(t) - \underline{r}_1(t) = \underbrace{-(I + G(z,\theta)C(z))^{-1}\underline{r}_1(t)}_{\text{transient } (T(t))} + \underbrace{(I + G(z,\theta)C(z))^{-1}H(z,\theta)\underline{e}(t)}_{\text{steady state } (R(t))} \quad (2\text{-}4)$$

The derivation is given in appendix A-3. The first term of Eq. (2-4) on the r.h.s. represents the transient behaviour of the system. For a stable closed-loop system the transient response tends to zero if the time tends to infinity under the assumptions that $\underline{r}_1(t)$ is constant and that there is an integrator in the system (which there is due to the integrator term of the PI-controllers). Therefore, the transient response will be neglected and not taken into account. The second part of Eq. (2-4) of the r.h.s. represents the steady state response which is of more importance. It is seen by the term $H(z,\theta)\underline{e}(t)$ that the steady state response is influenced by the disturbances in the system. It implies that we deal with a disturbance rejection problem and not a tracking problem. We will only consider the power contributions which corresponds to the steady state response. The steady state response is given by the signal $R(t)$. Before the power can be computed, first the power spectrum is computed for the difference of $\underline{y}(t)$ and $\underline{r}_1(t)$ for the steady state response and is given by

$$\Phi_{y-r_1}(\omega) = R(e^{j\omega})^*\Phi_e(\omega)R(e^{j\omega}) \qquad \text{with} \qquad \Phi_e(\omega) = \begin{bmatrix} \sigma_{e,1}^2 & & 0 \\ & \ddots & \\ 0 & & \sigma_{e,n}^2 \end{bmatrix}. \quad (2\text{-}5)$$

Here $(.)^*$ represent the complex conjugate of a matrix. The performance measure is then expressed in terms of the the power of the difference $\underline{y}(t) - \underline{r}_1(t)$ (and add up the elements of it). The latter is given by the following equation

$$\begin{aligned} J(C(z), G(z,\theta), H(z,\theta)) &= \frac{1}{2\pi}\int_{-\pi}^{\pi} \text{trace}\left(\Phi_{y-r_1}(\omega)\right) d\omega \\ &= \frac{1}{2\pi}\int_{-\pi}^{\pi} \text{trace}\left(R(e^{j\omega})^*\Phi_e(\omega)R(e^{j\omega})\right) d\omega. \end{aligned} \quad (2\text{-}6)$$

In case that $\Phi_e(\omega) = \sigma_e^2 I_n$, where I_n is a $n \times n$ identity matrix, the total power as computed by Eq. (2-6) can also be defined by taking the squared two norm which is then given by

$$J(C(z), G(z,\theta), H(z,\theta)) = \left|\left|(I + G(z,\theta)C(z))^{-1}H(z,\theta)\right|\right|_2^2 \sigma_e^2. \quad (2\text{-}7)$$

It needs to be established for which performance level a system is still able to produce products with an acceptable quality. Therefore, a threshold value β will be used and it will be verified whether the performance measure of Eq. (2-7) of the closed-loop system violates the threshold value. The threshold value β is chosen in such a way that it accounts for the maximum allowable performance in the closed-loop system for which the product quality is acceptable. If the performance of the closed-loop is found to be $J(C(z), G(z,\theta), H(z,\theta)) < \beta$, with this system an acceptable quality level will be achieved and if the performance level is equal or larger than β a performance deterioration is measured.

2-2-2 Performance Monitoring

The performance measure as given by the expression in Eq. (2-7) computes the total power of the difference of $\underline{y}(t) - \underline{r}_1(t)$ of the closed-loop system and will be used as a measure for the diagnosis methodology. However, over time the power of the closed-loop system can increase due to a change in the process dynamics $G_0(z)$ or a change in the disturbance characteristics $H_0(z)$. For that reason the performance needs to be monitored continuously. Performance monitoring will be used to detect performance deteriorations on-line. To be able to detect a performance degradation a performance measure will be used which is chosen to be an estimate of the power of the closed-loop system as given by Eq. (2-7). Information of the error between the measured outputs $\underline{y}(t)$ and set-points $\underline{r}_1(t)$ are used. The outputs will be measured over a time window from a time in the past k_{past} until a time k_{now}. By sampling with a sample time T_s the time window contains N_{win} data points. The measured data points can be used to compute the power of the error between the measured outputs and the chosen set-points. An often used classical performance measure as explained in Refs. [1, 3] to monitor the real-time performance, is given by

$$\hat{J}(k) = \frac{1}{N_{win}} \sum_{j=1}^{n} \sum_{i=k-N_{win}}^{k} (y_j(i) - r_{1,j}(i))^T \left(y_j(i) - \underline{r}_{1,j}(i) \right) \qquad \text{for } k \in \mathcal{N} \tag{2-8}$$

Here, $y_j(i) = \underline{y}(i)$ represents the measured discrete-time output signals and $r_{1,j}(i) = \underline{r}_1(i)$ the fixed set-point signals. There will be a difference between the measured outputs and set-points due to disturbances and white-noise contained in the system. It is also possible that there exists an off-set between the measured outputs w.r.t. the set-points. However, this thesis discusses closed-loop systems which includes an integrating action in the controller. The integrating action ensures that the off-set decreases to zero. Changes in the plant dynamics $G_0(z)$ or changes in the noise characteristics $H_0(z)$ will affect the performance measure in a negative way. The performance could deteriorate due to an increase in variance of the measured outputs $\underline{y}(i)$. If the variance increases, the difference between $\underline{y}(i)$ and $\underline{r}_1(i)$ increases which implies that the cost $\hat{J}(k)$ will also increase.

In case of a system in operation the performance can deteriorate over time. It needs to be defined at what moment a performance deterioration should be measured with the performance measure given by Eq. (2-8). In a similar way as applying a maximum bound on Eq. (2-7), a threshold value β is applied on the performance measure as given by Eq. (2-8). Despite the fact the performance measured by Eq. (2-8) is an estimate of Eq. (2-7) it is assumed that the estimate is close enough to make use of the same threshold value β. Thus for nominal performance it is found that $\hat{J}(k) < \beta$.

As discussed, the cost $\hat{J}(k)$ is measured for a certain discrete time window. It is of importance to choose this window correctly. A trade-off is made between two issues to find a desirable window size. The trade-off comprises the choice of the sensitivity of the performance measure (by considering the size of the window measured between k_{past} until k_{now}) and the accuracy of the detected performance deterioration. When taking a window which is too small the performance measure becomes very sensitive. This implies that the cost function may detect a performance drop which in reality is only a small fluctuation in the output compositions. The measured performance deterioration in this case could lead to a wrong conclusion which should be avoided. On the other hand, when taking the window too large

the opposite will happen. For a long period of time no deviations are detected, while in reality the performance is already deteriorated. Detecting the performance deterioration late implies that costs will increase for a longer period of time. Therefore, it is of importance to choose a window which is not sensitive for small composition fluctuations but sensitive enough to detect a real performance deterioration as quickly as possible.

2-3 Performance Diagnosis

As discussed earlier we need to distinguish between multiple causes which induce a performance deterioration. This is required because each cause has its own solution strategy to bring the deteriorated performance back to its nominal values. In the next sections it is explained what changes will be considered which cause the performance to deteriorate and how the performance diagnosis methodology is able to distinguish between the considered control relevant changes.

2-3-1 Control-Relevant System Changes

This thesis considers two causes which induce a performance deterioration and are discussed by the following two cases:

1) Change in disturbance characteristics.
   In the first case, the performance deteriorates due to changes in disturbance characteristics $H_0(z)$ as shown in Fig. 2-3 (left). Note that there could occur slight changes in the true process dynamics $G_0(z)$. However, these small changes in $G_0(z)$ alone do not cause the performance to deteriorate.

2) Change in control-relevant plant dynamics.
   In the second case, the performance deteriorates due to changes in plant dynamics $G_0(z)$ as presented in Fig. 2-3 (right). In this case the disturbance characteristics could also change slightly but does not induce a performance drop.

Note that in reality a change in disturbance characteristics occurs more often than a change in control-relevant plant dynamics. This possibly needs to be taken into account when making a decision. In the introductory chapter it was mentioned that each cause has its own solution strategy to restore nominal performance and for that reason a distinction needs to be made between both causes. The next section elaborates on that issue.

2-3-2 Hypothesis Testing and Decision Rule

Hypothesis testing will be used in the performance diagnosis to discriminate between the two causes. The hypotheses which will be adopted are based on the following definition.
Definition 1: Given the original disturbance characteristics $H(z, \theta_{com})$ and existing controller $C(z)$ in the closed-loop system, the domain $\mathcal{D}_{adm}$ represents the set of all transfer

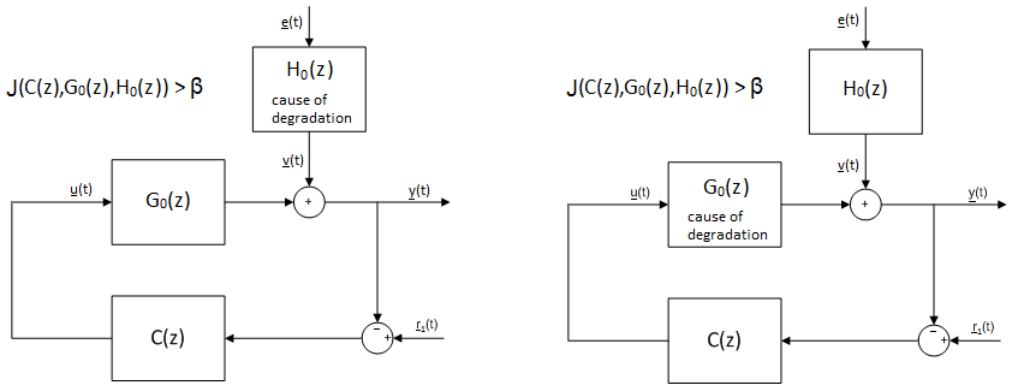

Figure 2-3: Left: the closed-loop model represents the case that a performance drop occurs due to changes in noise characteristics. The performance could change slightly due to changes in plant dynamics but does not deteriorate due to this possibly slight change. Right: the closed-loop model represents the case that a performance drop occurs due to changes in plant dynamics. The noise characteristics could also induce slight changes in performance, however, it does not induce the performance to deteriorate.

functions $G(z,\theta)$ which are stabilized by controller $C(z)$ and are able to achieve nominal performance, i.e., $J(C(z),G(z,\theta),H(z,\theta_{com})) < \beta$ (given by Eq. (2-7)). This set is given by

$$\mathcal{D}_{adm} = \{G(z,\theta)|J(C(z),G(z,\theta),H(z,\theta_{com}) < \beta\} \qquad \text{with } [C(z)\ G(z,\theta)] \text{ stable.} \tag{2-9}$$

These requirements are met at the commissioning stage, i.e., $G_0(z) \in \mathcal{D}_{adm}$ at commissioning.

To be able to distinguish between both causes and show the importance of set $\mathcal{D}_{adm}$ with regard to the hypotheses which we will adopt, the performance will be analysed for two closed-loop systems. The first closed-loop system is a fictive system where the true system $G_0(z)$ is considered which operates under the original disturbance characteristics $H(z,\theta_{com})$. The second closed-loop system which we will consider is the real system with the true plant model $G_0(z)$ and true disturbance characteristics $H_0(z)$. The fictive closed-loop system and real closed-loop system are denoted by, respectively:

$$1: \{C(z),G_0(z),H(z,\theta_{com})\} \qquad 2: \{C(z),G_0(z),H_0(z)\} \tag{2-10}$$

If for both closed-loop systems the performance is smaller than β it implies that there is no performance deterioration. Then consider that in the fictive closed-loop system the performance $J(C(z),G_0(z),H(z,\theta_{com})) < \beta$ and the performance in the real closed-loop system will be $J(C(z),G_0(z),H_0(z)) \geq \beta$. From the fictive closed-loop system it immediately implies that $G_0(z)$ did not deteriorated the performance. The performance deterioration is caused by changes in the disturbance characteristics $H_0(z)$ as is found from the true closed-loop system. The true system is located in set $\mathcal{D}_{adm}$, as shown in Fig. 2-4 (left), because it achieves nominal performance under the original disturbance characteristics $H(z,\theta_{com})$. If in both closed-loop systems the performance is equal or larger than β it implies that the performance deterioration is caused by changes in $G_0(z)$. In this case the true system $G_0(z) \notin \mathcal{D}_{adm}$ as shown in Fig. 2-4 (right), because the performance of the closed-loop system is deteriorated even under the original disturbance characteristics $H(z,\theta_{com})$.

Hypothesis testing can be used to verify that the true system $G_0(z)$ is located in-or outside set $\mathcal{D}_{adm}$. Both situations are depicted in Fig. 2-4 and the following hypotheses are

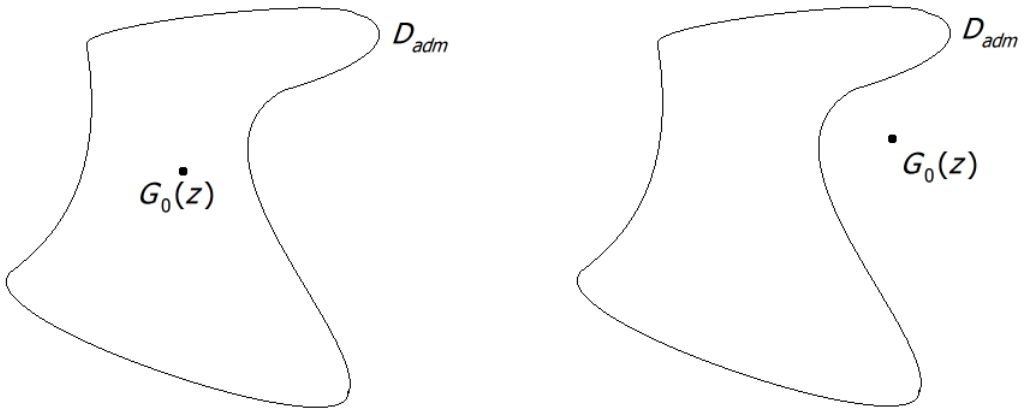

Figure 2-4: Left: All plant models inside set $\mathcal{D}_{adm}$ gives good performance. This is also the case for the true plant model $G_0(z)$ which lies inside set $\mathcal{D}_{adm}$. Right: the true system $G_0(z)$ lies outside set $\mathcal{D}_{adm}$ and will lead to a deteriorated performance

adopted:

$$\begin{aligned} \mathcal{H}_0 &: G_0(z) \in \mathcal{D}_{adm} \quad \text{(change in disturbance characteristics)} \\ \mathcal{H}_1 &: G_0(z) \notin \mathcal{D}_{adm} \quad \text{(change in plant dynamics)} \end{aligned} \tag{2-11}$$

The hypotheses are based on the true system dynamics $G_0(z)$ which is normally unknown. Therefore, it is not directly possible to make a clear distinction between the two causes and opt for one of the two adopted hypotheses as given in (2-11). To be able to make a distinction between the two causes, and find out whether the true system $G_0(z)$ is in or outside the set $\mathcal{D}_{adm}$ we will make use of an estimation of the true system dynamics and verify whether this model is contained in the set $\mathcal{D}_{adm}$.

A short closed-loop identification experiment is carried out on the true system as depicted in Fig. 2-1 (start fault diagnosis). A closed-loop identification experiment is performed, by making use of the direct closed-loop method (see Refs. [10, 11]), to estimate a plant model $G(z,\hat{\theta}_N)$ which describes the possibly changed process dynamics. The true system $G_0(z)$ is excited by the signals $\underline{r}_{ex}(t)$ as shown in Fig. 2-5 for $t = 0...N-1$ and data set $Z^N = \{\underline{u}(t), \underline{y}(t) | t = 0...N-1\}$ is collected. We assume that the true system dynamics can be described by a full order model structure $\mathcal{M} = \{G(z,\theta), H(z,\theta)\}$. Furthermore, there exists only one possible parameter vector θ_0 for which the full order model structure is able to describe the true system dynamics.
To estimate models in the set $\mathcal{M}$, the predictor and the prediction error are considered respectively:

$$\underline{\hat{y}}(t) = H(z,\theta)^{-1}G(z,\theta)\underline{u}(t) + \left(I - H(z,\theta)^{-1}\right)y(t), \tag{2-12}$$

$$\underline{\epsilon}(t,\theta) = \underline{y}(t) - \underline{\hat{y}}(t) = H(z,\theta)^{-1}(\underline{y}(t) - G(z,\theta)\underline{u}(t)). \tag{2-13}$$

Here, $\underline{y}(t)$ is given by Eq. (2-2) and $\underline{u}(t)$ is given by Eq. (2-3). The parameters which need to be estimated are contained in parameter vector $\hat{\theta}_N$ and can be computed by minimizing the prediction error as given by the criterion:

$$\hat{\theta}_N = \arg\min_{\theta} V_N(\theta, Z^N) = \arg\min_{\theta} \frac{1}{N}\sum_{t=0}^{N-1} \underline{\epsilon}(t,\theta)^T \underline{\epsilon}(t,\theta). \tag{2-14}$$

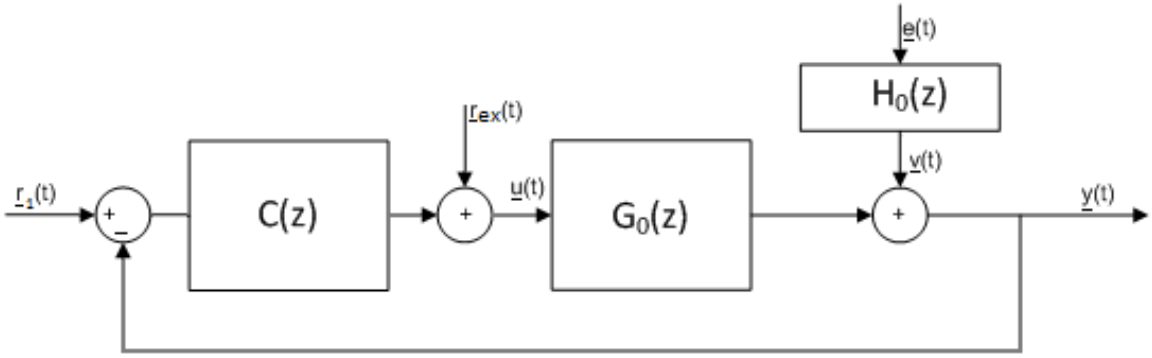

Figure 2-5: Closed-loop system with the controller given by $C(z)$, the true system dynamics by $G_0(z)$ and the noise characteristics by $H_0(z)$. The excitation signal is $r_{ex}(t)$, reference signal $r(t)$, input signal $u(t)$, output signal $y(t)$ and white noise signal $e(t)$ with variance Σ_e.

The identified parameter vector $\hat{\theta}_N$ is asymptotically normally distributed around the true parameter vector θ_0 provided that N is sufficiently large, i.e., $\hat{\theta}_N \sim \mathcal{N}(\theta_0, P_\theta)$. Here P_θ is a strictly positive definite variance matrix and is according to Ref. [12] for the MIMO case given by

$$P_\theta^{-1} = \mathbb{E}\Upsilon(t,\theta_0)\Sigma_e^{-1}\Upsilon^T(t,\theta_0). \tag{2-15}$$

Here, Σ_e^{-1} represents the covariance of $\underline{e}(t)$ and is given in section 2-2. Furthermore, the columns of matrix $\Upsilon(t,\theta_0)$ are represented by $v_i^T(t,\theta_0) = \frac{d\underline{\hat{y}}(t,\theta)}{d\theta}$ $(i = 1, ..., m)$. For further derivation see appendix A-5 and Ref. [12].

As already mentioned the true system dynamics $G_0(z)$ are unknown and it is not possible to choose for a hypothesis given by (2-11). Therefore, the decision will be based on the identified model $G(z,\hat{\theta}_N)$ and verify whether this model is contained in set $\mathcal{D}_{adm}$. The decision rule which is used to choose for one of the hypotheses is given as

$$\begin{aligned} G(z,\hat{\theta}_N) &\in \mathcal{D}_{adm} \rightarrow \mathcal{H}_0 && \text{(change in disturbance characteristics)} \\ G(z,\hat{\theta}_N) &\notin \mathcal{D}_{adm} \rightarrow \mathcal{H}_1 && \text{(change in plant dynamics)} \end{aligned} \tag{2-16}$$

To verify whether the estimated model is located in or outside $\mathcal{D}_{adm}$, as given in the decision rule (2-16), the performance of the closed-loop system $\left[C(z), G(z,\hat{\theta}_N), H(z,\hat{\theta}_N)\right]$ will be analysed. This is shown in Fig. 2-1 by the off-line fault diagnosis. Due to the fact that the estimated plant model, the original noise characteristics and the controller are all known it is rather easy to compute the performance $J(C(z), G(z,\hat{\theta}_N), H(z,\theta_{com}))$ as given by Eq. (2-7). It will be verified whether the estimated model is in or outside the set $\mathcal{D}_{adm}$ as defined by the decision rule given in (2-16).

Keep in mind that the decision, made with the decision rule (2-16), is based on the estimated model $G(z,\hat{\theta}_N)$. It is possible that with the estimated model $G(z,\hat{\theta}_N)$ a different performance is measured with respect to the true system $G_0(z)$, i.e., $J(C(z), G(z,\hat{\theta}_N), H(z,\hat{\theta}_N)) > \beta$ whereas $J(C(z), G_0(z), H_0(z)) \geq \beta$. For that reason it is possible that a wrong hypothesis is accepted to be true. In Fig. 2-6 two erroneous decisions are shown. On the left it can be seen that hypothesis $\mathcal{H}_0$ is accepted to be true because $G(z,\hat{\theta}_N) \in \mathcal{D}_{adm}$. However, the true system $G_0(z)$ is outside the set $\mathcal{D}_{adm}$. This implies that a performance deterioration

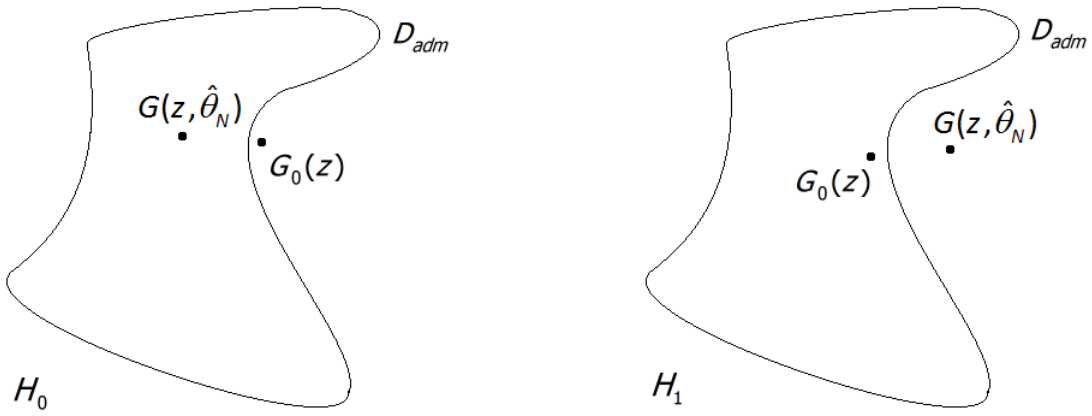

Figure 2-6: Erroneous decisions can be made. Left: the estimated model is located in set $\mathcal{D}_{adm}$ whereas the true system lies outside this set. Right: the estimated model is located outside set $\mathcal{D}_{adm}$ whereas the true system lies inside this set.

is caused due to a change in plant dynamics, while the cause is chosen to be a change in disturbance characteristics. On the right it is shown that the identified model $G(z,\hat{\theta}_N)$ is located outside set $\mathcal{D}_{adm}$ because it does not achieve nominal performance under the original noise characteristics and the cause is chosen to be a plant change. Whereas, in this situation the true system is located in set $\mathcal{D}_{adm}$ and the performance is actually deteriorated due to a change in disturbance characteristics.
It is shown that various wrong decisions can be made and therefore it is of importance to assess the confidence of opting for the correct hypothesis. The confidence will be assessed by performing a simulation case study. Within the next section the closed-loop performance analysis will be expanded and a method will be explained which possibly decrease the number of erroneous decisions.

2-3-3 Increase Confidence and Introduction of an Alternative Decision Rule

In the previous section it was discussed that after a performance deterioration is detected, first, an identification experiment is carried out on the true system. Secondly, by analysing the performance of the closed-loop system $\left\{C(z), G(z,\hat{\theta}_N), H(z,\theta_{com})\right\}$ we are able to verify whether the estimated model $G(z,\hat{\theta}_N)$ is located in or out the set $\mathcal{D}_{adm}$. However, this is not sufficient due to the erroneous situations which could occur. Therefore, the diagnosis will be expanded and we introduce an alternative decision rule and a change in decision rule (2-16).

To increase the confidence it is possible to constructing a confidence region as discusses in Mesbah et al. [2]. A confidence region can be build by considering a normal distribution as given by $\hat{\theta}_N \sim \mathcal{N}(\theta_0, P_\theta)$. The true parameter set θ_0 is contained in the uncertainty ellipsoid for a pre-specified probability level $Pr(\chi^2(k) < \mathcal{X}) = \alpha$. As discussed in Ref. [13] the uncertainty ellipsoid is given by

$$U = \{\theta | (\theta - \hat{\theta}_N)^T P_\theta^{-1} (\theta - \hat{\theta}_N) < \mathcal{X}\}. \tag{2-17}$$

Here $\mathcal{X} \in \mathbb{R}$ and $\chi^2(k)$ is a chi-square distribution with k degrees of freedom, where k represents the amount of parameters contained in the parameter set $\hat{\theta}_N$. The confidence

region with uncertainty ellipsoid is given by

$$\mathfrak{D}(\hat{\theta}_N, P_\theta) = \{G(z,\theta)|\theta \in U\}. \tag{2-18}$$

As discussed in Mesbah et al. [2] an uncertainty ellipsoid is created with a probability level of $\alpha = 95\%$. This implies that the true system is located inside the constructed ellipsoid $\mathfrak{D}(\hat{\theta}_N, P_\theta)$ with probability level α. If the whole ellipsoid is inside $\mathcal{D}_{adm}$, for a probability of at least 95% it can be adopted that the true system $G_0(z)$ is located inside $\mathcal{D}_{adm}$. However, in Ref. [2] it was mentioned that if the ellipsoid is not totally located in or outside the set $\mathcal{D}_{adm}$ the likelihood measure which is used becomes misleading. To be able to create any indication of confidence of the choice which will be made, even in the situation that the estimated model is close to the edge of the set $\mathcal{D}_{adm}$, a heuristic method will be applied. This method is possibly less confident than with a confidence region, however this method can be used in any situation even when $G(z,\hat{\theta}_N)$ is on the edge of $\mathcal{D}_{adm}$. Instead of considering a confidence region and verifying the worst and best case performance to obtain an estimation of the confidence of opting for the correct hypothesis, our decision will be based on replacing the confidence region $\mathfrak{D}(\hat{\theta}_N, P_\theta)$ by n discrete parameter vectors θ. The discrete parameters can be constructed by generating n values $\Delta\theta$ by making use of a normal distribution with mean zero and variance P_θ (from the estimated parameter vector). The realizations of $\Delta\theta$ can be generated by

$$\Delta\theta^{(i)} \sim \mathcal{N}(0, P_\theta) \qquad (i = 1...n). \tag{2-19}$$

The parameter vectors are then constructed by

$$\theta^{(i)} = \hat{\theta}_N + \Delta\theta^{(i)} \qquad (i = 1...n). \tag{2-20}$$

The constructed models $G(z,\theta^{(i)})$ are located around the estimated model $G(z,\hat{\theta}_N)$. It needs to be verified how likely it is of choosing a hypothesis correctly with the discrete method. This can be achieved by analysing/computing the performance of the closed-loop system $\left\{C(z), G(z,\theta^{(i)}), H(z,\theta_{com})\right\}$ for each constructed parameter vector as given in Eq. (2-20) and to verify in this way whether the plant model $G(z,\theta^{(i)})$ is located in or outside the set $\mathcal{D}_{adm}$. The percentage of models that are outside $\mathcal{D}_{adm}$ is computed by

$$\hat{Fr}_{out} = \frac{\text{Number of realizations when } G(z,\theta^{(i)}) \notin \mathcal{D}_{adm}}{n} \cdot 100\%. \tag{2-21}$$

Models inside the set $\mathcal{D}_{adm}$ is computed by the percentage $\hat{Fr}_{in} = 100 - \hat{Fr}_{out}$.
We want to investigate how likely it will be that the true system $G_0(z)$ is in or out the set $\mathcal{D}_{adm}$. To be able to increase the confidence for the choice which will be made, consider a threshold ν which represents the percentage of models that should at least be outside $\mathcal{D}_{adm}$ to opt for hypothesis $\mathcal{H}_1$. The threshold ν is a constant value somewhere between 0 and 100 which, in a simulation case study, is optimized to find the largest confidence of opting a hypothesis correctly. For a percentage $\hat{Fr}_{out} < \nu\%$, hypothesis $\mathcal{H}_0$ is more likely to be the correct hypothesis and is thus chosen. When percentage $\hat{Fr}_{out}$ is larger than $\nu\%$, it is more likely that the true system is outside set $\mathcal{D}_{adm}$. Therefore, when percentage $\hat{Fr}_{out}$ is large ($\geq \nu\%$) hypothesis $\mathcal{H}_1$ is chosen to be true. Summarizing the above the alternative hypothesis will become:

Alternative decision rule:

$$\begin{cases} \hat{Fr}_{out} = [0,\ \nu)\% \rightarrow \text{pick } \mathcal{H}_0 \\ \hat{Fr}_{out} = [\nu,\ 100]\% \rightarrow \text{pick } \mathcal{H}_1 \end{cases} \tag{2-22}$$

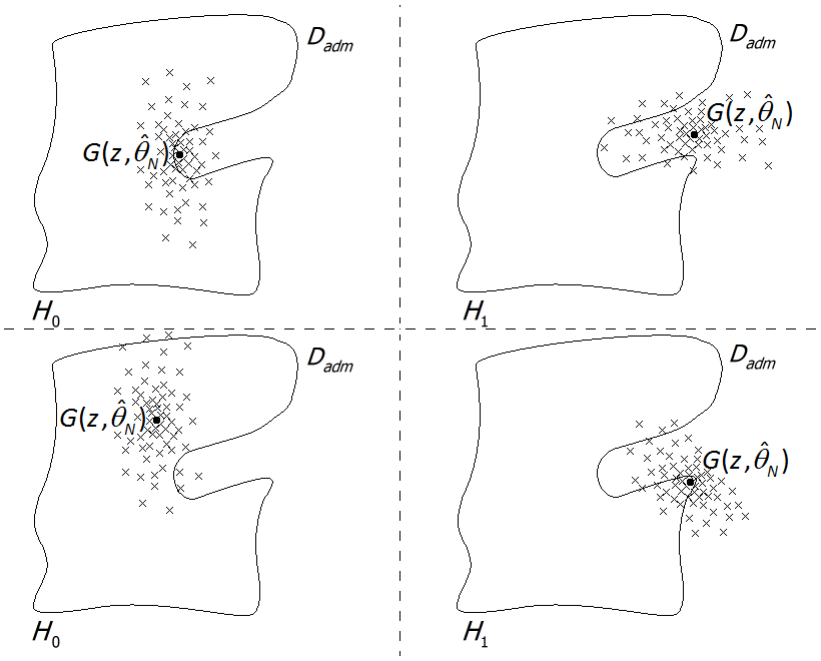

Figure 2-7: Upper left: The estimated $G(z,\hat{\theta}_N) \notin \mathcal{D}_{adm}$ and it is found that $\hat{Fr}_{out} < \nu$. Then hypothesis $\mathcal{H}_0$ is chosen. Upper right: The estimated $G(z,\hat{\theta}_N) \notin \mathcal{D}_{adm}$ and it is found that $\hat{Fr}_{out} \geq \nu$. Therefore, hypothesis $\mathcal{H}_1$ is chosen. Lower left: The estimated model is found to be $G(z,\hat{\theta}_N) \in \mathcal{D}_{adm}$ and $\hat{Fr}_{out} < \nu$, thus hypothesis $\mathcal{H}_0$ is chosen. Lower Right: The estimated model is found to be $G(z,\hat{\theta}_N) \in \mathcal{D}_{adm}$ and $\hat{Fr}_{out} \geq \nu$, thus hypothesis $\mathcal{H}_1$ is chosen.

An example is shown in Fig. 2-7 for all cases which can occur when the decision is based on (2-22). In the upper left it is shown that most of the models $G(z,\theta^{(i)})$ are located inside set $\mathcal{D}_{adm}$ ($\hat{Fr}_{out} < \nu\%$) and therefore hypothesis $\mathcal{H}_0$ is chosen (even when $G(z,\hat{\theta}_N) \notin \mathcal{D}_{adm}$). In the upper right, most of the models around the estimated model are located outside set $\mathcal{D}_{adm}$ ($\hat{Fr}_{out} \geq \nu\%$) and based on this observation hypothesis $\mathcal{H}_1$ is assumed to be true. In the lower left figure it is obviously found that $\hat{Fr}_{out} < \nu\%$ and hypothesis $\mathcal{H}_0$ is chosen. Finally, in the lower right figure it can be seen that most of the models are outside the set $\mathcal{D}_{adm}$ and thus hypothesis $\mathcal{H}_1$ is chosen (even when $G(z,\hat{\theta}_N) \in \mathcal{D}_{adm}$).

As earlier mentioned in section 2-3-1, due to the fact that in reality a change in disturbance characteristics appears much more often it is preferred to opt for a disturbance change. Furthermore, it was also mentioned that there is a large difference in economic costs with respect to the cause of a performance deterioration and the recovery of the systems performance. When opting for the wrong hypothesis it will be less costly when opting for hypothesis $\mathcal{H}_0$ while $\mathcal{H}_1$ is true instead of opting for hypothesis $\mathcal{H}_1$ while $\mathcal{H}_0$ is true. This increases the need of creating a preference for a change in disturbance characteristics even more. The latter can be taken into account by adjusting the decision rule of (2-16) and incorporating (2-22). it will be implemented as follows. We choose for hypothesis $\mathcal{H}_0$ when the estimated model $G(z,\hat{\theta}_N)$ is located in $\mathcal{D}_{adm}$. When the estimated model $G(z,\hat{\theta}_N)$ is not located in $\mathcal{D}_{adm}$ the decision is based on the percentage of models which are outside $\mathcal{D}_{adm}$ as computed by Eq. (2-21) and given by the decision from (2-22). The changed decision rule to make a decision between hypothesis $\mathcal{H}_0$ or $\mathcal{H}_1$ is given by

Changed decision rule with preference for $\mathcal{H}_0$:

$$\begin{aligned} G(z,\hat{\theta}_N) \in \mathcal{D}_{adm} & \quad \rightarrow \text{pick } \mathcal{H}_0 \\ G(z,\hat{\theta}_N) \notin \mathcal{D}_{adm} & \begin{cases} \hat{Fr}_{out} < \nu\% & \rightarrow \text{pick } \mathcal{H}_0 \\ \hat{Fr}_{out} \geq \nu\% & \rightarrow \text{pick } \mathcal{H}_1 \end{cases} \end{aligned} \tag{2-23}$$

The decision rule which is based on the estimated model only as given in (2-16) is different from the decision rule given by (2-23). The decision rule as described in (2-23) will lead to a preference for hypothesis $\mathcal{H}_0$, which implies it is more likely to opt for hypothesis $\mathcal{H}_0$ while $\mathcal{H}_1$ is true. On the other hand, it becomes less likely of choosing hypothesis $\mathcal{H}_1$ while $\mathcal{H}_0$ is true which is a preferred situation to minimize economic costs. With this decision rule it will be more likely to have the situations as shown in Fig. 2-7 (the upper left, upper right and the lower left figure). The case shown in the lower right figure is with decision rule (2-23) excluded to create the preference for hypothesis $\mathcal{H}_0$.

2-3-4 Recovery of the System Performance

Finally, it is of importance to know what needs to be done after a hypothesis is chosen. The last and most obvious question in the diagnosis therefore will be: **what should be done when a decision is made and one of the hypotheses is chosen?**

We have discussed the two situations where a change in disturbance characteristics and a change in control-relevant plant dynamics could cause the performance to deteriorate. Throughout the previous sections the importance of why a distinction needs to be made is discussed. As shown in Fig. 2-1 the last step is to recover nominal performance within the system.

In the first case of section 2-3-1, a (temporary) change in disturbance characteristics is considered. If the change is only temporary and shorter than a certain amount of time nothing should be done. However, if it seems not to be temporary it is possible to re-tune the controller.

In the second situation when it is found that the plant dynamics have changed, a full re-identification experiment needs to be performed. Within this experiment the changed plant dynamics are identified and new models are estimated. For model-based control systems possibly re-tuning of the controller is necessary. After estimation of the models and/or re-tuning of the controller it should be possible to operate at nominal performance again.

To summarize the methodologies; when a performance monitoring method is applied to a system we are able measure the performance on-line and detect a performance deterioration automatically. Secondly, a diagnosis method needs to be applied. With the diagnosis method it is automatically decided what the most likely origin of a performance deterioration will be. Finally, when a hypothesis is assumed to be true a decision can be made what should be done to resolve the problem. Detecting a performance deterioration, perform a diagnosis, opt for a cause and restore the systems performance needs to be performed as quickly as possible to achieve nominal performance again and at the same moment to minimize the costs.

The described methodologies are tested in a case study on a multiple-input multiple-output system. The MIMO system used is a binary distillation column. Within the case study, simulations are performed which mimic the dynamic behaviour of a binary distillation

column. First, the binary distillation column is discussed in more detail which is done in the next chapter, and secondly, results of the case study are treated.

Chapter 3

A Binary Distillation Column

3-1 Introduction

This chapter focusses on the system which will be used to test the methodologies of the previous chapter. This thesis solely focus on a binary distillation column which is a MIMO system. In section 3-2 a more detailed explanation is given about the distillation column and its parameters. Furthermore, the separation process is described in more detail. Section 3-2-2, shortly explains the system variables in terms of control and the control configuration and simplification of the system. To mimic the behaviour of a binary distillation column a simulation model is used. In section 3-3 a simulation model is elaborated which describes the true system dynamics. Also, the controller is given and both the plant model and controller are discretized. The way of modelling a change in process dynamics and disturbance characteristics is explained in section 3-3-3. Finally, in a simulator analysis it is explained whether the designed discrete controller is able to cope with the disturbances in the system and it is investigated whether the closed-loop behaviour is intuitively correct by making comparisons with models found in literature.

3-2 Processes in the Binary Distillation Column

A binary distillation column consist of a condenser, a reflux drum, a reboiler and the large distillation tower as shown in Fig. 3-1 which are all interconnected in a certain way.
Distillation is a process which is often used in industry. In general binary means that the mixture/feed that enters the distillation column consists of two components. This is called the binary feed, indicated by F, which can be separated into two individual components; a "heavy" and a "light" component in terms of molecular weight. The feed flow has a composition z_F which is given as the more volatile component, i.e., the component which has the lowest molecular weight and thus the lowest boiling point. Note that the boiling point of both components can be close to each other. In this case the evaporation rate of both compositions will be almost the same. Even in this case it is possible to separate the mixture into two

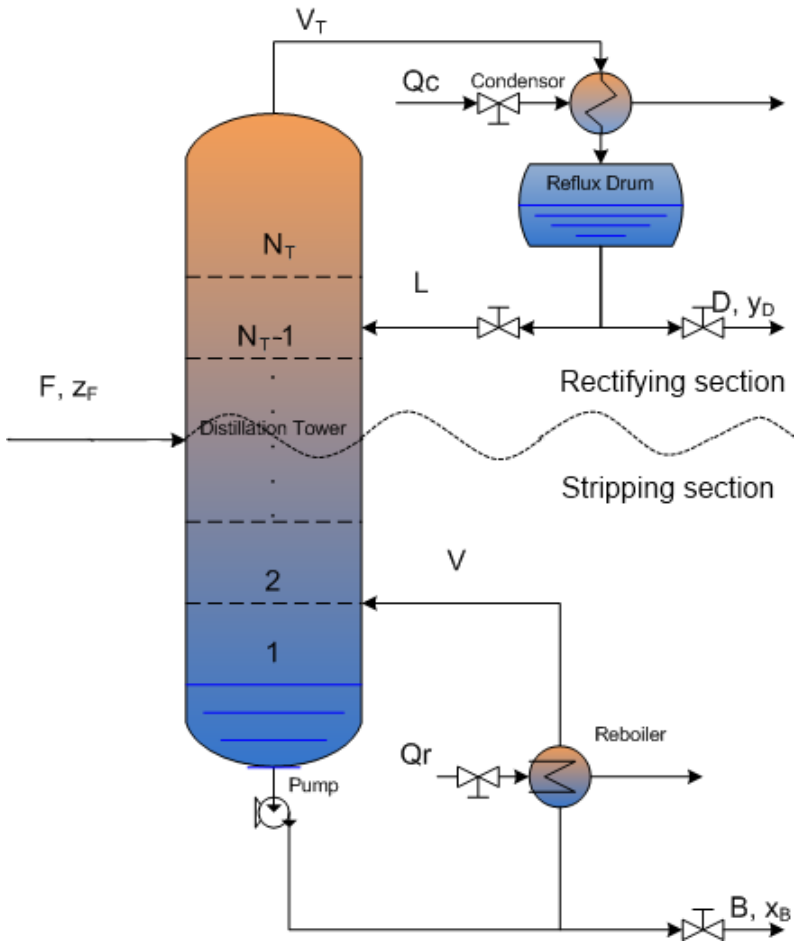

Figure 3-1: Binary distillation column with reflux and reboil flows L and V.

components, yet it is more difficult. The feed mixture is separated into two different products called the bottom flow B and the distillate flow D. Here, the bottom flow represents the high molecular weight or less volatile product with impurity composition x_B and the distillate flow represents the low molecular weight or more volatile product with purity composition y_D. With two components a relative volatility can be computed which is defined as:

$$\kappa = \frac{(k_i/l_i)}{(k_j/l_j)} \tag{3-1}$$

Here, k_i represents the more volatile component and k_j the less volatile component in the vapour phase and l_i the more volatile component and l_j the less volatile component in the liquid phase at a vapour-liquid equilibrium. Furthermore, it is shown that the distillation column contains trays which are represented by the numbers $1...N_T$, as shown in Fig. 3-1. A tray can be seen as a shallow flat receptacle with a raised edge to keep the liquid mixture in for short amount of time, as presented by Fig. 3-2. In this figure the liquid flow and vapour flow at a tray i are presented by L_i and V_i, respectively.

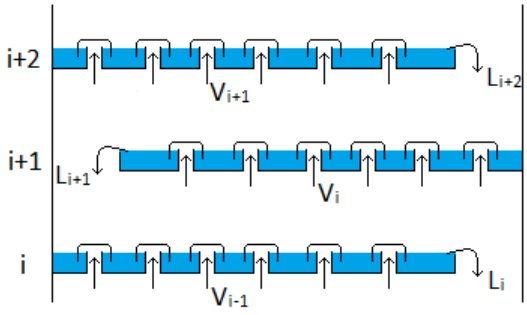

Figure 3-2: Three trays $i, i+1$ and $i+2$ are shown. It can be seen that the liquid flow L_i flows over the edge towards the bottom of the column and the vapour flow V_i rises through the liquid towards the top of the column.

3-2-1 Separation

To be able to separate the two components, a large part of the flow which leaves the bottom of the distillation column is heated. Heating of the liquid flow is done in a reboiler (where Q_r represents the heat input of the reboiler) until the liquid flow vaporizes. Then the vapour flow is fed back to the column as reboil flow V and the vapour gasses will rise through the column. At each tray the vapour flow will exchange heat, i.e., the liquid flow with lower temperature will absorb heat from the vapour flow which has a higher temperature. The heat exchange occurs due to the fact that the vapour flow V flows through the liquid at each tray, as shown in Fig. 3-2. The vapour flow will slightly cool down at each tray and the high molecular weight component contained in the vapour flow will partly condense. From the liquid flow, which slightly increases in temperature, the more volatile component will partly vaporize and rises towards the top. Over time, the liquid mixture contained in the feed flow will be separated into a liquid flow which mostly contains the high molecular weight component (which flows down the tray ladder) and a vapour flow which mostly contains the low volatile component (which will climb the ladder of trays). N_T trays are used to separate the mixture into a liquid and a vapour flow. The number of trays (N_T) which are at least needed to reach a certain purity can be calculated by making use of the McCabe Thiele Method, as discussed in Ref. [14]. At the top of the column the more volatile vapour flow, flows out of the column as indicated by V_T. This vapour flow will be completely condensed by making use of a total condenser by cooling, i.e., absorbing heat from the vapour flow with cooling input Q_c. The liquefied vapour is collected in a reflux drum. From the reflux drum the liquid flow, which mostly contains the low molecular weight component with impurities of the high molecular weight component, partly leaves the system as distillate flow D and is partly fed back to the column as reflux flow indicated by L. As mentioned the top vapour flow V_T is condensed in a condenser and will be collected in a reflux drum once it is liquid. The liquid level in this drum is controlled individually in order to maintain the liquid level to be almost constant. Enrichment of the distillate flow also occurs by increasing the reflux flow L compared to the output flow D. The ratio between these variables is called the reflux ratio, i.e., $r = L/D$. Almost the same is done at the bottom of the column. Here the outgoing flow at the bottom of the column will be separated in the bottom flow B and the reboil flow V. After heating the liquid flow, the vapour reboil flow is fed back to the column. By enlarging the reboil flow V compared to the bottom flow B the output flow B will be more enriched

with the high molecular weight component. The ratio between the reboil flow V and the bottom flow B is given by the reboil ratio $s = V/B$.

3-2-2 Process Variables and Control Configuration

To keep a binary distillation process running safely, certain variables needs to be controlled, i.e., controlled variables (CVs). To adjust the CVs, other variables can be manipulated which are the so-called manipulated variables MVs. Furthermore, there are disturbance variables (DVs) acting on the system (e.g. the feed rate F and feed composition z_F). In the case of the binary distillation column there are five variables which need to be stabilized around a certain set-point and there are five variables which can be manipulated in order to stabilize the system. The controlled variables are $y = (y_D \quad x_B \quad L_D \quad L_B \quad P)^T$. Here, the reflux drum liquid level is given by L_D, the distillation column liquid level is indicated by L_B and the pressure in the column is represented by P. The manipulated variables are $u = (L \quad V \quad D \quad B \quad V_T)^T$. Often the following assumptions are used.

- The pressure P can almost be kept constant by only manipulating the top vapour flow V_T. (There are multiple pressure control techniques as shown in Ref. [15])
- The two liquid levels, one in the reflux drum L_D and one in the distillation column L_B, can be controlled by using two of the four remaining manipulated variables.

By making use of these assumptions, two MVs remain to control two CVs. When for example the liquid levels are controlled by the distillate and bottom flow D and B the CVs and MVs become respectively:

$$CVs : \begin{bmatrix} y_D \\ x_B \end{bmatrix} \qquad MVs : \begin{bmatrix} L \\ V \end{bmatrix}. \tag{3-2}$$

This is called the LV-control configuration and is the configuration that we will consider in this thesis. Note that in literature various control configurations are discussed (see Refs. [16, 17]).

Within this section the necessary basics are presented in terms of what a binary distillation column is and for what reasons it is used. The next section treats a case study in which a simulator will be discussed. The simulator represents a binary distillation column which is used to perform simulations of the behaviour of such a column. Within the simulation model the LV-control configuration is used.

3-3 Simulating a Binary Distillation Column

Throughout this chapter the closed-loop binary distillation column is considered as shown in Fig. 3-3. Here, $G_0(s)$ represents the true continuous time plant dynamics and $C(s)$ represents the continuous time controller. The signals $r_{1,1}(t)$ and $r_{1,2}(t)$ are reference/set-point signals applied to the output compositions, $e_{r1}(t)$ and $e_{r2}(t)$ are the error signals which are fed to the controller, $r_{ex,1}(t)$ and $r_{ex,2}(t)$ are excitation signals used to perform a re-identification experiment when a performance drop is measured and a diagnosis is performed. disturbances are added to the system via the signals $v_1(t)$ and $v_2(t)$. The signals $u_1(t)$ and $u_2(t)$ are the

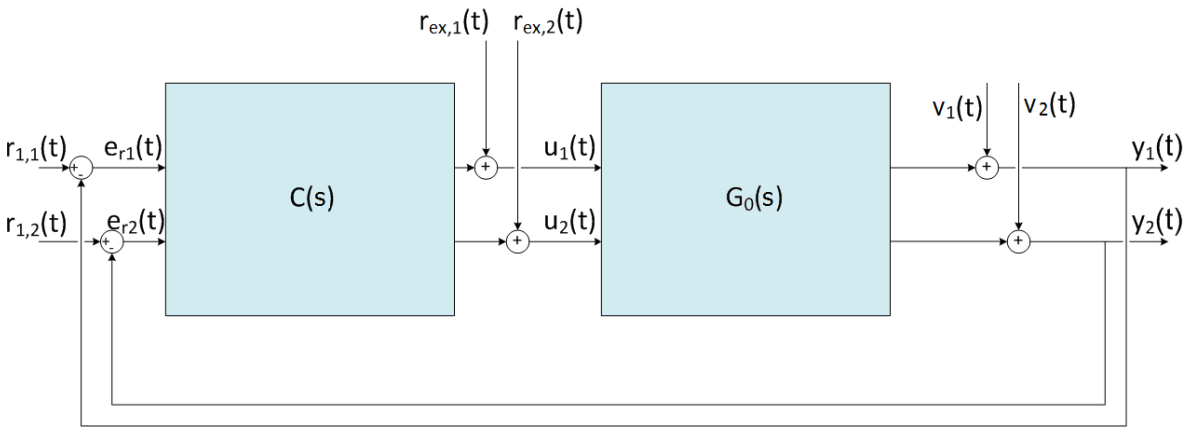

Figure 3-3: Closed-loop configuration of a binary distillation column.

input signals and $y_1(t) = y_D$ and $y_2(t) = x_B$ are the measured output compositions from the distillate and bottom flows.

3-3-1 Distillation Column Model and Controller

To mimic the behaviour of a binary distillation column, we will consider a dynamic model from Skogestad [18]. This model has the following properties: the distillation column contains $N_T = 41$ trays, a total condenser and a reboiler. Assumptions are that there are constant molar flows (for each vaporized mole of liquid also a mole of vapour is condensed), constant relative volatility $\kappa = 1.5$ between the two components and the pressure P is assumed to be constant. The feed enters the column at tray 21, the feed flow is $F = 1\frac{kmol}{min}$ with feed composition of $z_F = 0.5$ mole fraction.

Skogestad described the quite complex non-linear process by a first-order linear model, as discussed in Ref. [18]. The first-order linear model is given by

$$G_0(s) = \frac{1}{1+75s}\begin{bmatrix} 0.878 & -0.864 \\ 1.082 & -1.096 \end{bmatrix}. \tag{3-3}$$

The model given in (3-3) represents a good simplification of the binary distillation column as described above. A non-linear model could be used, however, the simplified model as shown in (3-3) represents the behaviour of a binary distillation column close enough for the purposes needed in this thesis (more of the closed-loop behaviour is shown in the simulator analysis). Emphasis is put on the application of a performance monitor and diagnosis method to a MIMO system.

Within the simulation of the distillation column, the outputs track pre-chosen set-points. The top composition y_D needs to track a purity set-point of $r_{1,1} = 0.95$ and the bottom composition x_B needs to track an impurity set-point of $r_{1,2} = 0.05$. To keep the outputs of the distillation column close around the set-points, the outputs need to be controlled which is done by two PI-controllers.
With the proportional gain and the integrating term the rise time will be decreased and the

steady state offset from both compositions will be eliminated. The controller $C(s)$ is given by two independent PI-controllers. The continuous time controller is given by

$$C(s) = \begin{pmatrix} kp_1 + \frac{ki_1}{s} & 0 \\ 0 & kp_2 + \frac{ki_2}{s} \end{pmatrix} \tag{3-4}$$

The values of both PI-controllers are given in Table 3-1. The values of both controllers could

Table 3-1: Values of both PI-controllers are shown.

	kp	ki
PI 1	1.523	0.142
PI 2	-2.830	-0.206

not be found by a heuristic method as for example the Ziegler-Nichols tuning rules because it is based on SISO systems. Therefore, tuning of both PI-controllers is performed by making use of Matlab/Simulink. Matlab chooses PID gains such that a balance is created between response time and bandwidth (performance) and phase margin (robustness). In the section about the simulator analysis the closed-loop behaviour is discussed. First the plant model and controller will be discretized.

3-3-2 Discretization

When a diagnosis is performed a re-identification experiment will be performed and a discrete model is estimated. Therefore, our simulator will also use a discrete plant model and discrete controller. For discretization a sample time needs to be used. The sample time is more or less related to the (closed-loop) bandwidth of the system which for this system will be close to $\omega_{BW} = 5 \cdot 10^{-3}$ rad/s. According to Ref. [19] to assure that the performance of a digital controller will match the performance of a continuous time controller a sampling time of at least 20 times the (closed-loop) bandwidth needs to be used. With this result we find a sampling rate of $(20 \cdot 5 \cdot 10^{-3})/2\pi = 0.0159$Hz, which gives a sampling time of $T_s = 1/0.0159 \approx 1$ min. The continuous time system and controller are discretized by making use of zero order hold and become:

$$G_0(z) = \frac{1}{z - 0.98} \begin{pmatrix} 1.16 & -1.14 \\ 1.43 & -1.45 \end{pmatrix} 10^{-2} \tag{3-5}$$

$$C(z) = \begin{pmatrix} \frac{kp_1 z + (ki_1 \cdot Ts - kp_1)}{z-1} & 0 \\ 0 & \frac{kp_2 z + (ki_2 \cdot Ts - kp_2)}{z-1} \end{pmatrix} \tag{3-6}$$

In the true system there are always disturbances acting on the controlled outputs. System disturbances occur due to fluctuations of the feed flow or feed flow compositions or due to measurement noise. In the simulator the disturbances and noisy behaviour is mimicked by applying stochastic noise on the measured outputs. In the model of the binary distillation column there are two zero-mean white noise signals $e_1(t)$ and $e_2(t)$ (as shown in Fig. 3-4) which are both chosen to have a variance of $\sigma_e^2 = 3.75e - 5$ and is filtered by a first-order filter. In the nominal situation the disturbances are presented by a quite noisy signal (for a

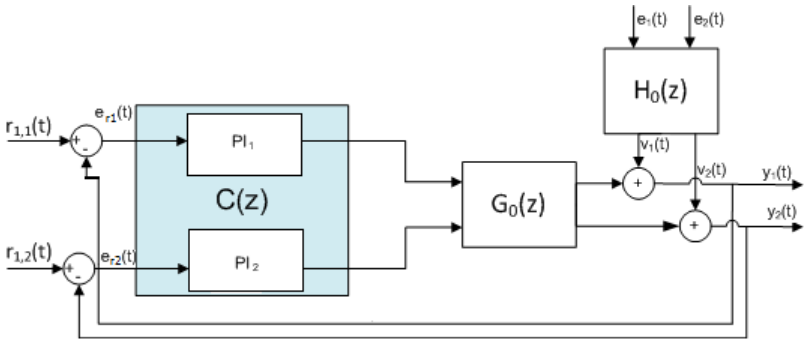

Figure 3-4: The discrete closed-loop system is shown of a distillation column which is stabilized by two PI-controllers ($C(z)$). Here, $G_0(z)$ represents the discrete process dynamics and $H_0(z)$ the discrete noise model.

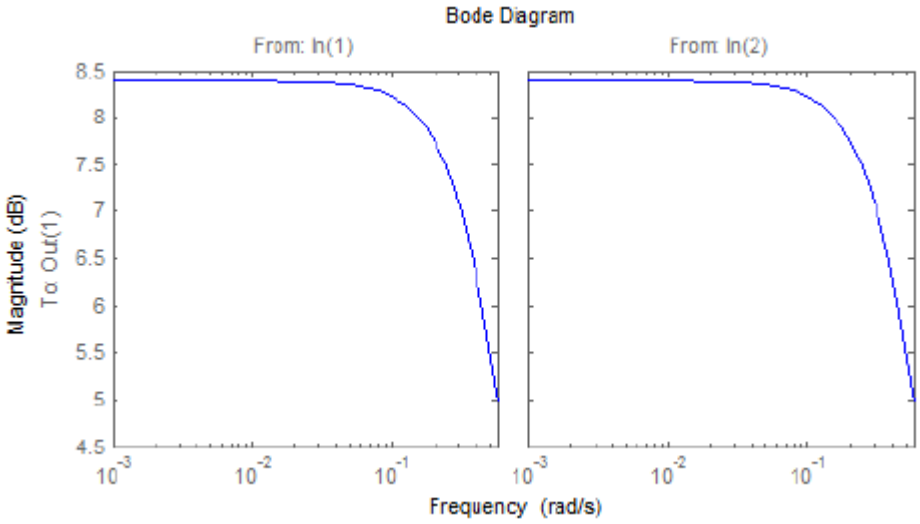

Figure 3-5: The power spectrum for both disturbance signals $v_1(t)$ (left) and $v_2(t)$ (right) are shown in the situation of nominal performance.

disturbance change more high frequencies will be filtered out as discussed later). The discrete noise filter $H_0(z)$, as shown in Fig. 3-4, is given by:

$$H_0(z) = \begin{bmatrix} \frac{z+0.05}{z-0.60} & 0 \\ 0 & \frac{z+0.05}{z-0.60} \end{bmatrix}. \tag{3-7}$$

The variance of the disturbance signals $v_1(t)$ and $v_2(t)$ are of order $\sigma_v^2 = 6.25 \cdot 10^{-5}$ and the spectrum is shown in Fig. 3-5. It can be seen that for frequencies larger than 10^{-1}rad/s the magnitude decreases. All frequencies smaller than 10^{-1}rad/s are taken into account to create lower frequency disturbances combined with a noisy behaviour and are applied by signals $v_1(t)$ and $v_2(t)$. The lower frequency output disturbances could correspond to e.g. changes in feed flow F or in feed composition z_F and measurement noise.

In reality a dynamic change or a change in disturbance characteristics could appear at any time. However, in a simulation environment a dynamic change needs to be applied in

order to let the performance of the system decrease. How the considered changes are modelled is discussed in the next section.

3-3-3 Modelling Changes

The performance monitoring and diagnosis methods as explained in chapter 2 are applied to the simulation model of the binary distillation column. These methods are tested by applying a plant change or disturbance change to the simulator. As mentioned, within the simulation model a change needs to be applied to create a performance deterioration. A change can be modelled for each of the two causes and is discussed in the following sections.

3-3-3-1 Plant Change

Over time the performance of a distillation column deteriorate. To simulate a performance drop caused by a plant change we will rotate the inputs of the system. Rotation of the inputs causes a larger variance on the outputs of the system. In Fig. 3-6 it is shown that there is an extra block ("rotation") added which rotates the inputs of the system. A rotation is applied to the input signals $u_1(t)$ and $u_2(t)$ by making use of rotation angle ψ. The rotation is implemented by making use of a rotation matrix and the rotated input signals are constructed by:

$$\begin{pmatrix} u_{1,rot}(t) \\ u_{2,rot}(t) \end{pmatrix} = \begin{pmatrix} cos(\psi) & -sin(\psi) \\ sin(\psi) & cos(\psi) \end{pmatrix} \begin{pmatrix} u_1(t) \\ u_2(t) \end{pmatrix} = \begin{pmatrix} cos(\psi)u_1(t) - sin(\psi)u_2(t) \\ sin(\psi)u_1(t) + cos(\psi)u_2(t) \end{pmatrix}. \tag{3-8}$$

In the nominal case $\psi = 0$ rad and $u_{i,rot}(t) = u_i(t)$ for $i = 1, 2$. When a plant change is applied to the system, the input signals are rotated by a chosen value of $\psi = -\pi/8$rad. This value is chosen such that the variance of the measured outputs increase more or less by a factor of order two to three. To show the difference between the true system and the dynamics of the rotated system, we will analyse the magnitude at each frequency. Therefore, in Fig. 3-7 the magnitude at each frequency is shown for both models. Here, it can be seen that the magnitude at each frequency from input $u_1(t)$ to both outputs will be increased due to the rotation and from input $u_2(t)$ to both outputs, the magnitude at each frequency will be decreased. Note, that the difference between both models is not large and therefore, in the performance diagnosis the re-identification length or power should be chosen with care to obtain an accurate estimate of the true system dynamics and to make the correct decision.

3-3-3-2 Disturbance Change

It is also possible that a performance drop is caused by variations in disturbance characteristics. A change in disturbance characteristics is actually very easy to implement in a simulation model. The variance of a white-noise signal can be increased and/or a different disturbance model can be implemented. To incorporate a change in disturbance characteristics in our simulation we will change the parameters of the noise transfer matrix, i.e.,

$$H_0(z) = \begin{bmatrix} \frac{z-0.05}{z-0.85} & 0 \\ 0 & \frac{z-0.05}{z-0.85} \end{bmatrix}. \tag{3-9}$$

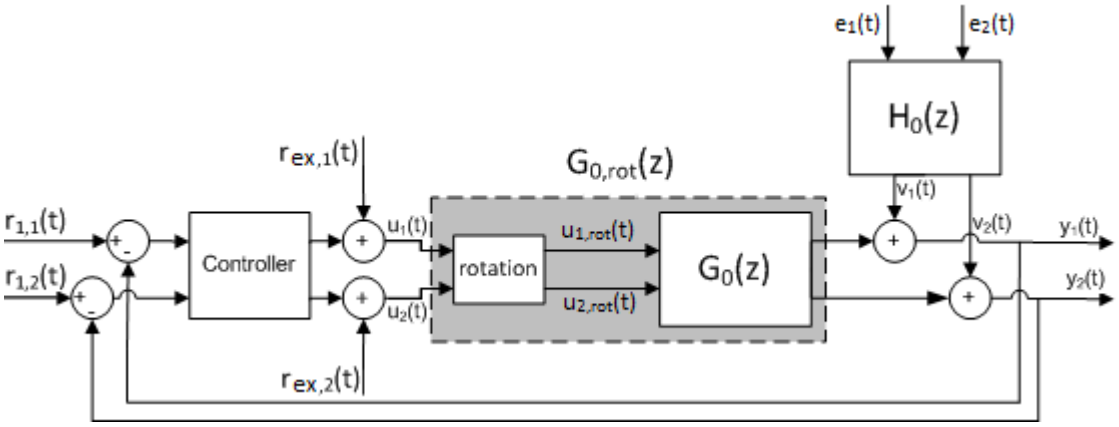

Figure 3-6: Closed-loop system with rotated inputs to the plant $G_0(z)$. The deteriorated true plant is indicated by $G_{0,rot}(z)$.

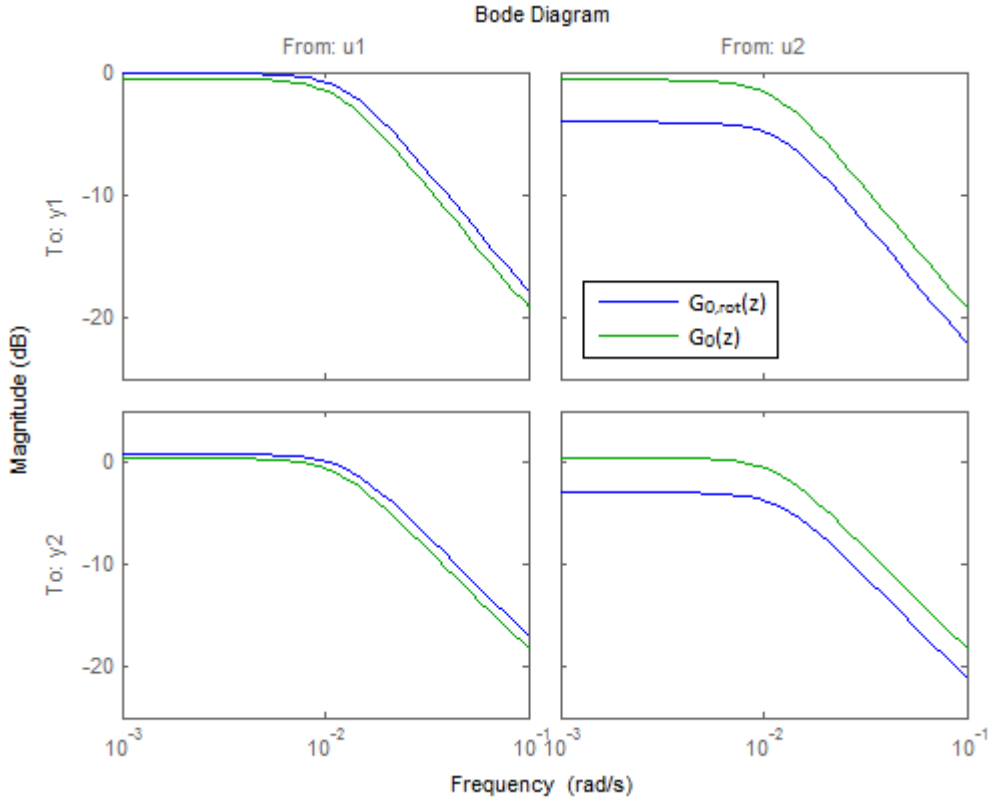

Figure 3-7: Magnitude-frequency plot for both the discrete model $G_0(z)$ and rotated model $G_{0,rot}(z)$.

By this change the variance of the outputs increase also more or less by a factor of two to three[1] and thus the performance $\hat{J}(k)$ will violate the threshold value β.

[1]The plant and disturbance change are chosen such that a relatively small performance deterioration occurs. If a small performance deterioration can be detected and the cause can be determined, a larger performance deterioration will of course be detected.

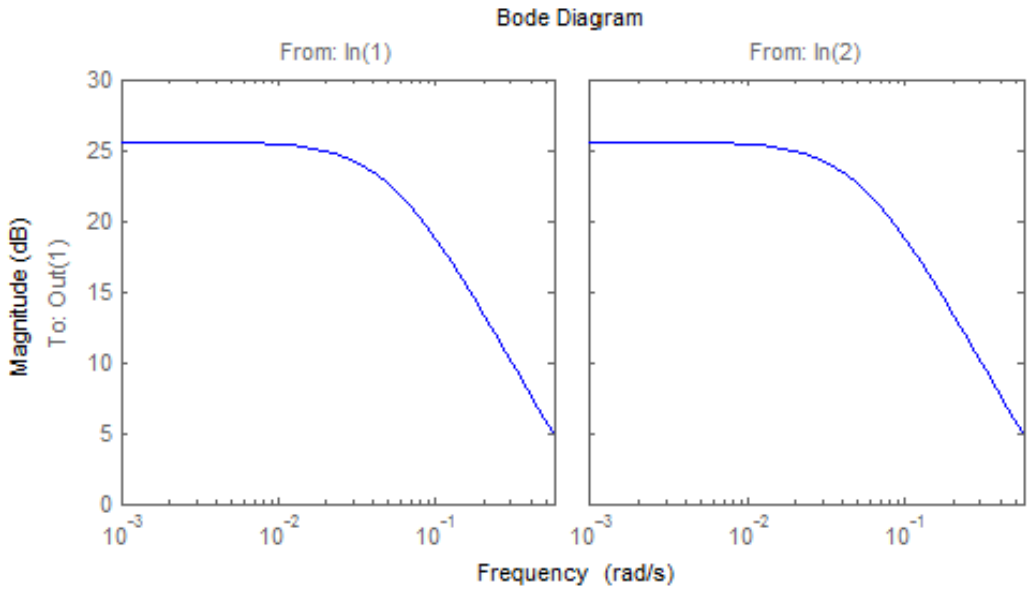

Figure 3-8: The spectrum for both disturbance signals $v_1(t)$ (left) and $v_2(t)$ (right) are shown in the situation of a change in disturbance characteristics.

The spectrum of the disturbances are shown in Fig. 3-5 for a system with nominal performance. In case of a disturbance change, the power of both disturbances $v_1(t)$ and $v_2(t)$ are of order $\sigma_v^2 = 1.25 \cdot 10^{-4}$ and the changed spectrum of both signals is shown in Fig. 3-8. It can be seen that compared to the original spectrum that the magnitude is larger for lower frequencies and creates larger disturbances. The low frequent disturbances with a larger magnitude affect the system and deteriorate the system performance. Due to these larger disturbances the performance will deteriorate.

3-3-3-3 Identification of System Changes

After a performance drop is created, the performance diagnosis method is applied and a short re-identification needs to be performed for this purpose[2]. To identify the system dynamics, excitation signals $u_i(t)$ (for $i = 1, 2$) are applied which are white-noise signals with variance of $\sigma_r^2 = 1 \cdot 10^{-2}$ and data $Z^{N_{id}} = [u_i(t), y_i(t) | t = 0...N_{id} - 1]$ is collected. To have a consistent estimate, a full-order model structure (Box-Jenkins) will be used to estimate a model for the plant dynamics and an independent model for the variations in disturbance characteristics[3]. By trial and error, the model structure used for re-identification is chosen to be:

$$y_1(t) = \frac{b_{11}z^{-1}}{1+f_{11}z^{-1}}u_1(t) + \frac{b_{12}z^{-1}}{1+f_{12}z^{-1}}u_2(t) + \frac{1+c_1z^{-1}}{1+d_1z^{-1}}e_1(t) \tag{3-10}$$

$$y_2(t) = \frac{b_{21}z^{-1}}{1+f_{21}z^{-1}}u_1(t) + \frac{b_{22}z^{-1}}{1+f_{22}z^{-1}}u_2(t) + \frac{1+c_2z^{-1}}{1+d_2z^{-1}}e_2(t). \tag{3-11}$$

[2]The direct closed-loop identification method is applied as explained in section 2-3-2.

[3]The diagnosis method tries to make a distinction between the two causes by making use of independent plant and disturbance dynamics, as explained in section 2-3.

Here, $[b_{11}, b_{12}, b_{21}, b_{22}, c_1, c_2, d_1, d_2, f_{11}, f_{12}, f_{21}, f_{22}]$ are the parameters which need to be estimated by making use of the criterion as given by Eq. (2-14). In the next section the closed-loop behaviour is discussed and it is verified whether the designed controller is able to cope with the chosen noise characteristics.

3-3-4 Simulator Analysis

This section elaborates on the simulator model and a short model analysis is made. In the next section a system that operates at nominal performance is analysed and also the situations when a disturbance or a plant change occurs will be discussed. This is done to verify that the discrete simulation model react more or less in the same way as a true distillation column would do. It is important to notice that the closed-loop behaviour depends on the designed PI-controllers. The system has fixed set-points and therefore, using the controller for reference tracking is less important. However, the behaviour will be shown for a set-point change and compared with models from literature. Secondly, more important is that the controller is able to cope with input uncertainty which arises e.g. due to modelling errors and is able to reject output disturbances due to e.g. changes in the feed flow or feed composition which could affect the system outputs.

3-3-4-1 Set-point Change

It will be shown what output behaviour is found with the simulator when a set-point change is applied (this is defined as an in or decrease of a set-point by 0.02). A set-point change is applied and the second set-point is kept unchanged to show the influence of each set-point change to each output. Secondly, both set-points are changed at the same time to show the influence at both outputs.

First, we discuss the behaviour when changing one set-point at a time. In this case the discrete system as shown in Fig. 3-4 is simulated for 40 time samples (Note that the noise signals $e_1(t)$, $e_2(t)$ will not be used and are chosen to be zero). The set-points for t<0 are $r_{1,1}(t) = 0.95$ and $r_{1,2}(t) = 0.05$. At time t=0 the set-point corresponding to the top composition is changed to $r_{1,1}(t) = 0.97$ and $r_{1,2}(t) = 0.05$ remains unchanged. In Fig. 3-9 (Upper left) it is shown what happens to both output compositions. The purity of the top composition (shown by the blue line) directly increases and settles around 25 time samples at the chosen set-point of 0.97. Due to the interconnection between the top and the bottom of the column also the purity of the bottom product decreases for a while[4] (which is shown by the green line). This is caused by the fact that it is easy to decrease the purity of one product and increase the purity of the other product.

Secondly, the same simulation is performed but this time set-point $r_{1,1}(t) = 0.95$ is kept unchanged and at time t=0, set-point $r_{1,2}(t)$ is increased to 0.07. In Fig. 3-9 (Upper right) again both compositions are shown (top composition in blue and bottom composition in green). Here, it is seen that the bottom composition directly increases and settles around 21 time samples. Also, in this case due to the interconnection between the top and the bottom of the column, the top composition increases for a short amount of time and settles at its fixed

[4]When the purity of the bottom product decreases it implies that the bottom composition increases, because the composition is given in terms of the more volatile product.

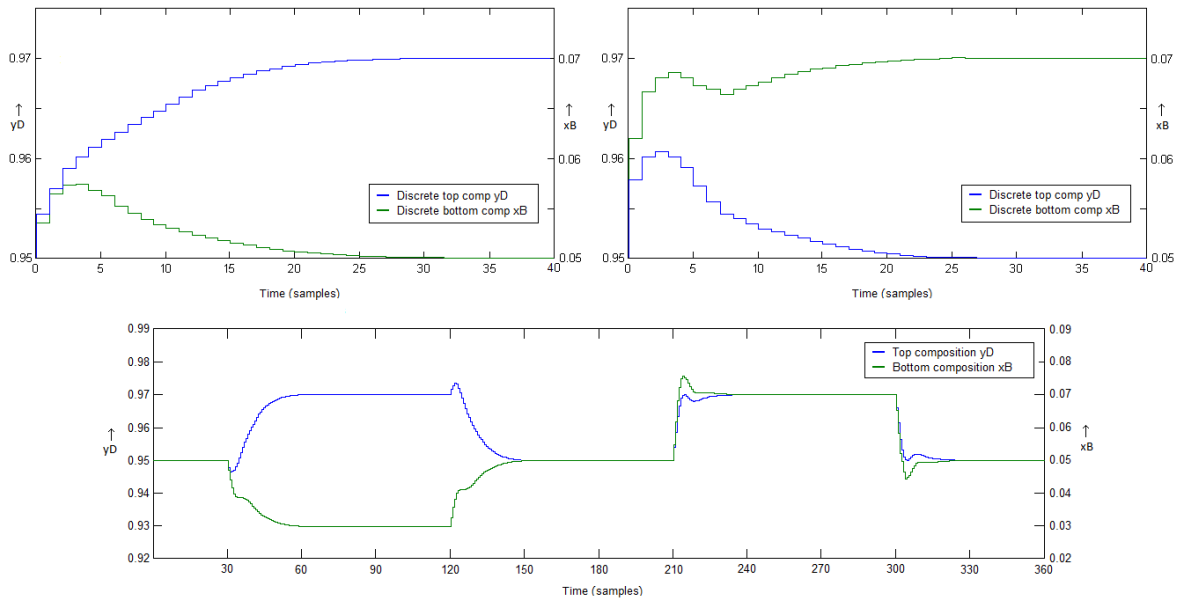

Figure 3-9: Upper left: A set-point change is applied onto the top composition at time t=0 and both output responses are shown. A settling time of around 25 time samples is found for the top composition. Upper right: A set-point change is applied onto the bottom composition at time t=0 and both output responses are shown. Also, a settling time of around 25 time samples is found for the bottom composition. Bottom: various set-point changes are applied to show the influence on both outputs.

set-point value at time sample 22. Furthermore, it is shown that the bottom composition reacts faster on a set-point change than the top composition. This is caused by the larger gain kp_2 in the second PI controller.

The third simulation runs for 360 time samples. In this case both set-points are changed. At time samples $[0,\ 30,\ 120,\ 210,\ 300]$ the set-points are $r_{1,1}(t) = [0.95,\ 0.97,\ 0.95,\ 0.97,\ 0.95]$ and $r_{1,2}(t) = [0.05,\ 0.03,\ 0.05,\ 0.07,\ 0.05]$ respectively to create all possible situations. In Fig. 3-9 (Bottom) again both compositions are shown (top composition in blue and bottom composition in green). At the first set-point change at time t=30 samples both product purities will increase. Due to the faster response of the bottom composition and the interconnection between the top and the bottom of the column, the top composition first decreases and within five time samples the top composition increases as what it should do. At the moment the top composition increases, the bottom composition is influenced as shown by the bump at time sample 35. Finally, both compositions settles within 30 time samples. It will take more time due to the fact that both product purities need to increase at the same time. At time sample 120 more or less the same behaviour is found but in the opposite direction. The bottom composition increases faster which let the top composition increase for a short amount of time and at the moment the top composition decreases the bottom composition react on the decrease as shown by the bump at time sample 125. At time sample 210, the purity of the top product increases and the purity of the bottom product decreases, i.e., both compositions increase at the same time. Due to the faster response of the bottom composition and the increase of both compositions at the same time, the bottom composition overshoots its corresponding set-point but settles faster w.r.t. a single set-point change as shown in Fig.

3-9 (Upper right). Due to the combined set-point change in the same (positive) direction both changes react faster and settles within a shorter amount of time samples which is near 20 time samples for both compositions. The last change at time sample 300 react also more or less the same but in the opposite direction and also settles in about 20 time samples.

3-3-4-2 Output Disturbances and Uncertainty

As mentioned, the outputs of a binary distillation column are often quite noisy which is caused by all kind of disturbances. Therefore, output disturbance rejection is important for such a system. The sensitivity of the system is of importance to shown what frequencies are amplified (or attenuated). The output sensitivity function is given by $S(z) = (I + G_0(z)C(z))^{-1}$. In Fig. 3-10 the magnitude between each disturbance input and measured outputs at each frequency is shown. Here, it can be seen from disturbance input $v_1(t)$ to output y_D and from disturbance input $v_2(t)$ to output x_B that the maximum magnitude is near zero dB at high frequencies. The maximum value near zero dB implies that noise and disturbances in the system will almost not be amplified by the feedback controller. In fact for frequencies smaller than $10^{-1} rad/s$ there is only attenuation of the noise in the system. Besides the sensitivity of the system we will also look at the system outputs and the corresponding control actions and how they react on output disturbances. Also, uncertainty in the system is taken into account to assure that the controller is able to cope with the output disturbances on the nominal system and even in the situations a plant or disturbance change occurs. Keep in mind that uncertainty for the original system $G_0(z)$ is different w.r.t. a system where a plant change occurs. For the original system the uncertainty can be seen as e.g. the modelling errors, which are considered to be quite small. The uncertainty of the model is defined by:

$$G(z,\theta) = \frac{1}{z-(0.985+c)} \begin{pmatrix} 1.16+a & -1.14+b \\ 1.43+a & -1.45+b \end{pmatrix}, \tag{3-12}$$

where, a represent $\pm 10\%$ uncertainty on the parameters of input one, b represent $\pm 10\%$ uncertainty on the parameter of input two. The uncertainties are chosen such that the physical couplings between the transfer function elements remain intact. In this way it is possible to analyse e.g. that $a = +10\%$ uncertainty and $b = -10\%$ or vice versa. Parameter c represents only a small uncertainty of $\pm 1\%$. Note that by making use of larger values the system could become unstable due to a pole which will be smaller than -1.

For a system where a dynamic change occurs, nothing is known about the changed dynamics. The unknown changed plant dynamics have, compared to the original model and w.r.t. the true system dynamics a larger error. Furthermore, each time a plant change occurs the plant dynamics will be different which causes more uncertainty in the system.
On the simulator, a plant change occurs by rotating the inputs of the system. The error between the rotated system and the true dynamics will be larger than the modelling errors of the original plant model (the larger error causes the performance deterioration). Note that we make use of one rotation angle ψ, which implies that the applied plant change is more or less the same every time. However, in reality each dynamic change is different. To take uncertainty into account w.r.t. the rotation it is possible to consider that there is uncertainty in the rotation angle ψ, which is given by

$$\psi = -\pi/8 \quad \pm 10\%$$

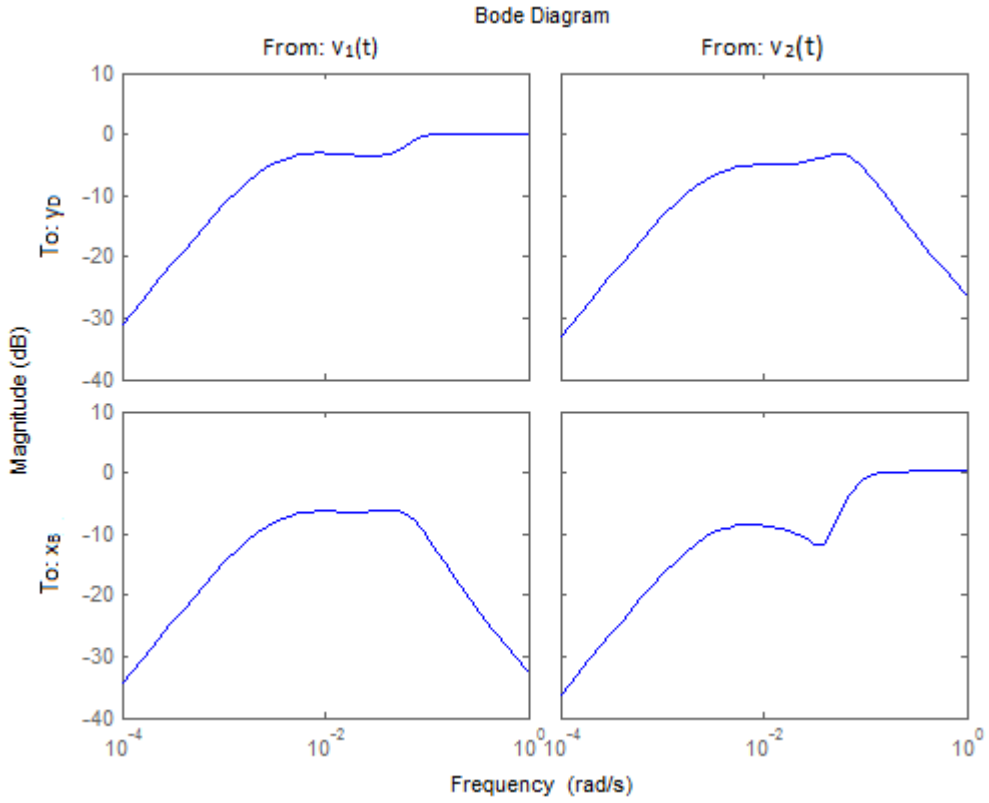

Figure 3-10: Sensitivity function from each input to each output.

This influences the rotation of the inputs $u_1(t)$ and $u_2(t)$ as given by Eq. (3-8).
The next step is to show the behaviour of the worst case system (within the range of the chosen uncertainties), i.e., the worst system performance and verify whether the controller can handle the output disturbances. If so, then the controller is assumed to be sufficient robust even for a considered plant or disturbance change.

Nominal situation

The discrete closed-loop system as shown in Fig. 3-4 will be considered where the process dynamics are given by (3-5) and controller is given by (3-6). The signals $e_1(t)$ and $e_2(t)$ are applied to the system as shown in Fig. 3-4 and are two white-noise signals which are filtered by $H_0(z)$ as given by (3-7). The white-noise signals both have a variance of $3.75 \cdot 10^{-5}$. The variance of the disturbance signals $v_1(t)$ and $v_2(t)$ is of order $6.5 \cdot 10^{-5}$. Both outputs have fixed set-points of $r_{1,1}(t) = 0.95$ and $r_{1,2}(t) = 0.05$. The distillation column will be simulated for 300 time samples to show the influence of the applied disturbances to the outputs of the system and the corresponding control action.

In Fig. 3-11 (Upper left) the top composition is shown and in Fig. 3-11 (Upper right) the bottom composition is shown for 300 time samples in case of the worst case considered uncertainty for the nominal situation (which is $a = -10\%, b = +10\%$ and $c = +1\%$ uncertainty). The top composition fluctuates around its set-point of 0.95 and the bottom composition around it set-point of 0.05. Keep in mind that when a performance deterioration occurs these fluctuations will increase. Both the top and bottom compositions have a variance of order $7.0 \cdot 10^{-5}$, the performance is then $\bar{J}(k) = 1.4 \cdot 10{-}4$. In Fig. 3-11 (Lower left) and in

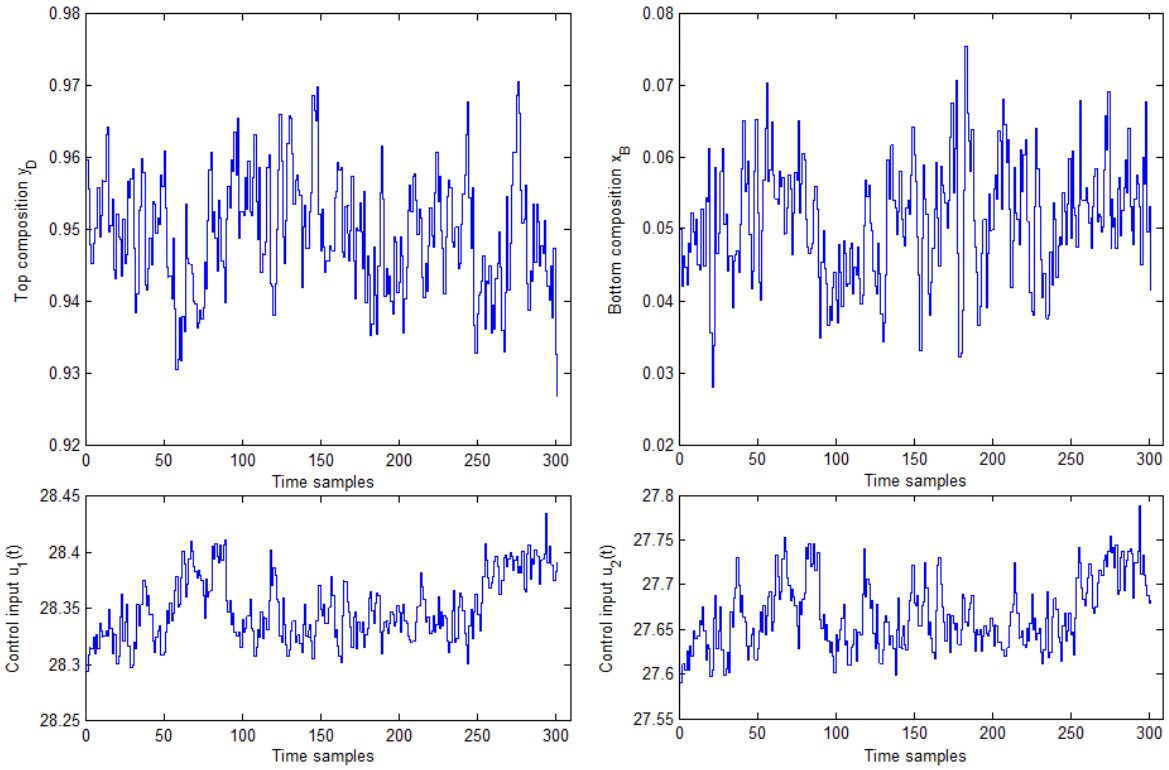

Figure 3-11: Upper left: the top composition is shown for 300 time samples for the worst case uncertainty scenario in case of nominal performance. Upper right: the bottom composition is shown also for 300 time samples for the worst case uncertainty scenario in case of nominal performance. Lower left: the control action is shown which corresponds to the top composition y_D. Lower Right: the control action is shown which corresponds to the bottom composition x_B.

Fig. 3-11 (Lower right) the corresponding control action is given for the top composition y_D and bottom composition x_B. When the top composition is measured and found to be larger than the chosen set-point the control action decreases in order to decrease the composition and thus the purity of the top product. On the other hand, if the bottom composition is larger than its set-point the control action needs to increase. This implies that the purity of the bottom product is lower than what it should be and needs to be increased. The latter can be seen in Fig. 3-11 (Upper and Lower left), where the control action at time sample interval $t = [50,\ 100]$ is relatively large because the top composition is in the same interval below its set-points of 0.95. Also, between the interval of $[250,\ 270]$ the top composition is below its set-point and the control action therefore increases. The same is shown for the bottom composition in Fig. 3-11 (Upper and Lower right). On the interval of $[90,\ 120]$ time samples the bottom composition is smaller than its corresponding set-point and less control action is needed because the purity should decrease. At the interval of $[250,\ 300]$ the bottom composition is larger than its set-point which implies that the purity needs to be increased what is done by the increasing control action.
Furthermore, it is shown that the controller does not react very aggressively to the disturbances in the system which can be seen by the small variations in control actions. It is important that the noise will not be amplified too much. As found with the sensitivity func-

tion almost no amplification of disturbance characteristics occurs. Finally, it can be seen that the compositions are quite close around its set-points and that the disturbances are sufficiently rejected by the controller.

Change in disturbance characteristics

Due to the importance of disturbance rejection, the influence of a change in disturbance characteristics will also be shown for the worst case uncertainty, i.e., the largest system performance (which is the same as in the nominal case, i.e., $a = -10\%, b = +10\%$ and $c = +1\%$ uncertainty). Again, the discrete closed-loop system as shown in Fig. 3-4 will be considered with plant model (3-5) and controller (3-6). As explained in section 2-3-1 the disturbance model will be changed to the model shown in (3-9). The output disturbances $e_1(t)$ and $e_2(t)$ are given by two white-noise signals which both have a variance of $3.75 \cdot 10^{-5}$. The variance of the disturbance signals $v_1(t)$ and $v_2(t)$ are of order $1.2 \cdot 10^{-4}$, which is almost an increase of two w.r.t. the nominal disturbances. Both outputs have fixed set-points of $r_{1,1}(t) = 0.95$ and $r_{1,2}(t) = 0.05$. The distillation column will be simulated for 300 time samples to show the influence of the changed disturbances to the outputs of the system.

In Fig. 3-12 (Upper left) the measured top composition is shown and in Fig. 3-12 (Upper right) the measured bottom composition is shown for the worst case uncertainty situation. The variance of both compositions increased by a factor two to $1.35 \cdot 10^{-4}$.
The change in disturbance characteristics can be seen in Fig. 3-12 by the larger fluctuations in the system outputs. Especially, for the top composition it is shown at time sample 75 and 250, that the composition decreases quite much. On the other hand, due to the large connection between the top and the bottom, the bottom composition increases quite much at time sample 250. These changes can also be seen in Figs. 3-12 (Lower left and right) which represent the corresponding control action. The control action also fluctuates more due to the change in disturbance characteristics. Even with the change in disturbance characteristics and the input uncertainty, the controller can handle the disturbances acting on the outputs of the system satisfactory.

Change in plant dynamics

Also, for a plant change with the worst case considered uncertainty[5], the output behaviour will be shown. Consider the discrete system as shown in Fig. 3-4 with plant model (3-5) and controller (3-6). The largest rotation angle $\psi = -\pi/8 \cdot 1.1$ is considered which causes the largest performance degradation. The signals $e_1(t)$ and $e_2(t)$ are applied to the system as shown in Fig. 3-4 and are two white-noise signals which are filtered by $H_0(z)$ as given by (3-7). The white-noise signals both have a variance of $3.75 \cdot 10^{-5}$. The variance of the disturbance signals $v_1(t)$ and $v_2(t)$ is of order $6.5 \cdot 10^{-5}$. Both outputs have fixed set-points of $r_{1,1}(t) = 0.95$ and $r_{1,2}(t) = 0.05$. The distillation column will be simulated for 300 time samples.

In Fig. 3-13 (Upper left and right) the top and bottom compositions y_D and x_B are shown. The plant change/rotation causes the outputs to fluctuate up and down with a more sinusoidal behaviour. This is also shown for the corresponding control actions which are shown in Fig. 3-13 (Lower left and right). At time sample 75, the control action $u_1(t)$ increases to increase the top composition. The bottom composition also increases, due to the

[5]This is the case for the largest possible angle ψ, due to the fact that for a larger rotation the performance degrades more.

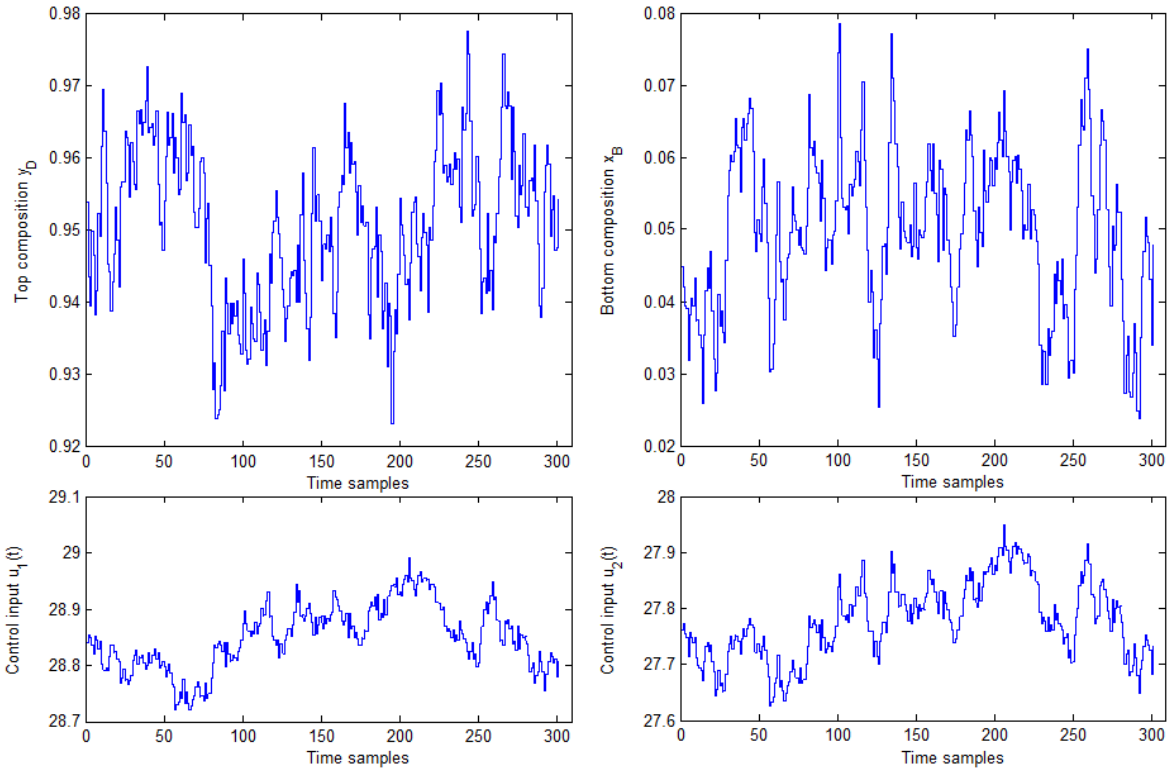

Figure 3-12: Upper left: the top composition is shown for 300 time samples for the worst case uncertainty scenario in case of a disturbance change. Upper right: the bottom composition is shown also for 300 time samples for the worst case uncertainty scenario in case of a disturbance change. Lower left: the control action is shown which corresponds to the top composition y_D. Lower Right: the control action is shown which corresponds to the bottom composition x_B.

increase of the top composition. At time sample 100, also the control action $u_2(t)$ starts to increase to decrease the bottom composition. Furthermore, it is shown that the control action $u_1(t)$ is much smaller than $u_2(t)$ when we compare those values with the nominal situation. This is caused by the rotation. By considering (3-8) it can be computed that $u_{1,rot}(t) = \cos(1.1 \cdot -\pi/8) \cdot 14.1 - \sin(1.1 \cdot -\pi/8) \cdot 37 = 28.3$ which is near $u_1(t)$ from the nominal situation (the factor 1.1 represents the worst considered case +10% uncertainty). The same can be done for the second output, which is $u_{2,rot}(t) = \sin(1.1 \cdot -\pi/8) \cdot 14.1 + \cos(1.1 \cdot -\pi/8) \cdot 37 = 27.7$ and also approaches the values of $u_2(t)$ from the nominal situation. It is shown that even if a plant change occurs and uncertainty is taken into account the controller is able to cope with these changes. Only, a more sluggish output behaviour arises, which is logical because the controller is designed on the original model and not on the changed plant dynamics. It seems that the controller is capable of handling a plant change sufficiently.

3-3-4-3 Discussion

From these results of the set-point changes it is found that the system react in the way as what was expected. If we compare the results of the set-point changes with the behaviour as found in literature (see Refs. [15, 18, 20]) it can be concluded that the system behaves

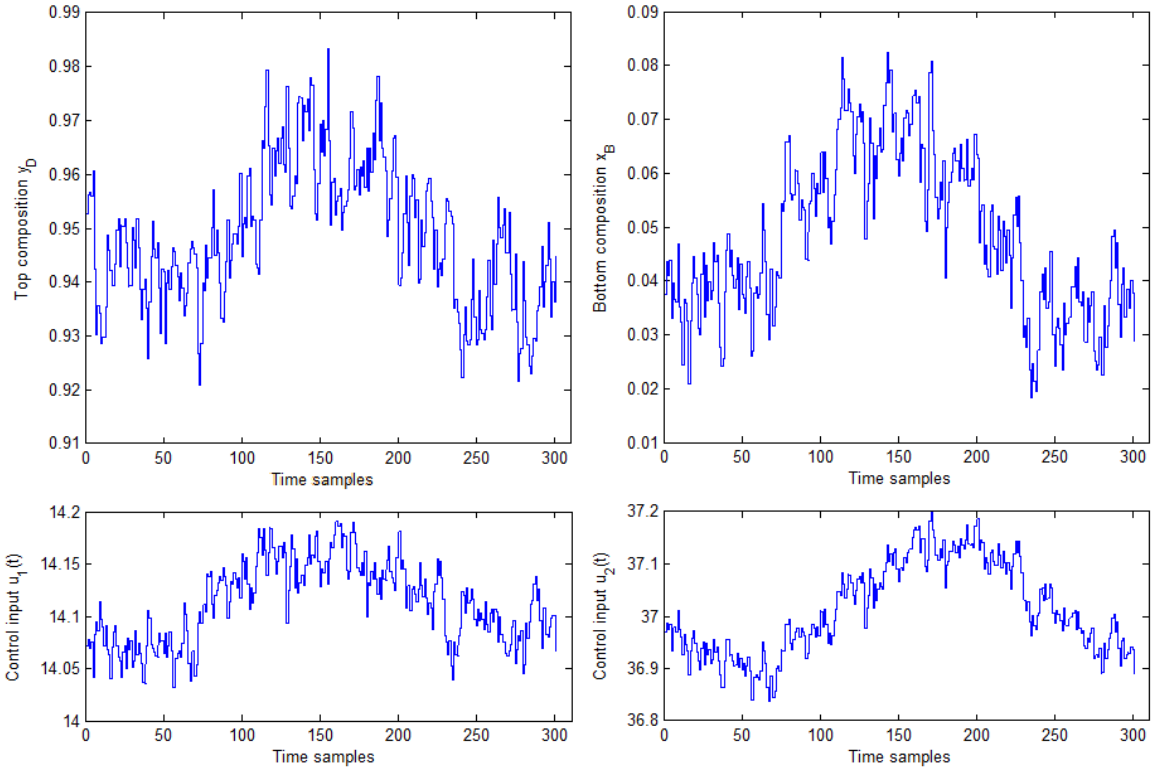

Figure 3-13: Upper left: the top composition is shown for 300 time samples for the worst case uncertainty scenario in case of a plant change. Upper right: the bottom composition is shown also for 300 time samples for the worst case uncertainty scenario in case of a plant change. Lower left: the control action is shown which corresponds to the top composition y_D. Lower Right: the control action is shown which corresponds to the bottom composition x_B.

and react in the same way on set-point changes. Furthermore, it is found that the designed controller is able to cope with the applied disturbance characteristics satisfactory. The closed-loop system does almost not amplify the disturbance characteristics, which is desired. Also, a change in plant dynamics can be handled satisfactory. Even with input uncertainty the controller is able to cope with the output disturbances and also in case of a plant change with uncertainties (on the rotation angle), the controller is capable of handle these situations sufficient. Therefore, the controller is found to be sufficiently robust and the closed-loop model is found to be a representative model to test the performance monitoring and diagnosis methodologies on.

Chapter 4

Numerical Results

4-1 Introduction

This chapter discusses the performed simulations and the results which are obtained with the simulator. Within this thesis it is investigated if the application of a performance monitoring and diagnosis method can be applied to a MIMO binary distillation column and how confident the made decision will be. The window size of the performance monitor is of importance and it will be investigated what size is an acceptable choice. Within the diagnosis method a small closed-loop identification experiment is carried out. Therefore, we consider the identification length to be an important variable and it will be investigated what a desirable length could be. Finally, multiple decision rules will be compared to increase the confidence of opting for the correct hypothesis. The simulation set-up and results of the application of the performance monitoring method to the simulator are discussed in section 4-2 and the application of the performance diagnosis is discussed in section 4-3.

4-2 Performance Monitor

Within this section results will be discussed concerning the choice of the window size which is used in the performance monitor. Before that is done, comparisons are made between systems which operate at nominal performance and systems which have a degraded performance. In case of a system with a degraded performance, results will be discussed concerning a plant change and a change in disturbance characteristics. Detection of one of the two considered changes can be done by making use of the following performance measure (which is discussed in section 2-2-2):

$$\hat{J}(k) = \frac{1}{N_{win}} \sum_{j=1}^{n} \sum_{i=k-N_{win}}^{k} \left(y_j(i) - r_{1,j}(i)\right)^T \left(y_j(i) - \underline{r}_{1,j}(i)\right) \qquad \text{for } k \in \mathcal{N} \tag{4-1}$$

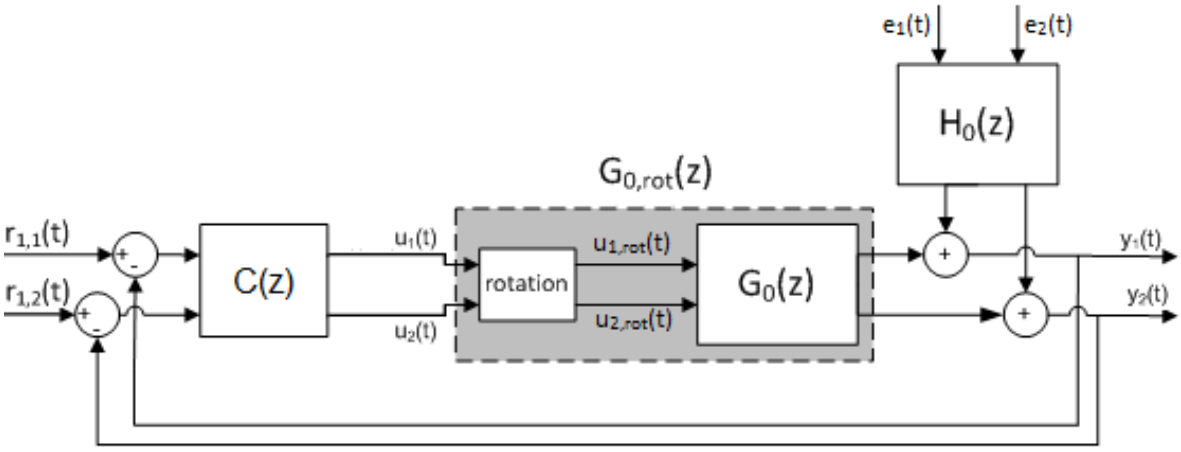

Figure 4-1: The closed-loop system is shown. The controller $C(z)$ is given by (3-6) and the plant model $G_0(z)$ is given by (3-5). The rotation angle (in block 'rotation') is set to $\psi = 0$ rad, for a system which operates at nominal performance or for a system where a disturbance change is applied. In case of a plant change the angle $\psi = -\pi/8$ rad, as discussed in section 2-3-1.

Here, $y_j(i)$ represents the measured discrete-time output signals and $r_{1,j}(i)$ the fixed set-point signals. The performance measure will be used to explain certain phenomena which are found within the simulation case study.

4-2-1 Nominal Situation

Two changes have been discussed which can occur in model-based control systems. First we will analyse results of a system which operates at nominal performance. The discrete closed-loop system as shown in Fig. 4-1 will be considered with plant model $G_0(z)$ as given by (3-5), the controller $C(z)$ as given by (3-6) and noise model $H_0(z)$ as given by (3-7). The rotation angle is set to $\psi = 0$ rad (no rotation). Stochastic signals are applied to the system via $e_1(t)$ and $e_2(t)$ with both a variance of $\sigma_e^2 = 3.75 \cdot 10^{-5}$. Furthermore, the outputs y_D and x_B have corresponding set-points of $r_{1,1}(t) = 0.95$ and $r_{1,2}(t) = 0.05$. The system is simulated for 10000 time samples. At time sample $t = 10000$, a plant change is applied by rotating the inputs over an angle $\psi = -\pi/8$ rad and the simulation is continued for another 10000 time samples.

In Fig. 4-2 (a) both output compositions are shown after subtraction of the corresponding set-points. The first 10000 data points shows a system which operates at nominal performance, where the outputs have a variance of order $\sigma_{y_D}^2 = \sigma_{x_B}^2 = 6.5 \cdot 10^{-5}$. Figure 4-2 (a) also shows the output compositions for a system where a plant change is applied. This is shown in the second 10000 data samples. For the case a plant change is applied, the output variance is increased to $\sigma_{y_D}^2 = \sigma_{x_B}^2 = 1.25 \cdot 10^{-4}$ which is almost a factor two.
Again, the same simulation is performed for 10000 time samples in case of the nominal system and at time sample 10000 the simulation is performed for another 10000 time samples where the disturbance model $H_0(z)$ is changed to (3-9).

In Fig. 4-2 (b) the output compositions are shown after subtraction of the corresponding set-points. Again, the first 10000 time samples shows the output compositions when the system operates at nominal performance and almost the same variance is achieved for both

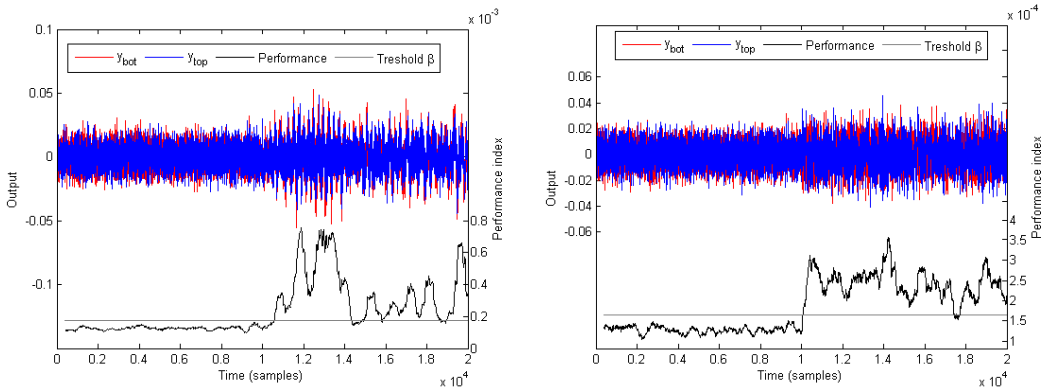

(a) The performance drop is caused by a plant change.

(b) The performance drop is caused by a disturbance change.

Figure 4-2: Both output compositions are plotted including the corresponding performance and threshold value. At the first 10^4 time samples the system operates at nominal performance and the outputs have a variance of order $\sigma^2_{y_D} = \sigma^2_{x_B} = 6.5 \cdot 10^{-5}$ and for the second 10^4 time samples a dynamics change is applied and the variance of the outputs changes to an order of $1.2 \cdot 10^{-4}$.

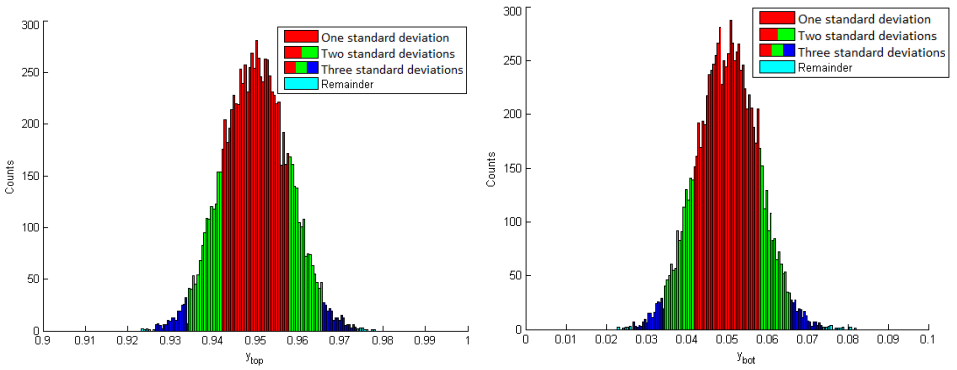

(a) Distillate output composition y_D.

(b) Bottom output composition x_B.

Figure 4-3: Both histograms show the one, two and three standard deviations and the remainder. The outputs are given for a system operating at nominal performance.

outputs $\sigma^2_{y_D} = \sigma^2_{x_B} = 6.57 \cdot 10^{-5}$. A disturbance change is applied at the second 10000 data points. Here, the variance increases to $\sigma^2_{y_D} = \sigma^2_{x_B} = 1.31 \cdot 10^{-4}$. At the bottom of both figures 4-2 (a and b) the performance $\bar{J}(k)$ as computed by Eq. (4-1) is shown including the threshold value $\beta = 1.60 \cdot 10^{-4}$. In case of the nominal situation the measured performance remains below the chosen threshold value when using a satisfactory value for N_{win}. How this variable is chosen is explained in section 4-2-4.

To show a degradation even better, the measured data of both output compositions y_D and x_B for a system that operates at nominal performance as shown in Figs. 4-2 is collected. In Fig. 4-3, a histogram is shown for both outputs at nominal performance when using the first 10000 collected data points from the simulation results as shown in Fig. 4-2. Within the histograms the one, two and three standard deviations and remainder are shown. This is done to easily show the difference between a system operating at nominal performance and a system where the performance degraded due to a plant or disturbance change.

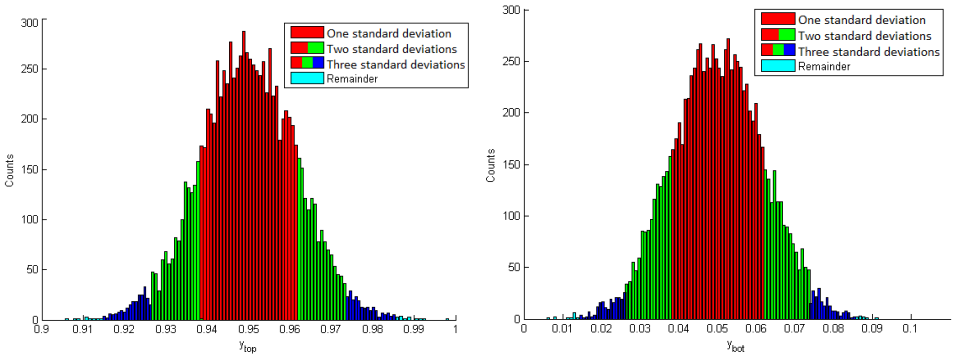

(a) Distillate output composition y_D. **(b)** Bottom output composition x_B.

Figure 4-4: Both histograms show the one, two and three standard deviations and the remainder. The outputs are given for a system where a plant change degraded the performance.

4-2-2 Plant Change

The situation when the system operates at nominal performance is compared with the situation that a plant change occurs. In the previous section the simulation set-up is already discussed. As shown in Fig. 4-2 (a), the output compositions are shown in the second 10000 data samples. It was found that the variance of the outputs is increased by a factor two to three. The performance level as shown below the output compositions increased and violated the threshold value. The degradation of $\bar{J}(k)$ can be explained by the fact that the difference between the outputs $y_i(t)$ and the set-points $r_{1,i}(t)$ (for $i = 1, 2$) is increased which implies a larger cost of Eq. (4-1). In Fig. 4-4 histograms are shown in the situation a plant change occurred which is simulated for 10000 data points (left the top and right the bottom composition). It can be seen that the standard deviations increased w.r.t. the nominal case. In table 4-1 the mean values and the values of one standard deviation is shown for the nominal situation and for the situation that a plant change occurred. Here, it is shown that the standard deviation of the output composition significantly increased at the moment a plant change occurs compared to the nominal situation.

4-2-3 Disturbance Change

Finally, the results of a change in disturbance characteristics will be compared with the results of a system with nominal performance. In Fig. 4-2 (b) the output compositions are shown in the second 10000 data points. It was found that the variance also increased by a factor two to three. The increase in the output compositions is detected by the performance measure (4-1) and the increase in performance is shown in Fig. 4-2 (b) below the output compositions. In Fig. 4-5, for the collected data set of 10000 time samples of the situation a disturbance change occurred, a histogram is shown (left the top and right the bottom composition). By comparing Fig. 4-3 and Fig. 4-5, the difference between the nominal situation and a disturbance change is obvious. In table 4-1 also the mean values and one standard deviations of a disturbance change is shown for both output compositions. For this cause it is seen that these values are also significantly larger than in the nominal situation and is of the same order as when a plant change occurs. This implies that there is almost

Table 4-1: The mean value and the one standard deviation is given for a dataset of 10^4 samples in case of nominal performance, a plant change and a change in disturbance characteristics. Histograms with these values are shown in Figs. 4-3, 4-4 and 4-5.

		Mean	One SD
Nominal situation	y_D	0.95	± 0.0080
	x_B	0.05	± 0.0078
Plant change	y_D	0.95	± 0.0118
	x_B	0.05	± 0.0107
Disturbance change	y_D	0.95	± 0.0113
	x_B	0.05	± 0.0119

no difference in the histograms as shown in Figs. 4-4 and 4-5. Note that even if we are able to measure a difference between a plant change and a disturbance change on the true system, in advance it is not known what the cause of the performance deterioration will be. A performance deterioration (and thus an increase in the measured variance of the output compositions) will be different each time a performance drop arises. Therefore, we need to use a diagnosis method to be able to distinguish between the plant and disturbance change.

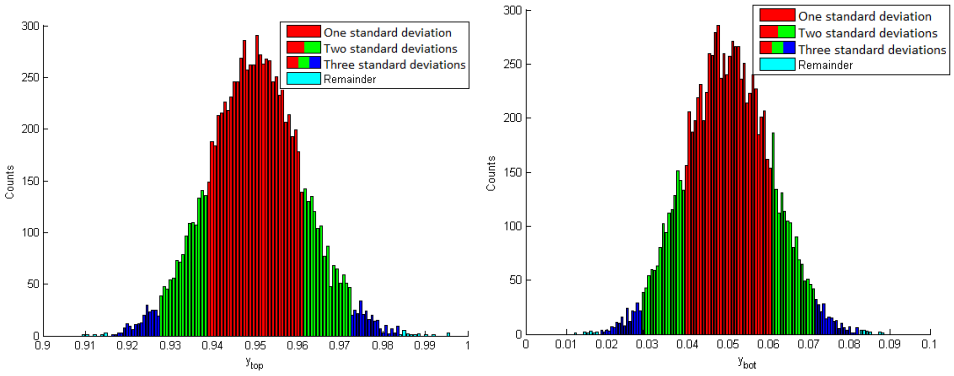

(a) Distillate output composition y_D. **(b)** Bottom output composition x_B.

Figure 4-5: Both histograms show the one, two and three standard deviations and the remainder. The outputs are given for a system where a change in disturbance characteristics degraded the performance.

The performance measure $\hat{J}(k)$ as given by Eq. (4-1), is capable of detecting both changes when they occur in a system. Note that in the previous results a satisfying window size is used of length $N_{win} = 400$ time samples. The size of the window is chosen in a heuristic way and is explained in more detail in the next section.

4-2-4 Performance Monitoring Method Window Size

In section 2-2-2 it was discussed why the size of the window of the performance monitoring method is of importance. To explain the importance of the window size we will again analyse the output compositions of a system which operates at nominal performance and a system where a plant change occurred. An exact same simulation is performed as discussed in section 4-2-1 and shown in Fig. 4-2 (a), where the discrete closed-loop system as shown in Fig. 4-1

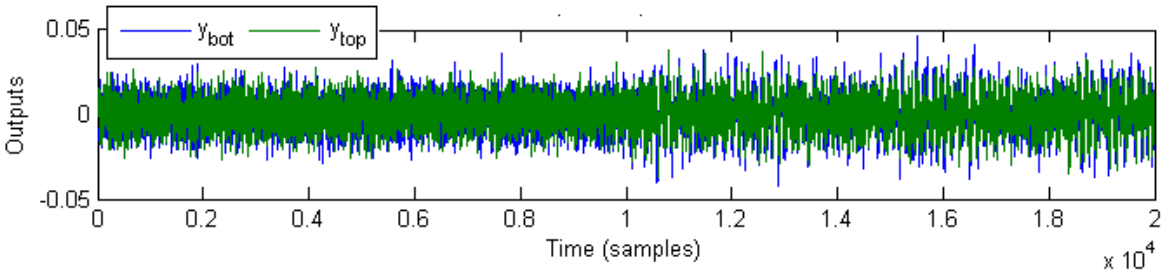

(a) Both output compositions are shown after subtraction of the corresponding references, i.e., $y_D - r_{1,1}(t)$ and $x_B - r_{1,2}(t)$.

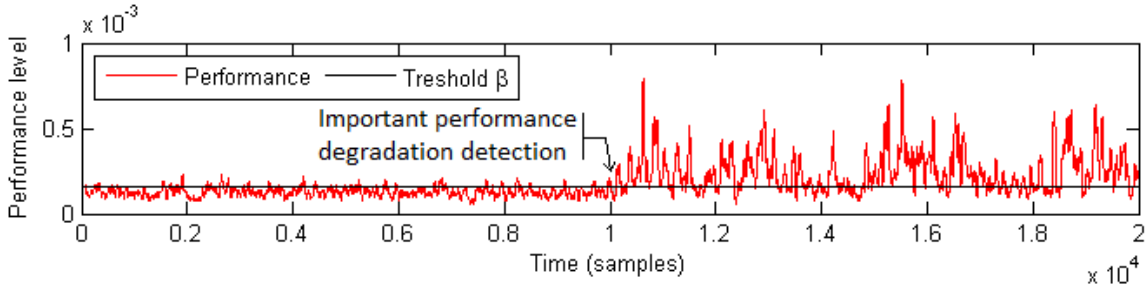

(b) The performance measure is shown which corresponds to the data of the measured compositions shown in Fig. 4-6 (a) with a window size of $N_{win} = 50$. Also, the threshold value $\beta = 1.60 \cdot 10^{-4}$ is shown.

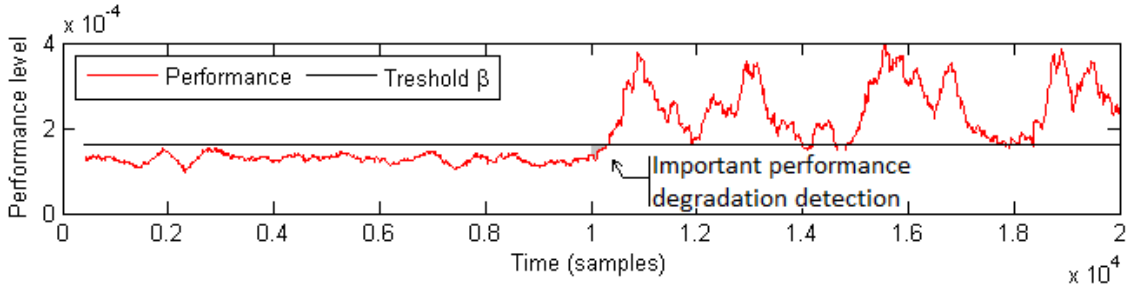

(c) The performance measure is shown which corresponds to the data of the measured compositions shown in Fig. 4-6 (a) with a window size of $N_{win} = 500$. Also, the threshold value $\beta = 1.60 \cdot 10^{-4}$ is shown.

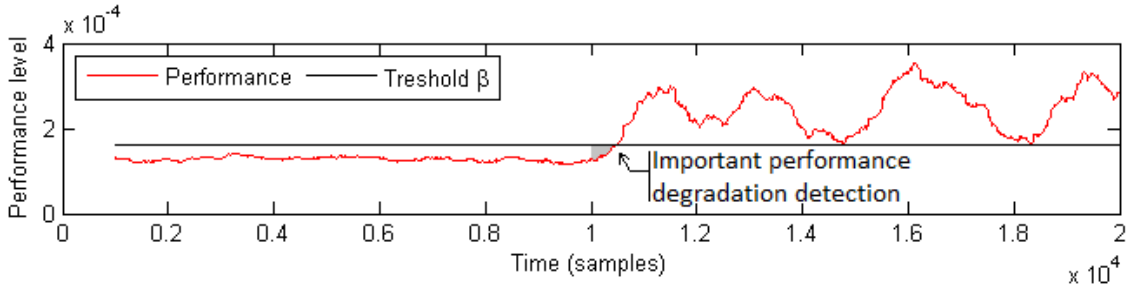

(d) The performance measure is shown which corresponds to the data of the measured compositions shown in Fig. 4-6 (a) with a window size of $N_{win} = 1000$. Also, the threshold value $\beta = 1.60 \cdot 10^{-4}$ is shown.

Figure 4-6: For both measured output composition the performance $\hat{J}(k)$ is shown for various window sizes N_{win}.

will be considered with plant model $G_0(z)$ as given by (3-5), the controller $C(z)$ as given by (3-6) and noise model $H_0(z)$ as given by (3-7). White-noise is applied to the system via $e_1(t)$ and $e_2(t)$ with both a variance of $\sigma_e^2 = 3.75 \cdot 10^{-5}$. Furthermore, the outputs y_D and x_B have corresponding set-points of $r_{1,1}(t) = 0.95$ and $r_{1,2}(t) = 0.05$. The rotation angle is set to $\psi = 0$ rad (no rotation). The system is simulated for 10000 data samples. Then the simulation is performed for again 10000 data samples but now the inputs are rotated over an angle $\psi = -\pi/8$ rad.

In Fig. 4-6 (a) the measured output compositions y_D and x_B are shown. In the first 10000 data points the variance of the outputs is of order $\sigma_{y_D}^2 = \sigma_{x_B}^2 = 6.5 \cdot 10^{-5}$. For the second 10000 data points the variance of both output compositions increased by a factor two to three. Furthermore, the performance measure (4-1) is given for three different window sizes $N_{win} = 50$, 500 and 1000 as shown in Fig. 4-6 (b, c and d) respectively. It is shown that with a small window $N_{win} = 50$ the performance measure is very sensitive and even though the system operates at nominal performance, the performance measure $\hat{J}(k)$ exceeds β many times which causes false alarms/detection errors (first 10^4 data samples). If one or both output compositions have a temporary decrease in purity due to a stochastic effect, with a small window size this can be seen as a performance deterioration. However, this is not desired because a performance diagnosis will be performed at the moment the performance measure violates the threshold value and unnecessary costs will be made. For that reason a larger window needs to be chosen. When taking a larger window $N_{win} = 500$ or 1000 time samples it can be seen that the performance measure stays below the threshold value in the first 10000 data points where the system runs at nominal performance. On the other hand, in Fig. 4-6 (b, c and d) the grey area shows the time it takes to detect a performance deterioration. This value increases when using a larger window size. By making use of a larger window the performance as measured by Eq. (4-1) is averaged over a larger window N_{win} and it will take more time to detect a performance deterioration. However, the time it takes to detect a performance deterioration should be small due to increasing operational costs which arise when a performance deterioration occurs. Therefore, a trade-off is made between the detection time and detection errors because they both depend on the window size. These variables can be defined as

Detection time:
This variable represents the time it takes from the moment a plant or disturbance change occurs in the system until the moment a performance drop is actually detected.

Detection errors:
At the moment the system operates at nominal performance it is possible that a performance deterioration is measured. This is mainly caused due to small fluctuations in the measured output compositions and/or due to a window size which is chosen too small. The (incorrectly) measured performance drops are called detection errors.

First the detection time and secondly the detection errors is investigated to find a satisfying window size. For both variables, Monte Carlo simulations will be used. This implies that one or more variables will be changed each simulation to collect a distribution of data in terms of the variables which will be investigated. This distribution/data set represents a large range of scenarios which could occur. The discrete closed-loop system as shown in Fig. 4-1 is used with controller C(z) (3-6), plant model $G_0(z)$ (3-5) and noise model $H_0(z)$ (3-7). Set-points are fixed at $r_{1,1}(t) = 0.95$ and $r_{1,2}(t) = 0.05$. For each window size $N_{win} = [50,\ 100,\ 200,\ 300,\ 400,\ 500,\ 750,\ 1000]$ time samples, 100 simulations are per-

formed and stochastic signals are applied via $e_1(t)$ and $e_2(t)$ and both have a variance of $\sigma_e^2 = 3.75 \cdot 10^{-5}$.

4-2-4-1 Detection Time

In each simulation the system runs first for 10000 time samples at nominal performance and at time sample $t = 10000$ a plant change is applied with a rotation of $\psi = -\pi/8$ rad. Then the simulation is continued for another 10000 data samples. In Fig. 4-7 the window size is plotted against the time it takes to detect a performance degradation, i.e., detection time. The plot shows the mean value and the standard deviation found from 100 simulations for each window size. As expected and found in Fig. 4-6 (b, c and d), the detection time increases as the window size increases and an almost linear increasing behaviour is found with respect to the window size. To explain the increase of the mean values of the detection time with respect to the window size we will make use of the performance measure as given by Eq. (4-1). It is shown that the sum for $i = 1, ..., N_{win}$ of the distance between $y_j(i)$ and $r_{1,j}(i)$ for $j = 1, ..., 2$ is averaged over the total window length given by the factor $\frac{1}{N_{win}}$ (and thus the performance which depends on those variables). The performance will be averaged over more data points when a larger window size N_{win} is chosen. By making use of a large window ($N_{win} \approx 1000$) for a longer period of time, data points where the system operated at nominal performance are taken into account. For example, with an average detection time of 300 time samples for a window size of $N_{win} = 1000$ still 700 data points are taken into account where the system operated at nominal performance. Compared to a window size of $N_{win} = 100$ samples, an average detection time of 35 data points are needed to detect a performance deterioration and only 65 data points are taken into account for which the system operated at nominal performance. By averaging over more data points implies that it will take more time until a performance deterioration is actually detected. Therefore, a performance deterioration is measured rather late with a large window compared to a small window size.

Furthermore, in Fig. 4-7 it is seen that the standard deviation increases when the window size increases, which is counter-intuitive due to an increasing window size. The increase can be explained by the fact that the detection time also depends on the size of the measured performance change. When the system runs at nominal performance and suddenly a change occurs in the system such that the performance increases, with a small window ($N_{win} \approx 50$) this is (almost) always measured within a small number of time samples (detection time < 100 data points) due to its sensitivity (independently of a small or large change $\hat{J}(k) \approx 2 \cdot 10^{-4}$ or $\hat{J}(k) \approx 1 \cdot 10^{-3}$ respectively). As shown in Fig. 4-6 (a) the performance is quite fluctuating up and down. The large peaks can also be seen as a large performance degradation and the lower area just above β as a small performance degradation. A large window ($N_{win} \approx 750 \sim 1000$) averages over more data points. This implies that a small performance deterioration will be detected at a later time moment because it will be averaged out for a longer period of time. On the other hand a large performance deterioration has a larger weight in the summation of the performance measure $\hat{J}(k)$ (4-1) and will be detected at an earlier time moment. When a performance degradation occurs, the measured output compositions will fluctuate more and also the performance measure as shown in Fig. 4-6 (b, c and d). Each time that a performance degradation occurs, the size of the degradation will be different. For a larger window the size of the degradation is more important than for a small window size and could explain the

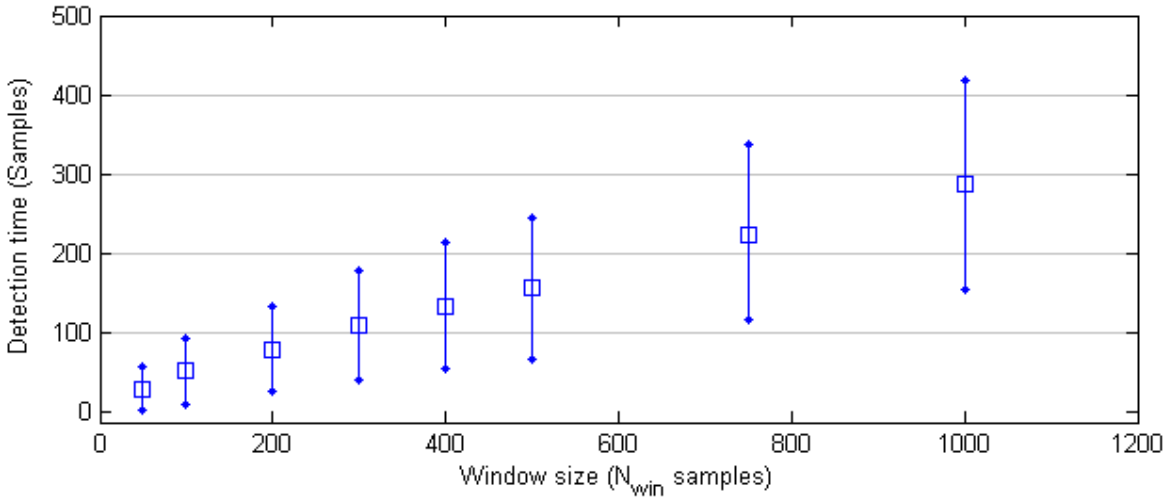

Figure 4-7: The window size is plotted against the time it takes to detect a performance degradation. 100 simulations have been performed for each window size and the mean value and one standard deviation are shown.

increasing standard deviation for larger window sizes.

It is found that the mean detection time of a window size of $N_{win} = 50$ is about 35 time samples. On the other hand, for a window size of 1000 samples the mean detection time is roughly ten times larger and varies more. It brings much extra costs with it and therefore, for this variable the window size should be chosen as small as possible (e.g. a mean value smaller than 150 time samples because there is a certain amount of operational cost attached to the length of the detection time).

4-2-4-2 Detection Errors

For the detection errors the same simulations are used as for the previous variable. However, we only need to investigate the performance measure for different window sizes at nominal performance. For the window sizes $N_{win} = [50,\ 100,\ 200,\ 300,\ 400,\ 500,\ 750,\ 1000]$ time samples the number of detection errors are measured. That is done for a certain amount of performance measurements $\hat{J}(k)$. The number of sample points of which $\hat{J}(k)$ can be computed depends on the window size and the simulation length of 10000 data points. For the largest window size $N_{win} = 1000$ the performance can only be measured for $10000 - 1000 = 9000$ data points. Whereas for a small window size $N_{win} = 100$ the performance can be measured for a total of $10000 - 100 = 9900$ data points, which is 900 more performance measurements (and thus more detection errors can be measured). To solve that problem for each window size only the last 9000 performance measurements are taken into account. A percentage is computed which represent the number of performance measurements in which a detection error occurs and is given by $(\#detectionerrors/9000) \cdot 100$.

In Fig. 4-6 (b) it is shown that a small window size ($N_{win} = 50$) is very sensitive and measures many detection errors (in 1.05% of all performance measurements $\hat{J}(k)$). Therefore, we expect that a large window is more useful, which is the opposite as found for the detec-

tion time. In Fig. 4-8 the mean value and the one standard deviations represent the total

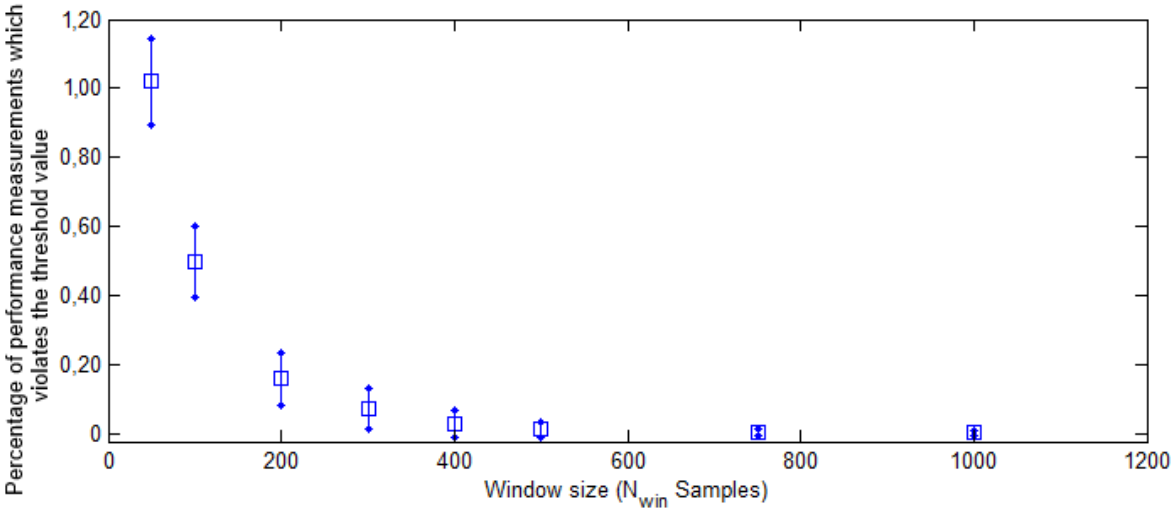

Figure 4-8: The window size is plotted against the percentage of performance measurement in which a detection error occurs. An error is detected at the moment that the system operates at nominal performance and yet the performance exceeds the threshold value β. A reliable performance measure is obtained when the number of detection errors is almost zero. 100 simulations have been performed for each window length and the mean value and one standard deviation is shown.

amount of detection errors which are measured for different window sizes N_{win}. This is done for 100 simulations for each window size. Here, it can be seen that the amount of detection errors exponentially increases when the window size is chosen smaller than $N_{win} = 500$ time samples. The asymptotic behaviour and the decreasing variance can be explained by looking at the performance measure from Eq. 4-1. The performance measure is basically a measure of the variance of the outputs. Therefore, we will look at an estimate of the mean value of a measured output (top composition y_D) for one window and its variance which in theory is computed by[1]

$$\bar{y}(k) = \frac{1}{N_{win}} \sum_{i=1}^{N_{win}} y(i), \qquad \text{with } y(i) \sim \mathcal{N}(0.95, \sigma_y^2) \tag{4-2}$$

According to the central limit theorem the estimate of the mean value is normally distributed by $\bar{y}(k) \sim \mathcal{N}(0.95, \sigma_y^2/N_{win})$. It can be seen that the variance decreases by $1/N_{win}$ when the window size increases. Furthermore, in Fig. 4-9 the distribution for a small and a large window size are shown. Here, r represents a constant value. For smaller window sizes ($N_{win} = 50$) the percentage $P(\bar{y}(k) \geq r)$ is much larger than for large window sizes ($N_{win} = 500$) as indicated by the shaded area. For that reason the total cost, computed by Eq. (4-1), is more often larger for a small window size compared to that from a large window size. This implies that the threshold value β is more often violated when monitoring with a small window size and the amount of detection errors increases. The number of detection errors also decreases more or less by a factor of $1/N_{win}$ which causes the asymptotic behaviour in Fig. 4-8.

[1]Notice that the performance $\hat{J}(k)$ does not use Eq. (4-2) and is only used to explain why the performance measure more often violates β when a small window size N_{win} is chosen.

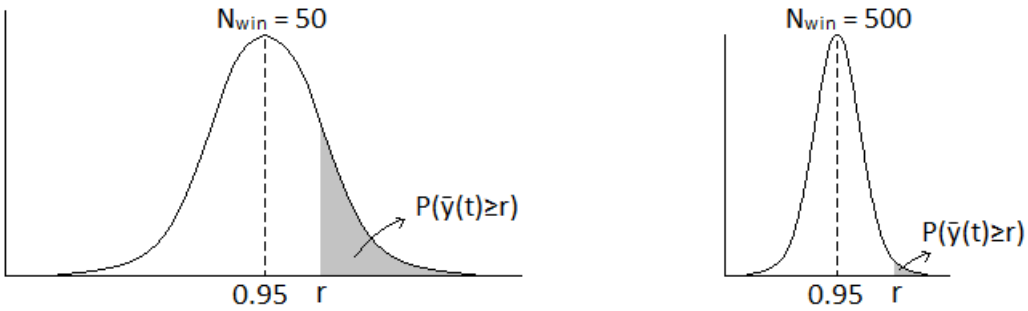

Figure 4-9: Normal distributions of the mean value $\bar{y}(k)$ for different performance measure window sizes. Shown is the probability $P(\bar{y}(k) \geq r)$ which is larger for a smaller window size.

To be able to choose a value for the window size a trade-off is made between the detection time and the amount of detection errors which occur. It needs to be taken into account that an increase in costs are involved when starting a performance diagnosis. Therefore, the number of errors should be as low as possible (near zero) and still have a detection time which is rather fast. On the other hand, a rather slow detection time also increases operational cost for a longer period of time. With, e.g. a cost analysis the choice of the window size can be made. However, nothing is known about any kind of costs and therefore a heuristic choice is made. For example, the detection should be near zero and the mean detection time needs to be smaller than 150 time samples. In Fig. 4-7 it is shown that the largest window having a mean value smaller than 150 samples is the window with $N_{win} \approx 450$. For ease we have chosen $N_{win} = 400$ because that is a window size we have used throughout this section and approaches the window of $N_{win} = 450$ the most. It can also be seen in Fig. 4-8 that with this window almost no detection errors are made. Therefore, a window size of $N_{win} = 400$ is a desirable choice.

4-3 Performance Diagnosis

This section examines the choice of the length of a short identification experiment, which is performed within the performance diagnosis. This is done to estimate model $G(z, \hat{\theta}_{N_id})$ which is used to make a decision. The found identification length is used in the diagnosis methodology. Note that it is also possible to vary the power of the excitation signal, but we have chosen to fix this value and vary the identification length. Furthermore, the decision rules as given in (2-16), (2-22) and (2-23) which have been discussed in section 2-3 will be compared to find out for which decision rule the largest confidence is found to opt for the correct hypothesis.

4-3-1 Identification Length

Within the performance diagnosis method a short identification experiment needs to be performed to estimate model $G(z, \hat{\theta}_{N_id})$. The identification length of this experiment is of importance to estimate a model which can accurately describe the true system dynamics. The accuracy of the estimated model will be of importance to make a correct decision. An

estimated model found with a large identification length will describe the true system dynamics more accurately than a model found with a short identification length. However, the costs of a diagnosis should be kept as low as possible. Due to the degraded performance of the system, e.g. operational cost increase and therefore the identification experiment should be kept as short as possible.
To find a satisfactory identification length we will perform simulations. The same discrete closed-loop system as shown in Fig. 4-1 with corresponding discrete models, set-points, stochastic signals are used as discussed in the previous section about performance monitoring. In the performance diagnosis the direct closed-loop method is used to perform a short closed-loop identification experiment. Input excitation signals are added to the inputs $u_1(t)$ and $u_2(t)$ of the system. These excitation signals are chosen to be white-noise signals with both a variance of $\sigma_r^2 = 1 \cdot 10^{-2}$. The identification length N_{id} will be varied by the following set $N_{id} = [100,\ 200,\ 300,\ 400,\ 500,\ 1000,\ 2000]$ data points. For each identification length a simulation is performed and data $Z^{N_{id}} = [\underline{u}(t), \underline{y}(t) | t = 0, ..., N_{id} - 1]$ is collected. As discussed in section 2-3-2, to estimate a model a full-order model structure is used and the criterion as given in (2-14) is considered.

According to Ref. [11], if an estimated parameter has a variance which is an order of magnitude smaller, the estimated parameter is required. In table 4-2 the values of each parameter is given including the variance for each parameter. This is shown for every identification length[2] and only for a disturbance change. It is found that for each identification length and for each parameter the order is at least of a magnitude smaller. It seems that the smallest identification length can be used. This was not expected and therefore we will also take into account that a decision is based on the closed-loop performance $J\left(C(z), G(z, \hat{\theta}_{N_{id}}), H(z, \theta_{com})\right)$ with the estimated model $H(z, \theta_{com})$ as given by (3-7)) . To take the closed-loop performance into account a different analysis will be performed.

The likeliness of opting for the correct decision depends on the accuracy of the estimated model. An estimated model found with a larger identification length could imply that the made decision is more likely to be true. Therefore, we try to find a relation between the identification length and the number of correctly made decisions. We use exactly the same simulation set-up as for the previous identification experiments. This time, the identification experiment for each identification length is repeated 100 times and the identification experiments are performed for the situation a plant change occurs and for the situation that a disturbance change occurs. Then we have chosen to use the decision rule from (2-16) which is only based on the closed-loop performance with the estimated model $G(z, \hat{\theta}_{N_{id}})$. Finally, it is verified for each simulation whether the estimated model is located in or outside the set $\mathcal{D}_{adm}$ to make a decision.

In table 4-3, both causes are shown for each considered identification length. For each identification length 100 simulations are performed and the number of correctly made decisions are shown. As expected, when using a small identification length more wrong decisions are made. As shown in table 4-2, the variance which correspond to each of the estimated parameters vary quite much between each identification length. For short identification lengths the true system can not be described accurate enough by the estimated model each time a model is estimated. Therefore, there could be quite a difference in performance of the closed-loop system with the estimated model w.r.t. the closed-loop performance of the true system.

[2]Except for the identification length of $N_{id} = 2000$, because it was found that a smaller identification length will suffice.

Table 4-2: Values of each parameter is shown which are contained in the estimated parameter vectors. Also, the variance of each parameter is given for all identification lengths. This is shown for a disturbance change.

Parameters .	N_{id} =100	N_{id} =200	N_{id} =300
$\bar{b}_{1,1}$	0.0124 ± 3.63e-06	0.0122 ± 1.62e-06	0.0122 ± 9.69e-07
$\bar{b}_{1,2}$	-0.0108± 3.30e-06	-0.0107 ± 1.49e-06	-0.0109 ± 9.03e-07
$\bar{b}_{2,1}$	0.0137 ± 3.74e-06	0.0136 ± 1.68e-06	0.0139 ± 1.06e-06
$\bar{b}_{2,2}$	-0.0149± 3.57e-06	-0.0146 ± 1.61e-06	-0.0147 ± 1.03e-06
$\bar{f}_{1,1}$	-0.9445± 2.66e-03	-0.9657 ± 4.73e-04	-0.9787 ± 1.18e-04
$\bar{f}_{1,2}$	-0.8981 ± 7.46e-03	-0.9524 ± 1.17e-03	-0.9732 ± 1.87e-04
$\bar{f}_{2,1}$	-0.9079 ± 4.09e-03	-0.9256 ± 1.57e-03	-0.9412 ± 8.26e-04
$\bar{f}_{2,2}$	-0.9679 ± 1.37e-03	-0.9800 ± 1.64e-04	-0.9831 ± 7.34e-05
Parameters	N_{id} =400	N_{id} =500	N_{id} =1000
$\bar{b}_{1,1}$	0.0122 ± 6.99e-07	0.0122 ± 5.29e-07	0.0117 ± 2.35e-07
$\bar{b}_{1,2}$	-0.0113 ± 6.41e-07	-0.0112 ± 4.77e-07	-0.0112 ± 2.15e-07
$\bar{b}_{2,1}$	0.0142 ± 7.32e-07	0.0144 ± 5.70e-07	0.0142 ± 2.45e-07
$\bar{b}_{2,2}$	-0.0145 ± 6.95e-07	-0.0145 ± 5.36e-07	-0.0146 ± 2.30e-07
$\bar{f}_{1,1}$	-0.9815 ± 6.17e-05	-0.9817 ± 4.27e-05	-0.9842 ± 1.33e-05
$\bar{f}_{1,2}$	-0.9761 ± 1.13e-04	-0.9797 ± 6.26e-05	-0.9836 ± 1.34e-05
$\bar{f}_{2,1}$	-0.9694 ± 1.82e-04	-0.9690 ± 1.26e-04	-0.9851 ± 1.06e-05
$\bar{f}_{2,2}$	-0.9836 ± 3.20e-05	-0.9847 ± 2.27e-05	-0.9855 ± 7.77e-06

This difference could imply that the true system is located inside the set $\mathcal{D}_{adm}$ whereas the estimated model is outside the set (or vice versa). A quite large difference is found for the number of correctly made decisions for small identification lengths $N_{id} = 100$ or 200 between plant and disturbance changes. A plant change is caused by a rotation of the inputs of the system. In Fig. 3-7 the quite small difference is shown between the true and the rotated plant. With a small identification length the variance is quite large which implies that it is more likely to estimate models that are close to the true (not rotated) system. Therefore, more wrong decisions can be made when the identification length is chosen to short. Furthermore, it can be seen from the data that for large identification lengths the number of correctly made decisions tends to 100%. This is explained by the fact that when the identification length tends to infinity the variance tends to zero and the true system can exactly be described by the estimated model, i.e., $G(z, \hat{\theta}_{N_{id}}) \to G_0(z)$. This implies that the closed-loop performance will also be the same and thus the number of correct decisions increase to 100%. This is reached near an identification length of $N_{id} = 2000$ data samples, which is quite large for a short performance diagnosis identification experiment. Therefore, in a more or less heuristic way we have chosen a value of near 95% of correct decisions is sufficient. This corresponds to an identification length of around $N_{id} = 400$ data samples which is used to keep diagnosis costs low. By making use of the found identification length, in the next section the quality of the made decision will be assessed and various decision rules will be compared.

Table 4-3: For both causes and each considered identification length N_{id}, the number of correctly made decisions are shown for 100 simulations for each identification length. The decision is based on decision rule (2-16).

Cause\ Identification length N_{id}	100	200	300	400	500	1000	2000
Plant change	55	73	84	92	92	96	99
Disturbance change	86	91	94	97	99	100	100

4-3-2 Increase Confidence of Making the Correct Decision by Comparison of Three Decision Rules

At this moment we have discussed the performance monitoring method and the choice of the identification length. As explained in section 2-3-2 and 2-3-3 various decision rules are introduced. These decision rules will be compared to find the largest confidence to opt for the correct decision. To be able to make these comparisons we will consider the discrete closed-loop system as shown in Fig. 4-1 with controller $C(z)$, plant model $G_0(z)$ and disturbance model $H_0(z)$ as given by (3-6), (3-5) and (3-7) respectively. The set-points are fixed at $r_{1,1}(t) = 0.95$ and $r_{1,2}(t) = 0.05$. Monte Carlo simulations are performed. Stochastic noise is applied to the system via the signals $e_1(t)$ and $e_2(t)$ with a variance of $3.75 \cdot 10^{-5}$. In 250 simulations an identification experiment is performed on a system where a plant change occurred and in 250 simulations an identification experiment is performed on a system where a disturbance change occurred. A closed-loop identification experiment is performed exactly the same as explained in the previous section, but this time only the chosen identification length of $N_{id} = 400$ data points is used. For estimation of a model a full-order model structure is used and the parameters are estimated with the chosen criterion as given by (2-14).

In section 2-3-2 and 2-3-3, three decision rules are discussed which will be compared to investigate for which decision rule the largest percentage is found of opting a hypothesis correctly. The decision rule based on the estimated model (only) is given by:
Decision rule 1:

$$\begin{aligned} G(z,\hat{\theta}_{N_{id}}) \in \mathcal{D}_{adm} &\rightarrow \text{ pick } \mathcal{H}_0 \\ G(z,\hat{\theta}_{N_{id}}) \notin \mathcal{D}_{adm} &\rightarrow \text{ pick } \mathcal{H}_1 \end{aligned}$$

The second decision rule is based on the proposed heuristic method (only) and is given by:
Decision rule 2:

$$\begin{cases} \hat{Fr}_{out} = [0,\ \nu)\% \rightarrow \text{ pick } \mathcal{H}_0 \\ \hat{Fr}_{out} = [\nu,\ 100]\% \rightarrow \text{ pick } \mathcal{H}_1 \end{cases}$$

The third decision rule is a combination of the previous two decision rules. First, the estimated model is considered and dependent on whether the estimated model is located in or outside set $\mathcal{D}_{adm}$, the decision could be based on the heuristic method as given by:
Decision rule 3:

$$\begin{aligned} G(z,\hat{\theta}_{N_{id}}) \in \mathcal{D}_{adm} &\rightarrow \text{pick } \mathcal{H}_0 \\ G(z,\hat{\theta}_{N_{id}}) \notin \mathcal{D}_{adm} &\begin{cases} \hat{Fr}_{out} < \nu\% \rightarrow \text{pick } \mathcal{H}_0 \\ \hat{Fr}_{out} \geq \nu\% \rightarrow \text{pick } \mathcal{H}_1 \end{cases} \end{aligned}$$

With the first and third decision rules the decision is directly based on the performance of the closed-loop system $\left\{C(z), G(z,\hat{\theta}_{N_{id}}), H(z,\theta_{com})\right\}$[3] as computed by Eq. (2-7). For the third decision rule when $G(z,\hat{\theta}_{N_{id}}) \notin \mathcal{D}_{adm}$ and for the second decision rule, the decision is based on the heuristic method as discussed in section 2-3-3 where $\hat{Fr}_{out}$ also makes use of the set $\mathcal{D}_{adm}$.

To asses the quality of the diagnosis method, we will investigate how often an (in)correct decision is made. The percentage of opting a hypothesis incorrectly can be computed by

$$Pr_{incorrect} = Pr(\mathcal{H}_1|\mathcal{H}_0)Pr(\mathcal{H}_0) + Pr(\mathcal{H}_0|\mathcal{H}_1)Pr(\mathcal{H}_1). \tag{4-3}$$

Here $Pr(\mathcal{H}_1|\mathcal{H}_0)$ represents the percentage that is found when opting for hypothesis $\mathcal{H}_1$ while $\mathcal{H}_0$ is true. The percentage $Pr(\mathcal{H}_0|\mathcal{H}_1)$ represents vice versa of $Pr(\mathcal{H}_1|\mathcal{H}_0)$, because now hypothesis $\mathcal{H}_0$ is chosen while $\mathcal{H}_1$ is true. Furthermore, the percentages of opting for the incorrect and correct hypotheses are given by $Pr_{incorrect}$ and $Pr_{correct}$ (total of both plant and disturbance changes). Here, $Pr_{correct} = 1 - Pr_{incorrect}$. The percentage $Pr(\mathcal{H}_0)$ corresponds to $Pr(\mathcal{H}_0) = 1 - Pr(\mathcal{H}_1)$ and represents how often a plant or disturbance change occurs. Furthermore, the ratio of how often a plant or disturbance change occurs is varied. This ratio is called the plant to disturbance ratio which is varied by the following set:

$$\text{Plant to Disturbance ratio } \frac{Pr(\mathcal{H}_1)}{Pr(\mathcal{H}_0)} = [90/10,\ 70/30,\ 50/50,\ 30/70,\ 10/90]\% \tag{4-4}$$

The percentages $Pr(\mathcal{H}_0)$ and $Pr(\mathcal{H}_1)$ from Eq. (4-3) will thus be varied. It is known that a change in disturbance characteristics occurs more often in a binary distillation column and a small ratio is obtained. However, when this is not the case the percentages of opting a hypothesis (in)correctly is different. Therefore, it is also investigated what will happen when the plant to disturbance ratio will be varied.

4-3-2-1 Decision Rule One

In this section we consider decision rule one which implies that the decision is based on the performance of the closed-loop system $\left\{C(z), G(z,\hat{\theta}_{N_{id}}), H(z,\theta_{com})\right\}$ which is computed by Eq. (2-7). The performed simulations are used to determine how often an erroneous situation occurs, i.e., we want to determine $Pr(\mathcal{H}_1|\mathcal{H}_0)$ and $Pr(\mathcal{H}_0|\mathcal{H}_1)$. First, the performance is computed with the estimated model in each of the 500 simulations. The closed-loop performance of 250 simulations where a plant change occurred are shown in Fig. 4-10a and for the 250 simulations where a disturbance change occurred in Fig. 4-10b. Also the threshold value β is given in these figures. Here, it is seen that for a plant change in most simulations the performance is computed between the interval of $[1.35 \cdot 10^{-4},\ 4.0 \cdot 10^{-4}]$. It is detected how often an erroneous situation occurs. For example, from the 250 simulations where a plant change occurred, 22 times a wrong decision was made due to a measured performance which is smaller than β and thus it was found that $G(z,\hat{\theta}_{N_{id}}) \in \mathcal{D}_{adm}$. This erroneous percentage is computed by $Pr(\mathcal{H}_0|\mathcal{H}_1) = \frac{22}{250} = 0.088$. Thus in 8.8% of the simulations the closed-loop performance was smaller than β which indicates that in these simulations a wrong hypothesis is chosen. Note that it is preferred to opt for a disturbance change while a plant change occurs instead of the opposite as explained in section 1. Furthermore, in Fig. 4-10b it is found

[3]Here, $H(z,\theta_{com})$ is given by (3-7)

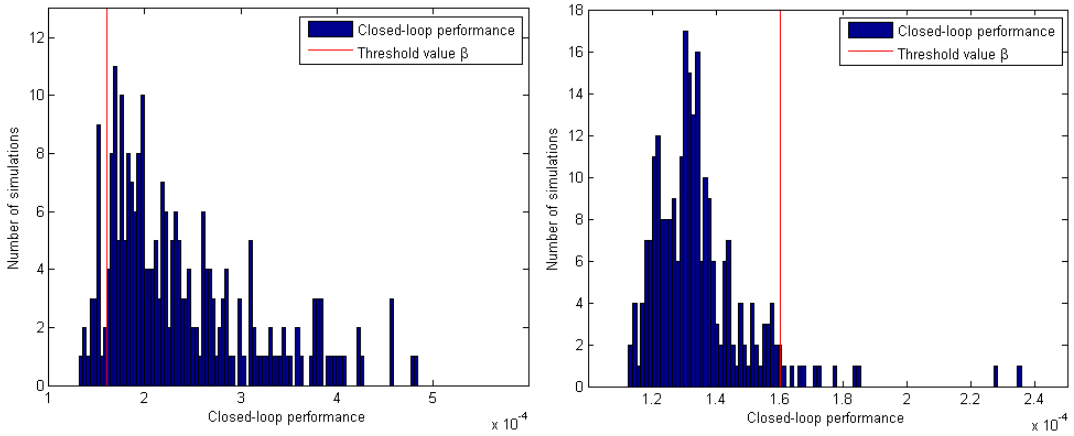

(a) Change of plant dynamics. **(b)** Change in disturbance characteristics.

Figure 4-10: The closed-loop performance is given for the estimated model $G(z, \hat{\theta}_{N_{id}})$, the original noise characteristics $H(z, \theta_{com})$ and controller $C(z)$. This is shown for 250 simulations for each of the causes. Decision rule one can be instantly applied with these results.

Table 4-4: With decision rule one the percentages are given when opting the wrong hypothesis for each cause and percentages are given when opting for incorrect and correct hypotheses (total correct and incorrect choices for both causes; plant and disturbance change). This is done for different ratios of how often a plant or disturbance change occurs.

Ratio Plant/Dist change	$\Pr(\mathcal{H}_0\|\mathcal{H}_1)$	$\Pr(\mathcal{H}_1\|\mathcal{H}_0)$	$\Pr_{incorrect}$	$\Pr_{correct}$
90/10	0.088	0.044	0.084	0.916
70/30	0.088	0.044	0.075	0.925
50/50	0.088	0.044	0.066	0.934
30/70	0.088	0.044	0.057	0.943
10/90	0.088	0.044	0.048	0.952

that most of the computed closed-loop performances, when a disturbance change occurred, are within the interval $[1.1 \cdot 10^{-4},\ 1.7 \cdot 10^{-4}]$. In this case from the 250 simulations where a disturbance change occurred in only 11 simulations the performance was measured to be larger than β which implies that $G(z, \hat{\theta}_{N_{id}}) \notin \mathcal{D}_{adm}$. This erroneous percentage is computed by $Pr(\mathcal{H}_1|\mathcal{H}_0) = \frac{11}{250} = 0.044$. Thus in 4.4% of the 250 simulations it was found that a wrong decision is made. In these cases we do not want to opt for a plant change due to the high costs which arise. Therefore, this percentage needs to be decreased which can possibly achieved with the second or third decision rule.

The erroneous decisions can be found in table 4-4 for each plant to disturbance ratio $\frac{Pr(\mathcal{H}_0)}{Pr(\mathcal{H}_1)}$. The percentage $Pr(\mathcal{H}_0|\mathcal{H}_1)$ does not equal $Pr(\mathcal{H}_1|\mathcal{H}_0)$ and by varying the plant to disturbance ratio $\frac{Pr(\mathcal{H}_0)}{Pr(\mathcal{H}_1)}$ in Eq. (4-3), a difference arise in $Pr_{incorrect}$ for each plant to disturbance ratio as shown in table 4-4. Finally, the percentage of correctly made decisions is found by $Pr_{correct} = 1 - Pr_{incorrect}$. Furthermore, it is shown in table 4-4 that a disturbance change is less often detected incorrectly because the percentage $Pr(\mathcal{H}_1|\mathcal{H}_0)$ is smaller than $Pr(\mathcal{H}_0|\mathcal{H}_1)$. This is mainly caused by the choice of β. When β was chosen to be slightly smaller, from Figs. 4-10a and 4-10b it can be seen that more plant changes will be chosen correctly and more disturbance changes will be chosen incorrectly, i.e., the percentage

Table 4-5: With decision rule two the percentages are given when opting for the wrong hypothesis for each scenario and percentages are given when opting for incorrect and correct hypotheses (both plant and disturbance changes). This is done for different ratios of how often a plant or disturbance change occurs. The threshold value(s) ν is/are given at the minimum values of $Pr_{incorrect}$ (and maximum values of $Pr_{correct}$).

Ratio Plant/Dist change	ν%	$\Pr(\mathcal{H}_0\|\mathcal{H}_1)$	$\Pr(\mathcal{H}_1\|\mathcal{H}_0)$	$\Pr_{incorrect}$	$\Pr_{correct}$
90/10	54 - 55	0.016	0.14	0.028	0.972
70/30	65 - 67	0.036	0.06	0.043	0.957
50/50	65 - 74	0.064	0.032	0.048	0.952
30/70	78 - 82	0.100	0.004	0.033	0.967
10/90	81 - 82	0.112	0	0.011	0.989

$Pr(\mathcal{H}_0|\mathcal{H}_1)$ will decrease and that $Pr(\mathcal{H}_1|\mathcal{H}_0)$ will increase.

A minimum percentage of opting a hypothesis correctly is found of 91.6% for the largest plant to disturbance ratio of 90/10 and a maximum percentage of opting a hypothesis correctly of 95.2% is found for the smallest plant to disturbance ratio of 10/90.

It is preferred to increase the confidence to opt for the correct hypothesis and therefore we will make use of the heuristic method and the corresponding decision rules two and three.

4-3-2-2 Decision Rule Two

In case of decision rule two the decision is only based on the heuristic method as discussed in section 2-3-3 and the percentage $\hat{Fr}_{out}$ as computed by Eq. (2-21). This percentage was based on the closed-loop performance $\left\{C(z), G(z,\theta^{(i)}), H(z,\theta_{com}\right\}$ of $i = 1...n$ constructed models around the estimated model. In each simulation a different percentage $\hat{Fr}_{out}$ of models is found which are outside the set $\mathcal{D}_{adm}$ and the number of incorrectly made decisions is based on the threshold value ν. Therefore, we vary threshold ν from 0 to 100% and compute at each integer value in between this interval, the percentages of the incorrectly made decisions $Pr(\mathcal{H}_1|\mathcal{H}_0)$ and $Pr(\mathcal{H}_0|\mathcal{H}_1)$. For example, from the 250 simulations where a plant change is applied, at a value $\nu = 50\%$, in four simulations a wrong decision is made because $\hat{Fr}_{out} < \nu$. Thus the percentage $Pr(\mathcal{H}_0|\mathcal{H}_1) = \frac{4}{250} = 0.016$ at threshold $\nu = 50\%$. The computed value can be found in Fig. 4-11, at $\nu = 50\%$, by the yellow/black dotted line which represents the percentage $Pr(\mathcal{H}_0|\mathcal{H}_1)$. Furthermore, the percentage $Pr(\mathcal{H}_1|\mathcal{H}_0)$ is given by the cyan/black dotted line and is computed in the same way as $Pr(\mathcal{H}_0|\mathcal{H}_1)$ and represents the percentage of incorrectly made decisions when a disturbance change occurred. The remaining lines represent the percentage of the correctly made decisions $Pr_{correct}$ for all five plant to disturbance ratios at all values ν on the interval of [0, 100].

The decreasing shape of the cyan/black dotted percentage line $Pr(\mathcal{H}_1|\mathcal{H}_0)$ from 1 to 0 in Fig. 4-11 can be explained by the fact that the decision rule is based on percentage $\hat{Fr}_{out}$ which on its turn depends on ν. When threshold is $\nu = 0\%$ it is found that fraction $\hat{Fr}_{out}$ cannot be smaller than ν and thus there is no possibility to opt for hypothesis $\mathcal{H}_0$ and thus $Pr(\mathcal{H}_1|\mathcal{H}_0) = 1$. When increasing the threshold ν it is found that in more simulations a correct decision is made and at $\nu = 81\%$ in all 250 simulations where a disturbance change is applied a correct decision is made which implies that $Pr(\mathcal{H}_1|\mathcal{H}_0) = 0$.
For a plant change the percentage of incorrectly made decisions $Pr(\mathcal{H}_0|\mathcal{H}_1)$, as shown in Fig.

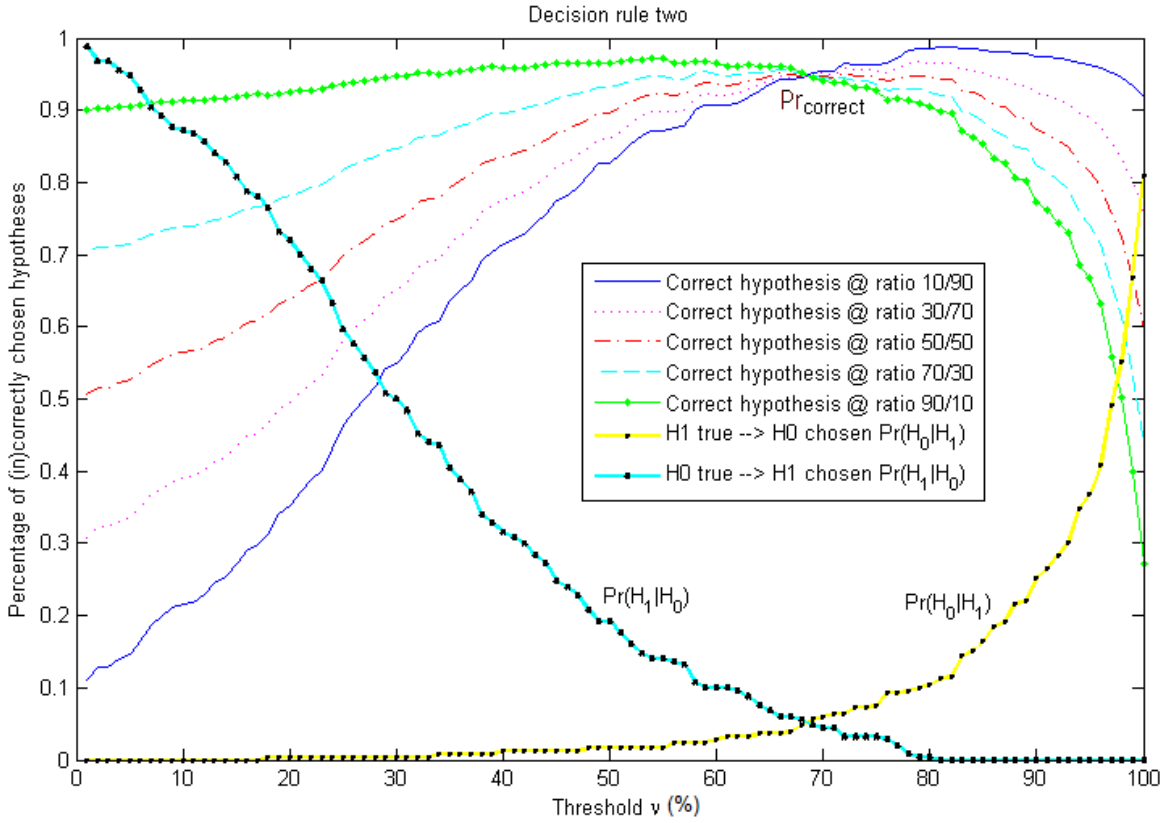

Figure 4-11: In this plot the percentage of opting a hypothesis correctly or incorrectly is shown. This is plotted against the minimum percentage of models that should lie outside set $\mathcal{D}_{adm}$, i.e., threshold value ν. The shown values are found by making use of decision rule two.

4-11 by the yellow/black dotted line, increases when ν increases. This is because we opt for a disturbance change (hypothesis $\mathcal{H}_0$) when it is found that $\hat{Fr}_{out} < \nu$. When $\nu = 0\%$, all plant changes are chosen correctly because in this case it is not possible to opt for a disturbance change.

To explain why the percentage $Pr(\mathcal{H}_1|\mathcal{H}_0)$ decreases slower than that percentage $Pr(\mathcal{H}_0|\mathcal{H}_1)$ increases, the following will be considered[4]. An error is made in case of a disturbance change when $\hat{Fr}_{out} \geq \nu$. The slow decreasing behaviour of $Pr(\mathcal{H}_1|\mathcal{H}_0)$ implies that in more simulations a percentage $\hat{Fr}_{out}$ is found which are larger than zero (somewhere between 10 and 50 %). This can be caused by the fact that $\hat{Fr}_{out}$ is based on the number of constructed models $G(z, \theta^{(i)})$ which are outside the set $\mathcal{D}_{adm}$. This is only the case when these models are located on the edge of set $\mathcal{D}_{adm}$ or when the variance of the estimated model is large and the constructed models are located quite some distance from the estimated model (and thus achieve a performance larger than β). The percentage $Pr(\mathcal{H}_0|\mathcal{H}_1)$ can decrease faster by decreasing the variance of the estimated parameters which can be achieved by increasing the identification length or increasing the power of the excitation signal during the re-identification experiment.

The percentages $Pr_{correct}$ as found in Table 4-5 are computed by $1 - Pr_{incorrect}$, where $Pr_{incorrect}$ is computed by Eq. (4-3), and correspond to the maximum percentages of correctly

[4]These percentages are shown by the cyan/black dotted line and by the yellow/black dotted line in Fig. 4-11 respectively.

made decisions as shown in Fig. 4-11 for each plant to disturbance ratio. It is the maximum of the blue solid, magenta dotted, red dashed-dotted, cyan dashed and green solid-dotted lines. The threshold values ν and percentages $Pr(\mathcal{H}_1|\mathcal{H}_0)$ and $Pr(\mathcal{H}_0|\mathcal{H}_1)$ as found in Table 4-5 are used to compute the maximum percentages $Pr_{correct}$ as found in Fig. 4-11, e.g., the blue solid line with plant to disturbance ratio of 10/90, has its maximum of 0.989 and has erroneous percentages of $Pr(\mathcal{H}_1|\mathcal{H}_0) = 0$ and $Pr(\mathcal{H}_0|\mathcal{H}_1) = 0.112$ at $\nu = 81 \sim 82\%$. (see Table 4-5)

For a plant to disturbance ratio of 90/10, the minimum incorrect percentage is $Pr_{incorrect} = 0.028$ as computed by Eq. (4-3) and is found for a threshold value $\nu = 55\%$ and percentages $Pr(\mathcal{H}_1|\mathcal{H}_0) = 0.016$ and $Pr(\mathcal{H}_0|\mathcal{H}_1) = 0.14$. For the smallest plant to disturbance ratio of 10/90, it is found that the minimum incorrect percentage is at $Pr(\mathcal{H}_1|\mathcal{H}_0) = 0$ and $Pr(\mathcal{H}_0|\mathcal{H}_1) = 0.112$ with $\nu = 81\%$ and is given by $Pr_{incorrect} = 0.011$.
Note that the percentages $Pr_{correct}$ from large to small plant to disturbance ratios first decreases and for smaller plant to disturbance ratios of 50/50 the percentages increases. This is caused by the decreasing and increasing behaviour of the percentages $Pr(\mathcal{H}_1|\mathcal{H}_0)$ and $Pr(\mathcal{H}_0|\mathcal{H}_1)$ and more or less same increasing and decreasing behaviour of the percentages $Pr(\mathcal{H}_0)$ and $Pr(\mathcal{H}_1)$ to compute $Pr_{incorrect}$ as given by Eq. (4-3).

4-3-2-3 Decision Rule Three

With the third decision rule we combine the first and second decision rules. The decision is first based on the performance of the closed-loop system $\left\{C(z), G(z,\hat{\theta}_{N_{id}}), H(z,\theta_{com})\right\}$. When the performance, computed with Eq. (2-7), is larger than the threshold value β only than the decision is based on the heuristic method as discussed in section 2-3-3, i.e., decision rule two. Therefore, the expectations are that with the third decision rule the confidence of opting for the correct hypothesis will increase w.r.t. decision rule one. Note that when variable $\nu = 0\%$ it implies that decision rule three equals decision rule one (because $\hat{Fr}_{out}$ can not be smaller than zero and thus when $G(z,\hat{\theta}_N) \notin \mathcal{D}_{adm}$ it is not possible to opt for hypothesis $\mathcal{H}_0$).

Again, at each threshold value ν on the interval $[0,\ 100]\%$ the incorrectly made percentages $Pr(\mathcal{H}_1|\mathcal{H}_0)$ and $Pr(\mathcal{H}_0|\mathcal{H}_1)$ are computed based on decision rule three. For example, in 250 simulations a disturbance change is applied. At an arbitrarily chosen threshold value $\nu = 30\%$, in eleven simulations a wrong decision is made due to the fact that the closed-loop performance is larger than β, thus $G(z,\hat{\theta}_{Nid}) \notin \mathcal{D}_{adm}$ and due to $\hat{Fr}_{out} \geq \nu$. The percentage is given by $\frac{11}{250} = 0.044 = 4.4\%$ which represents $Pr(\mathcal{H}_1|\mathcal{H}_0)$ and is shown in Fig. 4-12 by the cyan/black dotted line at $\nu = 30\%$. Furthermore, the yellow/black dotted line represents the percentage $Pr(\mathcal{H}_0|\mathcal{H}_1)$ which represent the number of incorrectly made decisions when a plant change occurred. In the same way as for decision rule two, for each of the plant to disturbance ratios the total percentage of correctly and incorrectly made decisions $Pr_{correct}$ and $Pr_{incorrect}$ are computed. The maximum and minimum of those percentages respectively, can be found in Table 4-6. The threshold values ν and percentages $Pr(\mathcal{H}_1|\mathcal{H}_0)$ and $Pr(\mathcal{H}_0|\mathcal{H}_1)$ are given to compute the minimum and maximum percentages $Pr_{incorrect}$ and $Pr_{correct}$ respectively. $Pr_{correct}$ is shown in Fig. 4-12 for all plant to disturbance ratios as shown by the blue solid, magenta dotted, red dashed-dotted, cyan dashed and green solid-dotted lines and for all threshold values ν.

The shape of the cyan/black dotted percentage line $Pr(\mathcal{H}_1|\mathcal{H}_0)$ in Fig. 4-12 is totally

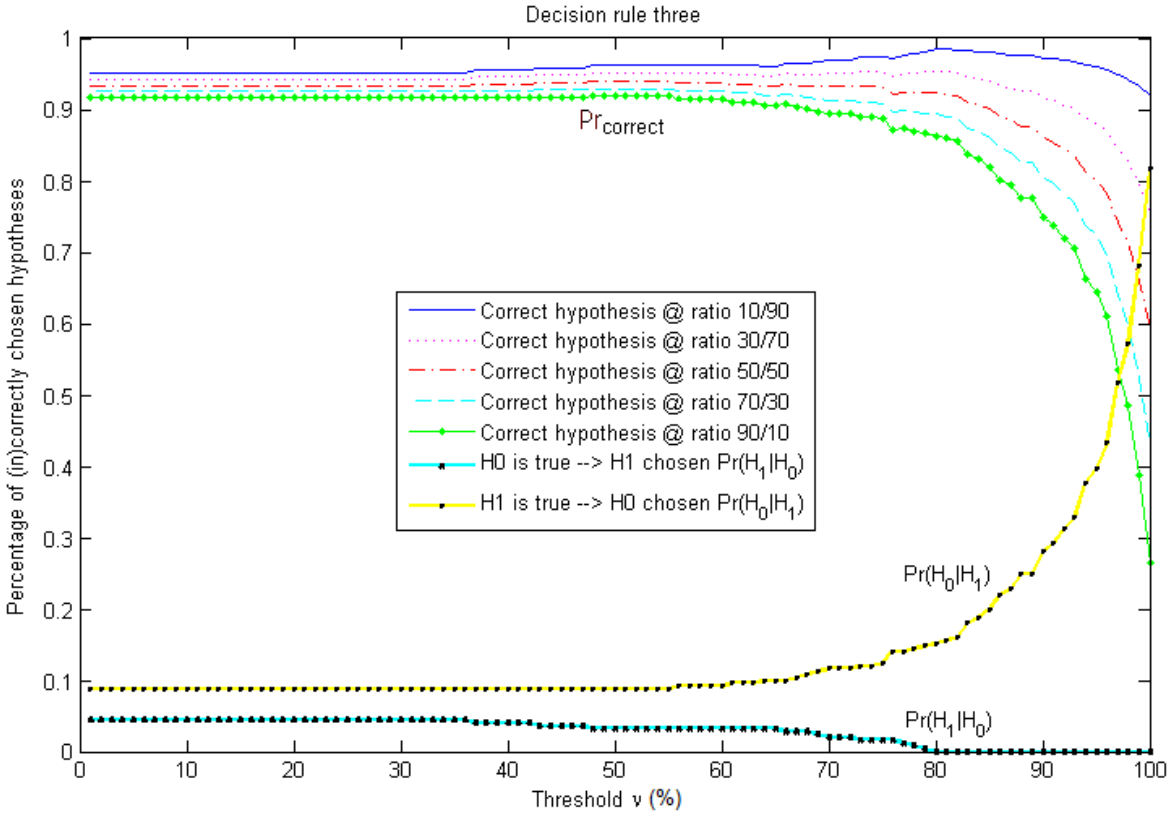

Figure 4-12: In this plot the percentage of opting a hypothesis correctly or incorrectly is shown. This is plotted against the minimum percentage of models that should lie outside set $\mathcal{D}_{adm}$, i.e., threshold value ν. The shown values are found by making use of decision rule three.

different w.r.t. Fig. 4-11. The maximum percentage of opting a disturbance change incorrectly is given by only 4.4% for an interval $\nu = [0,\ 35]\%$ and slightly decreases for $\nu \geq 35\%$. In many simulations the performance of the closed-loop system with the estimated model $G(z, \hat{\theta}_{N_{id}})$ is found to be smaller than β which implies that $G(z, \hat{\theta}_{N_{id}}) \in \mathcal{D}_{adm}$ and hypothesis $\mathcal{H}_0$ is chosen. Again, at $\nu = 80\%$ the percentage $Pr(\mathcal{H}_1|\mathcal{H}_0) = 0$ which was also found for decision rule two. This is the same because the decrease in $Pr(\mathcal{H}_1|\mathcal{H}_0)$ depends on the threshold ν and in none of the 250 simulations where a disturbance change is applied, a percentage larger than $\hat{Fr}_{out} = 80\%$ is found. The shape of the yellow/black dotted percentage line $Pr(\mathcal{H}_0|\mathcal{H}_1)$ in Fig. 4-12 almost corresponds to the yellow/black dotted line in Fig. 4-11. Due to the fact that first a decision is based on the closed-loop performance with the estimated model, it is found that for 22 of the 250 simulations a wrong decision is made. Thus $Pr(\mathcal{H}_0|\mathcal{H}_1) = \frac{22}{250} = 0.088 = 8.8\%$ as shown in Fig. 4-12 for $\nu = [0,\ 55]\%$. The second wrong decision which can be made is by finding a percentage $\hat{Fr}_{out}$ which is smaller than ν. When choosing a threshold $\nu \geq 55\%$ more wrong decisions are made as shown by the increasing yellow/black dotted line in Fig. 4-12.

The threshold value is the most important variable for which the minimum percentage of incorrectly made decisions $Pr_{incorrect}$ can be found. For a plant to disturbance ratio equal or larger than 50/50 it is found that the minimum incorrectly made decisions are made for a threshold value which is chosen between the interval of $[48,\ 55]\%$. At these threshold values

Table 4-6: With decision rule three the percentages are given when opting the wrong hypothesis for each scenario and percentages are given when opting for incorrect and correct hypotheses (both plant and disturbance changes). This is done for different ratios of how often a plant or disturbance change occurs. The threshold value(s) ν is/are given at the minimum values of $Pr_{incorrect}$ (and maximum values of $Pr_{correct}$).

Ratio Plant/Dist change	ν%	$\Pr(\mathcal{H}_0\|\mathcal{H}_1)$	$\Pr(\mathcal{H}_1\|\mathcal{H}_0)$	$\Pr_{incorrect}$	$\Pr_{correct}$
90/10	48 - 55	0.088	0.032	0.083	0.918
70/30	48 - 55	0.088	0.032	0.071	0.929
50/50	48 - 55	0.088	0.032	0.060	0.940
30/70	80	0.152	0	0.046	0.954
10/90	79 - 81	0.152	0	0.015	0.985

the percentages are $Pr(\mathcal{H}_1|\mathcal{H}_0) = 0.032$ and $Pr(\mathcal{H}_0|\mathcal{H}_1) = 0.088$. For plant to disturbance ratios larger than 50/50 the number of incorrectly made decisions when a plant change occurs is more important, due to the fact that a plant change occurs more often. Therefore, with the results as found with decision rule three, $Pr(\mathcal{H}_0|\mathcal{H}_1)$ should be as small as possible which is found for threshold values between $[0, 55]$ %. Then it is verified at which of the found threshold values ν $Pr(\mathcal{H}_1|\mathcal{H}_0)$ is as small as possible. When the plant to disturbance ratio decreases (smaller than 50/50) a disturbance change occurs more often. For that reason it is more important that $Pr(\mathcal{H}_1|\mathcal{H}_0)$ is as small as possible which it is for threshold values between $\nu = [80,\ 100]\%$. Secondly, the smallest value of $Pr(\mathcal{H}_0|\mathcal{H}_1)$ is found for threshold value near $\nu = 80\%$. It can be noticed that $Pr(\mathcal{H}_0|\mathcal{H}_1)$ is for each plant to disturbance ratio larger than $Pr(\mathcal{H}_1|\mathcal{H}_0)$. This is mainly caused by the heuristic method which will be used when $G(z, \hat{\theta}_{N_{id}}) \notin \mathcal{D}_{adm}$. It is then still possible to opt for hypothesis $\mathcal{H}_0$. On the other hand, it will be more likely to make a wrong decision when a plant change occurs because with this decision rule hypothesis $\mathcal{H}_1$ can only be chosen when $G(z, \hat{\theta}_{N_{id}}) \notin \mathcal{D}_{adm}$ and $\hat{Fr}_{out} \geq \nu$.

4-3-2-4 Comparison of the Decision Rules

As expected, with the first decision rule the smallest confidence is found of opting a hypothesis correctly for each of the plant to disturbance ratios and compared to decision rules two and three. As explained in section 2-3-2, various erroneous decisions can occur by making a decision which is only based on the estimated model $G(z, \hat{\theta}_{N_{id}})$.

To increase the confidence of opting for the correct hypothesis and decrease the number of erroneous situations, a heuristic method was proposed as given in section 2-3-3. With decision rule two it is, for each plant to disturbance ratio, found that the confidence increased of opting for the correct decision compared to decision rule one. There is an increase of 1.8% for a plant to disturbance ratio of 50/50 up to an increase of 5.6% for the largest plant to disturbance ratio of 90/10. Thus by making use of the heuristic method as explained in section 2-3-3 and choose threshold value ν, the confidence $Pr_{correct}$ can be increased.

The first and second decision rules are combined to construct decision rule three. With the third decision rule we created a preference to opt for hypothesis $\mathcal{H}_0$. It is found that by creating this preference, the confidence to opt for the correct decision decreases w.r.t. the second decision rule. The decrease is caused because the decision is again at first instance based on the closed-loop performance of the estimated model only. When $G(z, \hat{\theta}_{N_{id}}) \notin \mathcal{D}_{adm}$ the heuristic method is used. The reduction of confidence was found by the upward shift

of 8.8% of percentage $Pr(\mathcal{H}_0|\mathcal{H}_1)$ as shown by the yellow/black dotted line in Fig. 4-12 w.r.t. Fig. 4-11. Therefore, for large plant to disturbance ratios ($\geq 50/50$), the minimum incorrectly made decisions as computed by Eq. (4-3) is larger for the results as found in Table 4-6 compared to decision rule two and corresponding $Pr_{incorrect}$ in Table 4-5. For the plant to disturbance ratios $< 50/50$ the increase of $Pr(\mathcal{H}_0|\mathcal{H}_1)$ is of less importance due to the fact that more often a disturbance change occurs ($Pr(\mathcal{H}_1) < Pr(\mathcal{H}_0)$). Therefore, the confidence is only a slightly smaller for small plant to disturbance ratios compared to decision rule two. The slightly smaller confidence is shown by $Pr_{correct}$ in Table 4-6 compared to $Pr_{correct}$ from decision rule two and Table 4-5.

Finally, it can be seen that a decision based on the performance of the closed-loop system $\left\{C(z), G(z,\hat{\theta}_{N_{id}}), H(z,\theta_{com})\right\}$ only, gives less confidence of opting for the correct decision compared to decision rules two and three. Also, for plant to disturbance ratios $\geq 50/50$, decision rule three has only a slightly larger confidence of making the correct decision compared to the first decision rule. Furthermore, the third decision rule is compared with the first decision rule and it is found that an increase of 1 to 3% is obtained for plant to disturbance ratios $< 50/50$. Therefore, decision rule three is preferred above decision rule one. With decision rule two quite more confidence is found for plant to disturbance ratios $\geq 50/50$ and only slightly more confidence is found for ratios of $< 50/50$. This result shows that making use of the heuristic method only, the largest confidence is achieved of opting for the correct decision for each plant to disturbance ratio. However, it is important to have $Pr(\mathcal{H}_1|\mathcal{H}_0)$ as small as possible (near zero). This is not the case for decision rule two for plant to disturbance ratios of $\geq 50/50$. For that reason the chosen decision rule depends on a trade-off between having less confidence of making the correct decision and making more erroneous decisions when a disturbance change occurs. Note that this trade-off is made for plant to disturbance ratios of $\geq 50/50$. For smaller plant to disturbance ratios (which mostly occur in a system), decision rule two achieves a slightly larger confidence than decision rule three and is preferred to be used when applying the diagnostic tools to a MIMO system such as a binary distillation column.

Chapter 5

Conclusions and Future Work

In this thesis existing methodologies have been applied to a simulation model of a (MIMO) binary distillation column to monitor the performance on-line, detect a performance drop and find the cause of the performance drop. Also, the confidence of the made decision was analysed. A problem which can occur in model-based control systems has been discussed. The main concern is the decreasing performance of MIMO systems due to the occurrence of a control-relevant plant change or variations in disturbance characteristics over time.

The performance monitoring method of Ref. [1] is based on past measurements of the controlled outputs. The past measurements were used to estimate the power difference from the measured outputs and the corresponding set-points. A control-relevant plant or disturbance change increases the variance of the controlled outputs which implies that the difference between the set-point and output increases (and causes a decrease in performance). Furthermore, it was discussed that the number of past measurements are of importance, i.e., the window size is important. Using a small window size implies that a small number of data is used. The performance measure will be very sensitive with a small window and could give many false alarms, i.e., detection errors. When using a large window size, the power is averaged out for a longer period of time and it takes more time from the moment a change occurs until a performance drop is detected (detection time).

With the performance diagnosis method of Mesbah et. al. [2] a distinction is made between the considered causes by making use of hypothesis testing. Hypothesis $\mathcal{H}_0$ represents a disturbance change and hypothesis $\mathcal{H}_1$ a control-relevant plant change. Then a region $\mathcal{D}_{adm}$ is considered that contains all plant dynamics with which a satisfactory closed-loop performance can be achieved with the existing controller and under the original disturbance characteristics. Since the true dynamics are unknown a short closed-loop identification will be performed. On basis of the closed-loop performance with the estimated model one of the hypotheses is chosen. Furthermore, a heuristic method was used as discussed in section 2-3-3 and an alternative decision rule (given by (2-22)) is introduced to compare the confidence of the made decision. Finally, a third decision rule consists of a combination of the first and second decision rules as given by (2-23). To compare the decision rules, the confidence of the made decision is assessed by performing Monte Carlo simulations.

With the performance monitoring method of Ref. [1] and by applying a threshold on

the performance, a control-relevant plant change or variations in disturbance characteristics as discussed in section 3-3-3-1 degrades the performance. The performance then violates the threshold value which implies that such a change can be detected correctly each time one of these changes arises. It is discussed that the choice of the window size depends on a trade-off between the detection time and the detection errors. It is found that the performance measure having a window size of around 400 data points detects almost no errors and have a relatively short detection time for the MIMO binary distillation column. Note that a different window size can be chosen depending on the choice of the importance of one of the issues (detection errors and detection time).

To investigate how confident we are of making the correct decision, with the performance diagnosis methodology of Mesbah et. al. [2] various decision rules were compared. This is done to find the largest confidence of opting for the correct hypothesis. It was found that with the decision rule, which is based on the heuristic method (2-22), the largest confidence is achieved to opt for the correct hypothesis. In case that much more disturbance changes occur over time compared to plant changes, 98.9% of the decisions will be chosen correctly which is a quite satisfactory result.

It can be concluded that the performance monitoring method is able to measure the performance on a discrete basis and is able to detect any of the considered performance deteriorations. It is found that the diagnostic tools, function sufficiently within a MIMO system such as a binary distillation column due to the satisfactory confidence of opting for the correct hypothesis.

In this thesis only one classical performance monitoring method is applied to measure the performance. In case of a model-based control system, it may occur that a different kind of performance monitoring method will give a more accurate measure or possibly a faster detection time and less detection errors. One on-line monitoring method for example makes use of measured output data and data of the control input signals (i.e., an LQG objective function) as explained in Ref. [6] or even another method can be used where a trade-off is made between operational costs and a so-called constraint violation cost as explained in Ref. [5]. In future work it is possible to compare various performance monitoring methods to find out which method performs the best in a MIMO system such as a binary distillation column when considering the detection time and detection errors.

It is argued that the confidence of the made decision in the performance diagnosis partly depends on the accuracy of the estimated model and partly on the chosen decision rule. Besides increasing the confidence of the decision, economical cost should be kept as small as possible. What we have done is performing a quite costly re-identification experiment by exciting the whole frequency range. By only exciting the control-relevant dynamics it is possible to decrease economical costs. It is possible that it will affect the length of the excitation or the power of the excitation signal. Therefore, in future work it can be investigated whether the same kind or a higher confidence can be obtained (compared to the results in this thesis), but with less costly excitation signals (exciting only control-relevant dynamics and using shorter identification lengths and/or a lower excitation power).

Appendix A

Derivations

A-1 Closed-loop outputs

The open-loop outputs $\underline{y}(t)$, the input of system $G(z,\theta_0)$ and the errors $\underline{\epsilon}(t)$ are given by

$$\begin{aligned} \underline{y}(t) &= G(z,\theta_0)\underline{u}(t) + H(z,\theta_0)\underline{e}(t). && \text{(A-1)} \\ \underline{u}(t) &= C(z)\underline{\epsilon}(t). && \text{(A-2)} \\ \underline{\epsilon}(t) &= \underline{r}_1(t) - \underline{y}(t). && \text{(A-3)} \end{aligned}$$

Substitute Eq. (A-3) into Eq. (A-2) which gives

$$\underline{u}(t) = C(z)(\underline{r}_1(t) - \underline{y}(t)). \tag{A-4}$$

Then substitute Eq. (A-4) into Eq. (A-1) which gives

$$\underline{y}(t) = G(z,\theta_0)C(z)(\underline{r}_1(t) - \underline{y}(t)) + H(z,\theta_0)\underline{e}(t) \tag{A-5}$$

and rewrite $\underline{y}(t)$ to the left hand side

$$(I + G(z,\theta_0)C(z))\underline{y}(t) = G(z,\theta_0)C(z)\underline{r}_1(t) + H(z,\theta_0)\underline{e}(t). \tag{A-6}$$

Finally, we obtain

$$\underline{y}(t) = (I + G(z,\theta_0)C(z))^{-1}(G(z,\theta_0)C(z)\underline{r}_1(t) + H(z,\theta_0)\underline{e}(t)). \tag{A-7}$$

A-2 Closed-loop inputs

For the closed-loop inputs we will substitute Eq. (A-1) and Eq. (A-3) into Eq. (A-2) which gives:

$$\underline{u}(t) = C(z)\left(\underline{r}_1(t) - G(z,\theta_0)\underline{u}(t) - H(z,\theta_0)\underline{e}(t)\right). \tag{A-8}$$

Then rewrite $\underline{u}(t)$ to the left hand side

$$(I + C(z)G(z,\theta_0))\underline{u}(t) = C(z)\underline{r}_1(t) - C(z)H(z,\theta_0)\underline{e}(t). \tag{A-9}$$

Finally, we obtain the input signals by

$$\underline{u}(t) = (I + C(z)G(z,\theta_0))^{-1}C(z)\underline{r}_1(t) - (I + C(z)G(z,\theta_0))^{-1}C(z)H(z,\theta_0)\underline{e}(t). \tag{A-10}$$

A-3 Closed-loop error signal

Start with $\underline{y}(t)$ from Eq. A-7 and subtract $\underline{r}_1(t)$ gives:

$$\begin{aligned}
\underline{y}(t) &= (I + G(z,\theta_0)C(z))^{-1}(G(z,\theta_0)C(z)\underline{r}_1(t) + H(z,\theta_0)\underline{e}(t)) \\
\underline{y}(t) - \underline{r}_1(t) &= (I + G(z,\theta_0)C(z))^{-1}((G(z,\theta_0)C(z) - I)\underline{r}_1(t) + H(z,\theta_0)\underline{e}(t)) \\
&= (I + G(z,\theta_0)C(z))^{-1}(G(z,\theta_0)C(z) - (I + G(z,\theta_0)C(z)))\underline{r}_1(t) \\
&\qquad + (I + G(z,\theta_0)C(z))^{-1}H(z,\theta_0)\underline{e}(t) \\
&= -(I + G(z,\theta_0)C(z))^{-1}\underline{r}_1(t) + (I + G(z,\theta_0)C(z))^{-1}H(z,\theta_0)\underline{e}(t)
\end{aligned} \tag{A-11}$$

A-4 Closed-loop inputs with excitation signal

In the open-loop situation the inputs are given by

$$\underline{u}(t) = C(z)\underline{\epsilon}(t) + \underline{r}_{ex}(t). \tag{A-12}$$

To obtain the closed-loop inputs we substitute Eq. (A-1) and Eq. (A-3) into Eq. (A-2) which gives:

$$\underline{u}(t) = C(z)\left(\underline{r}_1(t) - G(z,\theta_0)\underline{u}(t) - H(z,\theta_0)\underline{e}(t)\right) + \underline{r}_{ex}(t). \tag{A-13}$$

Replace $C(z)\underline{r}_1(t) + \underline{r}_{ex}(t)$ by $\underline{r}(t)$ and write $\underline{u}(t)$ to the left hand side

$$(I + C(z)G(z,\theta_0))\underline{u}(t) = \underline{r}(t) - C(z)H(z,\theta_0)\underline{e}(t). \tag{A-14}$$

The outputs with excitation signal are then given by

$$\underline{u}(t) = (I + C(z)G(z,\theta_0))^{-1}\underline{r}(t) - (I + C(z)G(z,\theta_0))^{-1}C(z)H(z,\theta_0)\underline{e}(t). \tag{A-15}$$

A-5 MIMO covariance matrix

Substitute Eqs. (2-2) and (2-3) in Eq. (2-12) the columns and the transpose of the columns can be defined for $i = 1, ..., m$ by

$$\upsilon_i^T(t,\theta_0) = \frac{d\bar{\underline{y}}(t,\theta)}{d\theta} = F_r^i(t,\theta_0)\underline{r}(t) + F_e^i(t,\theta_0)\underline{e}(t), \tag{A-16}$$

$$\upsilon_i(t,\theta_0) = \mathrm{vec}(F_r^i(t,\theta_0))(I_m \otimes \underline{r}(t)) + \mathrm{vec}(F_e^i(t,\theta_0))(I_m \otimes \underline{e}(t)). \tag{A-17}$$

Here, $\otimes$ represents the tensor product of two vector spaces and $vec(.)$ represents a vectorization of a matrix. The matrix Υ is given by

$$\Upsilon(t,\theta_0) = \begin{pmatrix} \upsilon_1(t,\theta_0) \\ \upsilon_2(t,\theta_0) \\ \vdots \\ \upsilon_m(t,\theta_0) \end{pmatrix} \tag{A-18}$$

Furthermore, $F_r^i(t,\theta_0)$ and $F_e^i(t,\theta_0)$ are

$$F_r^i(t,\theta_0) = H_0(z)^{-1}\frac{dG(z,\theta)}{d\theta_i}S(z,\theta) \qquad i=1,...,m \tag{A-19}$$

$$F_r^i(t,\theta_0) = H_0(z)^{-1}\left(\frac{dH(z,\theta)}{d\theta_i} - \frac{dG(z,\theta)}{d\theta_i}S(z,\theta)C(z)H_0(z)\right) \tag{A-20}$$

Bibliography

[1] M. L. Tyler and M. Morari, "Performance monitoring of control systems using likelihood methods," *Automatica*, vol. 32, no. 8, pp. 1145–1162, 1996.

[2] A. Mesbah, X. Bombois, J. H. Ludlage, and P. M. Van den Hof, "Closed-loop performance diagnosis using prediction error identification," in *Decision and Control and European Control Conference (CDC-ECC), 2011 50th IEEE Conference on*, pp. 2969–2974, IEEE, 2011.

[3] M. Basseville and A. Benveniste, "Sequential detection of abrupt changes in spectral characteristics of digital signals," *Information Theory, IEEE Transactions on*, vol. 29, no. 5, pp. 709–724, 1983.

[4] R. Isermann, "Supervision, fault-detection and fault-diagnosis methodsŮan introduction," *Control engineering practice*, vol. 5, no. 5, pp. 639–652, 1997.

[5] M. Potters, M. Lundh, P. Modén, and X. Bombois, "Advanced autonomous model-based operation of industrial process systems," 2012.

[6] J. Schäfer and A. Cinar, "Multivariable mpc system performance assessment, monitoring, and diagnosis," *Journal of Process Control*, vol. 14, no. 2, pp. 113–129, 2004.

[7] F. Gustafsson and S. F. Graebe, "Closed-loop performance monitoring in the presence of system changes and disturbances," *Automatica*, vol. 34, no. 11, pp. 1311–1326, 1998.

[8] P. M. Frank, "Fault diagnosis in dynamic systems using analytical and knowledge-based redundancy: A survey and some new results," *Automatica*, vol. 26, no. 3, pp. 459–474, 1990.

[9] B. Huang and E. C. Tamayo, "Model validation for industrial model predictive control systems," *Chemical Engineering Science*, vol. 55, no. 12, pp. 2315–2327, 2000.

[10] L. Miškovic, A. Karimi, D. Bonvin, and M. Gevers, "Direct closed-loop identification of 2× 2 systems: Variance analysis," *CDROM Proc. of*, pp. 873–878, 2006.

[11] P. van den Hof, *System Identification (TUDelft Course Reader)*. 2006.

[12] M. Barenthin, X. Bombois, H. Hjalmarsson, and G. Scorletti, "Identification for control of multivariable systems: Controller validation and experiment design via lmis," *Automatica*, vol. 44, no. 12, pp. 3070–3078, 2008.

[13] M. Gevers, X. Bombois, B. Codrons, G. Scorletti, and B. Anderson, "Model validation for control and controller validation in a prediction error identification frameworkŮpart i: theory," *Automatica*, vol. 39, no. 3, pp. 403–415, 2003.

[14] M. Doherty and M. Malone, *Conceptual Design of distillation columns*. McGraw-Hill, 2001.

[15] Luyben, *Practical Distillation Control*. Van Nostrand Reinhold, 1992.

[16] S. Skogestad, P. Lundström, and E. Jacobsen, "Selecting the best distillation control configuration," *AIChE Journal*, vol. 36, no. 5, pp. 753–764, 1990.

[17] S. Skogestad, "The dos and don'ts of distillation column control," *Chemical Engineering Research and Design*, vol. 85, no. 1, pp. 13–23, 2007.

[18] S. Skogestad and I. Postlethwaite, *Multivariable Feedback Control analysis and design*. John Wiley & Sons Ltd., 1996.

[19] A. E.-N. G.F. Franklin, J.D. Powell, *Feedback control of dynamic systems*. Pearson, Presentice Hall.

[20] S. Skogestad, E. W. Jacobsen, and M. Morari, "Inadequacy of steady-state analysis for feedback control: Distillate-bottom control of distillation columns," *Industrial & Engineering Chemistry Research*, vol. 29, no. 12, pp. 2339–2346, 1990.

Abbreviations and Nomenclature

Table A-1: Abbreviations

BJ	Box-Jenkins
CV/PV	Controlled/Process Variable
DV	Disturbance Variable
MIMO	Multiple-Input Multiple-Output
MPC	Model Predictive Control
MV	Manipulated Variable
RGA	Relative Gain Array
SISO	Single-Input Single-Output

Table A-2: Nomenclature

LaTeX Code	Symbol	Meaning
`$B$`	B	Bottoms flow
`$D$`	D	Distillation flow
`$F$`	F	Feed flow
`$L$`	L	Reflux flow
`$V$`	V	Reboil flow
`$V_T$`	V_T	Condensing flow
`$z_B$`	z_B	composition of the bottom flow
`$z_D$`	z_D	composition of the distillate flow
`$z_F$`	z_F	composition of the feed flow
`$Q_c$`	Q_c	heat duty of the condenser
`$Q_r$`	Q_r	heat duty of the reboiler
`$L_D$`	L_D	liquid height in the reflux drum
`$L_B$`	L_B	liquid height in the distillation column
`$P$`	P	pressure in the distillation column
`$N_T$`	N_T	number of trays contained in the column

Table A-3: Nomenclature

LaTeX Code	Symbol	Meaning
`$r$`	r	reflux ratio $\frac{L}{D}$
`$s$`	s	reboil ratio $\frac{V}{B}$
`$\hat{J}(k)$`	$\hat{J}(k)$	performance measure
`$d$`	d	difference of the absolute value of the mean of the outputs minus a constraint
`$P_{viol}(k)$`	$P_{viol}(k)$	boundary value violation probability
`$c_d, c_p$`	c_d c_p	weights or cost factors
`$N_{win}$`	N_{win}	number of data points measured in one window
`$N_{viol}$`	N_{viol}	number of data points violating the boundary value
`$\beta$`	β	threshold value for the performance
`$y(k)$`	y(k)	discrete values of controlled variable
`$\bar{y}(k)$`	$\bar{y}(k)$	mean value of the discrete values of $y(k)$
`$u(t)$`	$u(t)$	input signal of a system
`$e(t)$`	$e(t)$	zero-mean white noise signal
`$y(t)$`	$y(t)$	output signal of a system
`$G_0(z)$`	$G_0(z)$	true transfer function matrix of the process
`$G(z,\hat{\theta}_N)$`	$G(z,\hat{\theta}_N)$	estimated model of the process transfer function matrix
`$H_0(z)$`	$H_0(z)$	true transfer function matrix of the noise
`$H(z,\hat{\theta}_N)$`	$H(z,\hat{\theta}_N)$	estimated transfer function matrix of the noise
`$C(z)$`	$C(z)$	controller in closed-loop system
`$\theta_0$`	θ_0	true parameter values
`$\hat{\theta}_N$`	$\hat{\theta}_N$	estimated parameter values
`$\theta_{com}$`	θ_{com}	parameter values of the model used at the commissioning stage
`$\mathcal{D}_{adm}$`	$\mathcal{D}_{adm}$	set of all transfer functions $G(z,\theta)$ which give nominal performance
`$Z^N$`	Z^N	obtained input and output data set
`$\epsilon(t)$`	$\epsilon(t)$	one-step-ahead prediction error
`$\mathcal{M}$`	$\mathcal{M}$	chosen model parametrization
`$\mathcal{S}$`	$\mathcal{S}$	true system $y(t) = G_0(z)u(t) + H_0(z)e(t)$
`$\mathcal{G}$`	$\mathcal{G}$	true process system
`$P_{\theta}$`	P_θ	variance matrix
`$\bar{E}$`	$\bar{E}$	expectation operator
`$\sigma_e^2$`	σ_e^2	variance of signal e(t)
`$N, N_{id}$`	N, N_{id}	identification length
`$\hat{Fr}_{out}$`	$\hat{Fr}_{out}$	Number of models which give bad performance
`$\nu$`	ν	threshold value for number of models $G(z,\theta) \notin \mathcal{D}_{adm}$ to opt for a hypothesis
`$amp$`	amp	amplification factor for rotation of input signals
`$\psi$`	ψ	rotation angle of signal u(t)